



CT Angiography in Ischemic Stroke: Optimization and Accuracy

Cécile de Monyé

CT Angiography in Ischemic Stroke: Optimization and Accuracy

Cécile de Monyé

CT Angiography in Ischemic Stroke: Optimization and Accuracy

CT Angiografie bij Herseninfarct:
Optimalisering en Accuratesse

Proefschrift

ter verkrijging van de graad van doctor aan de
Erasmus Universiteit Rotterdam
op gezag van de
rector magnificus

Prof.dr. H.G. Schmidt

en volgens besluit van het College voor Promoties.

De openbare verdediging zal plaatsvinden op
woensdag 13 Juni 2012 om 13.30 uur

door

Cécile de Monyé
geboren te Eindhoven

Cover design: Cécile de Monyé and A.W. Everaers

Layout: A.W. Everaers

Printed by: Ipskamp Drukkers BV

ISBN: 978-90-9026726-5

© 2012 Cécile de Monyé

All rights reserved. No part of this thesis may be reproduced or transmitted in any form or by any means, electronic or mechanical, including photocopying, recording, or any information storage and retrieval system, without prior written permission from the copyright owner.



Promotiecommissie:

Promotores: Prof.dr. A. van der Lugt
Prof.dr. D.W.J. Dippel

Overige leden: Prof.dr. M.G.M. Hunink
Prof.dr. H.J.M. Verhagen
Prof.dr. W.P.Th.M Mali

Contents

Chapter 1	General Introduction	9
Chapter 2	Sixteen-detector Row CT Angiography of Carotid Arteries: Comparison of Different Volumes of Contrast Material with and Without a Bolus Chaser	19
Chapter 3	Optimization of CT Angiography of the Carotid Artery with a 16-MDCT Scanner: Craniocaudal Scan Direction Reduces Contrast Material–related Perivenous Artifacts	39
Chapter 4	High Iodine Concentration Contrast Material for Noninvasive Multislice Computed Tomography Coronary Angiography: Iopromide 370 Versus Iomeprol 400	55
Chapter 5	Diagnostic Accuracy of CT Angiography and Duplex Ultrasound for the Detection of Carotid Artery Stenosis in TIA or Minor Stroke Patients	67
Chapter 6	Suspected Carotid Artery Stenosis: Cost-Effectiveness of CT Angiography in Work-up of Patients with Recent TIA or Minor Ischemic Stroke	81
	Appendix	107
Chapter 7	Assessment of Atherosclerotic Carotid Plaque Volume with Multidetector Computed Tomography Angiography	127
Chapter 8	Is a Fetal Origin of the Posterior Cerebral Artery a risk Factor for TIA or Ischemic Stroke? A Study With 16-multidetector-row CT Angiography	145
Chapter 9	MDCT Detection of Fibromuscular Dysplasia of the Internal Carotid Artery	159
Chapter 10	Summary and Conclusions	167
Chapter 11	Samenvatting en Conclusies	177
Chapter 12	Dankwoord	187
	List of Publications	191
	PhD Portfolio	195
	Curriculum Vitae	199

Chapter 1

General Introduction

General introduction

Stroke is the third leading cause of death after coronary heart disease and cancer. The clinical burden of stroke now exceeds that of coronary heart disease.¹ Especially in the aging population stroke is a major disease. By the year 2020 the incidence of stroke in the Netherlands is expected to have increased to 2.5 per 1000 and the prevalence to 8.7 per 1000 for the whole population.² Stroke is also the most common cause of disabilities in adults. Therefore not only the disease impact but also the healthcare impact of stroke is substantial.³

Stroke is defined as the clinical syndrome of rapid onset of focal or global cerebral deficit with a presumed vascular cause. Different pathological mechanisms can be responsible for a stroke: cerebral ischemia ($\approx 80\%$), primary intracerebral hemorrhage ($\approx 15\%$), and subarachnoid hemorrhage ($\approx 5\%$). Ischemic stroke is confined to an area of the brain perfused by a specific artery and lasts longer than 24 hours or has led to death. Transient ischemic attack (TIA) is a brief episode of neurological dysfunction caused by focal brain or retinal ischemia, with clinical symptoms usually lasting less than 24 hours, and without evidence of acute infarction.

Three main pathophysiological mechanisms of ischemic stroke and TIA can be acknowledged. The first cause is large vessel disease. About 50% of all ischemic strokes and TIA's are probably due to atherothrombotic disease of the extracranial, or less commonly large intracranial arteries. The main locations are the aortic arch, the carotid artery bifurcation, the carotid siphon, the origo of the vertebral arteries and the intracranial vertebral artery and basilar artery. Cerebral ischemia can occur when an atherosclerotic lesion significantly obstructs the blood flow to the brain (near occlusion), or when an atherosclerotic lesion ruptures and, due to thrombus formation and subsequent thrombus and/or plaque material embolization, obstructs a smaller vessel in the brain. The latter mechanism is by far the most common.³ The second cause is small vessel disease. About 25% of all ischemic strokes and TIA's are caused by lacunar infarcts, which are related to occlusion of small arteries perforating the brain. The third cause is cardiac disease. About 20% of all ischemic strokes and TIA's arise from emboli from the heart. The emboli can be caused by a variety of cardiac conditions, but the most common is atrial fibrillation with presumed thrombus in the right atrium. Other possible conditions include recent myocardial infarction, prosthetic valves, dilated cardiomyopathy, and infectious endocarditis. Finally, the remainder ($\approx 5\%$) of all ischemic strokes and TIA's are due to some rare causes like vasculitis, arterial dissection and fibromuscular dysplasia.

The management of acute ischemic stroke in the acute phase consists of treatment with intravenous thrombolytics in patients presenting within 4.5 hours, aspirin, surveillance on a stroke unit and optimization of vital functions. Only in a selected group of patients presenting within 6 hours with persisting intracranial arterial occlusion after onset of symptoms intra-arterial thrombolytic therapy is used.

The estimated risk of stroke after a TIA or minor stroke is 8-12% at seven days and 11-15% at one month.⁴ Most ischemic strokes after TIA occur in the first days after the TIA.⁵ Therefore, secondary prevention of stroke is of utmost importance. Medical treatment with antiplatelet drugs and oral anticoagulants and treatment of the most important cardiovascular risk factors, such as smoking, elevated blood pressure and elevated plasma cholesterol levels, reduces the risk of recurrent ischemic events. Secondary prevention focuses also on the underlying cause of ischemic stroke. Recurrent stroke risk ipsilateral to an atherosclerotic carotid artery stenosis is higher the more extreme the stenosis. Two large randomized trials (NASCET (North American Symptomatic Carotid Endarterectomy Trial) and ECST (European Carotid Surgery Trial)) have shown that carotid endarterectomy (CEA) in patients with severe symptomatic carotid artery stenosis (70–99%) is effective in the reduction of recurrent symptoms.^{6,7} These studies showed that the 5 years risk for ipsilateral ischemic stroke is more than 25% in patients with a stenosis of 70-99% and more than 15% in patients with a stenosis of 50-69%. The absolute risk reduction after surgery is 16% if the degree of stenosis is 70–99% and 4.6% if the degree of stenosis is 50–69%.⁸ Furthermore, the benefit of CEA also depends on the timing of surgery after the ischemic event. For symptomatic stenoses the benefit from surgery falls rapidly with increasing delay.⁹ In the past few years, endovascular treatment with placement of a stent has emerged as an alternative to CEA, although recent data show a higher periprocedural risk of stroke with stenting than with endarterectomy.¹⁰

It is important to select patients for surgical or endovascular treatment based on the severity of stenosis with a high accuracy. Besides severity of stenosis, plaque vulnerability is currently considered to play an essential role in cerebrovascular events. Detection of plaque vulnerability might improve risk prediction and could be used in the selection of patients for intervention. A wide range of plaque features have been related to plaque vulnerability: plaque volume, plaque composition, plaque ulceration, inflammation and neovascularisation.^{11,12}

Digital subtraction angiography (DSA) remains the reference standard for diagnosing a carotid artery stenosis, according to the large randomized trials, such as NASCET and ECST.⁶⁻⁸ The inherent risk of this invasive procedure has led to a less invasive diagnostic strategy in which patients were screened with duplex ultrasound (DUS). If a stenosis was found by DUS, DSA was performed to confirm the stenosis and assess the severity of stenosis. Since then, multiple studies have been performed to demonstrate that magnetic resonance angiography (MRA) can replace DSA as a confirmative study and is as accurate as DSA in the assessment of the severity of stenosis.¹³⁻¹⁵ With the introduction of spiral CT, CT angiography (CTA) entered clinical practice. Evaluation of CTA in the assessment of a significant stenosis in the carotid artery ($>70\%$) has revealed a high sensitivity and specificity.¹⁶ However, single slice CTA has not gained much popularity in the diagnostic work-up of patients with suspected symptomatic carotid artery stenosis. This may have been related to limitations in required volume of contrast material (CM) (>100 ml), scan range (<120 mm), slice thickness (≥ 2 mm) and available post-processing techniques.

Multidetector-row CT (MDCT) has eliminated several of these limitations. It allows full vascular imaging from the aortic arch to the circle of Willis. Therefore, also other important predilection sites of atherosclerosis, like the aortic arch, the origin of the supra-aortic vessels, the carotid siphon, and the vertebrobasilar arteries can now be evaluated. This allows the evaluation of other and rare causes of ischemic stroke. MDCT offers an improved spatial resolution of less than 1 mm slice thickness and shorter acquisition times of <15 sec. Lower doses of CM are required. Another advantage of MDCT angiography for atherosclerotic plaque evaluation is the increased in plane resolution and the subsequent ability to obtain near isotropic voxels. More detailed analysis of atherosclerotic plaque morphology and luminal plaque surface may now be possible.

The work in this thesis is focused on three topics. One: the optimization of the CTA scan protocol. Two: the accuracy of CTA in the detection of carotid artery stenosis and plaque composition. Three: the role of CTA in the workup of rare causes of ischemic stroke.

Optimization of the scan protocol

To evaluate the supra-aortic vessels a homogeneous high intraluminal attenuation is desirable. This can be achieved by injection of a large amount of contrast media with a high injection rate. However, we have to search for the lowest volume of CM necessary for optimal analysis for several reasons. Firstly, the high cost of CM forces the radiologist to search for ways to decrease CM volume. Secondly, the risk of nephrotoxicity is related to the volume of CM and decreasing the volume of CM may influence the risk of subsequent nephrotoxicity. Patients referred for carotid imaging are usually of higher age and often show generalized arteriosclerosis combined with impaired renal function.^{17, 18} These patients would specifically benefit from a reduced amount of contrast media.^{19, 20} Thirdly, in acute stroke patients, CTA of the carotid artery is often combined with CT perfusion of the brain, which requires an additional injection of 50 mL of CM^{21, 22}. In such studies the total volume of CM should be restricted to what is necessary for optimal analysis. An optimal CM injection protocol had not yet been established for CTA of the carotid artery with a 16-row MDCT. The application of a saline bolus chaser after the injection of the CM might improve enhancement and thus may lead to a reduction in the volume of CM. In **chapter 2** different volumes of intravenous CM with and without a bolus chaser were prospectively compared in order to find the optimal CM injection protocol for 16-row MDCT angiography of the carotid arteries.

With bolus tracking the CTA scan can be optimally synchronized with the passage of CM in the arteries.²³ Normally, the CTA scan starts before the end of contrast injection. This results in undiluted CM in the subclavian vein, brachiocephalic vein and superior vena cava which produces artifacts that project over the ascending aorta and the origin of the supra-aortic arteries.^{24, 25} Such artifacts can obscure adjacent structures and thus hide or suggest stenosis or occlusion of the proximal supra-aortic arteries. The addition of a bolus chaser to the main contrast bolus may lead

to a reduced frequency of these artifacts by clearing the veins of CM. However, the timing of the CTA scan is not altered by the addition of a bolus chaser and artifacts do still occur. A craniocaudal scan direction, opposite to the flow direction, may reduce the number of artifacts due to delayed scanning of the apex of the thorax. In **chapter 3** a caudocranial scan direction versus a craniocaudal scan direction was compared for the influence on enhancement of the carotid artery and on perivenous artifacts in CTA with a MDCT scanner.

CTA with MDCT scanners, with considerably more rapid acquisition times, requires a high attenuation in a short period of time without a concomitant increase in CM volume. One way to achieve this is by modifying the iodine administration rate although a more practical way might entail the use of a CM with higher iodine concentration. In **chapter 4** two different CM (iopromide 370 mgI/mL and iomeprol 400 mgI/mL), were prospectively compared in terms of the attenuation obtained in an extended territory comprising the coronary arteries as well as the ascending and descending thoracic aorta and pulmonary arteries.

The diagnostic imaging work-up of carotid artery disease

Although DUS as the only modality in the workup of stroke patients proved to be a cost-effective strategy²⁶, most clinicians like to confirm a stenosis diagnosed on DUS with a second angiographic modality. In practice, this two-step strategy can be time-consuming due to logistic problems. Moreover, apart from the degree of carotid stenosis and vascular risk factors, the benefit of CEA also depends on the timing of surgery after the ischemic event. For symptomatic stenoses the benefit from surgery falls rapidly with increasing delay⁹. Since CT of the brain is recommended in the diagnostic work-up of patients with TIA or minor ischemic stroke CTA can easily be added to the CT protocol. CTA could be the initial and only diagnostic modality in the evaluation of symptomatic carotid arteries²⁷. In **chapter 5** the diagnostic accuracy of MDCT angiography alone and DUS alone in a consecutive cohort of patients with TIA or minor stroke symptoms was studied. For each patient only the severity of stenosis of the carotid artery on the symptomatic side was included in the analysis. CTA and DUS were compared with a reference standard. In case of agreement between CTA and DUS on a stenosis of <50% or an occlusion, DUS and CTA were used as the reference standard. If both CTA and DUS showed a stenosis of 80-99% and DSA was not performed to prevent treatment delay, DUS and CTA were used as the reference standard. In all other cases the reference standard was DSA.

Beside the accuracy of an imaging technique, costs are a relevant item in the decision on the optimal imaging strategy. We propose CTA as the only diagnostic modality in the evaluation of the symptomatic carotid artery in all patients, while CTA is more expensive than DUS. In **chapter 6** the effectiveness and cost-effectiveness of state-of-the-art noninvasive diagnostic imaging strategies, including MDCT angiography, in patients with a TIA or a minor stroke who are suspected of having carotid artery stenosis was studied. Particular attention was paid to the time window

between the first ischemic symptoms and carotid endarterectomy, and the cutoff value chosen as an indication for surgery (70–99% vs 50–99% stenosis).

Atherosclerotic plaque rupture plays an important role in acute events, like TIA and minor stroke.^{11, 28} The vulnerable rupture-prone plaques have specific morphological features: the most frequently seen vulnerable plaque type has a large lipid-rich core with a thin fibrous cap and has proved to be an independent predictor of ischemic cerebrovascular events.¹² It is therefore hypothesized that the amount of atherosclerotic plaque and its components (calcifications, fibrous tissue, and lipid core) could be better predictors of acute events than the degree of stenosis. An in vitro and in vivo study showed that quantification of the area (two dimensional) of atherosclerotic carotid plaque and its components is possible in axial thin section MDCT angiography images, in good correlation with histology.^{29, 30} Further developments in the quantification software now enable to quantify the volume of atherosclerotic plaque and the volume of different plaque components. In **chapter 7** this software tool for atherosclerotic plaque and plaque component volume measurements in MDCT angiography images of the carotid artery was evaluated and the observer variability of these measurements was assessed.

Rare causes of ischemic stroke

In approximately 5 to 10% of patients with a TIA or minor stroke the ischemia is located in the territory of the posterior cerebral artery (PCA). Most commonly, the PCA derives from the basilar artery. However, in 10–20% of normal subjects the PCA derives from the internal carotid artery (ICA) through a patent posterior communicating artery, while the connection with the basilar artery is hypoplastic or even aplastic.³¹⁻³⁵ Such a fetal origin of the PCA in combination with atherosclerotic disease or dissection of the carotid artery may cause an ischemic stroke in the occipital lobe.³⁶⁻³⁸ Patients with a TIA or a minor stroke in the territory of the ICA combined with an ipsilateral carotid artery stenosis of more than 70% benefit from CEA.^{6, 39} It follows that patients with a TIA or mild stroke in the territory of the PCA who have a fetal origin of the PCA and atherosclerotic disease in the ICA might also be candidates for CEA. Whether patients with a fetal origin of the PCA have a higher risk of TIA or ischemic stroke in this arterial distribution is not known.³¹ In **chapter 8** the frequency of a fetal origin of the PCA in a clinical series, and the degree of stenosis of the ipsilateral ICA in patients with a TIA or infarct in the territory of the PCA was assessed with MDCT angiography.

A less common possible cause of stroke is fibromuscular dysplasia (FMD) of the cervical arteries. It can be detected with conventional angiography and less sensitive with DUS or MRA. In the study described in chapter 6 in which we screened patients with symptoms of a TIA or minor stroke for atherosclerosis and stenosis of the carotid artery with CTA, we encountered 2 cases of FMD of the ICA in a group of 400 consecutive patients. In **chapter 9** these 2 cases, where FMD of the ICA was diagnosed with CTA are presented.

References

1. Rothwell PM, Coull AJ, Silver LE, et al. Population-based study of event-rate, incidence, case fatality, and mortality for all acute vascular events in all arterial territories (Oxford Vascular Study). *Lancet* 2005; 366:1773-83.
2. Struijs JN, van Genugten ML, Evers SM, Ament AJ, Baan CA, van den Bos GA. Modeling the future burden of stroke in The Netherlands: impact of aging, smoking, and hypertension. *Stroke* 2005; 36:1648-55.
3. Warlow C, Sudlow C, Dennis M, Wardlaw J, Sandercock P. Stroke. *Lancet* 2003; 362:1211-24.
4. Coull AJ, Lovett JK, Rothwell PM. Population based study of early risk of stroke after transient ischaemic attack or minor stroke: implications for public education and organisation of services. *BMJ* 2004; 328:326.
5. Rothwell PM, Giles MF, Flossmann E, et al. A simple score (ABCD) to identify individuals at high early risk of stroke after transient ischaemic attack. *Lancet* 2005; 366:29-36.
6. Beneficial effect of carotid endarterectomy in symptomatic patients with high-grade carotid stenosis. North American Symptomatic Carotid Endarterectomy Trial Collaborators. *N Engl J Med* 1991; 325:445-53.
7. Randomised trial of endarterectomy for recently symptomatic carotid stenosis: final results of the MRC European Carotid Surgery Trial (ECST). *Lancet* 1998; 351:1379-87.
8. Rothwell PM, Eliasziw M, Gutnikov SA, et al. Analysis of pooled data from the randomised controlled trials of endarterectomy for symptomatic carotid stenosis. *Lancet* 2003; 361:107-16.
9. Rothwell PM, Eliasziw M, Gutnikov SA, Warlow CP, Barnett HJ. Endarterectomy for symptomatic carotid stenosis in relation to clinical subgroups and timing of surgery. *Lancet* 2004; 363:915-24.
10. Ederle J, Dobson J, Featherstone RL, et al. Carotid artery stenting compared with endarterectomy in patients with symptomatic carotid stenosis (International Carotid Stenting Study): an interim analysis of a randomised controlled trial. *Lancet* 2010; 375:985-97.
11. Naghavi M, Libby P, Falk E, et al. From vulnerable plaque to vulnerable patient: a call for new definitions and risk assessment strategies: Part I. *Circulation* 2003; 108:1664-72.
12. Polak JF, Shemanski L, O'Leary DH, et al. Hypochoic plaque at US of the carotid artery: an independent risk factor for incident stroke in adults aged 65 years or older. Cardiovascular Health Study. *Radiology* 1998; 208:649-54.
13. Nederkoorn PJ, Mali WP, Eikelboom BC, et al. Preoperative diagnosis of carotid artery stenosis: accuracy of noninvasive testing. *Stroke* 2002; 33:2003-8.
14. Nonent M, Serfaty JM, Nighoghossian N, et al. Concordance rate differences of 3 noninvasive imaging techniques to measure carotid stenosis in clinical routine practice: results of the CARMEDAS multicenter study. *Stroke* 2004; 35:682-6.
15. Wardlaw JM, Chappell FM, Best JJ, Wartolowska K, Berry E. Non-invasive imaging compared with intra-arterial angiography in the diagnosis of symptomatic carotid stenosis: a meta-analysis. *Lancet* 2006; 367:1503-12.

16. Koelmay MJ, Nederkoorn PJ, Reitsma JB, Majoie CB. Systematic review of computed tomographic angiography for assessment of carotid artery disease. *Stroke* 2004; 35:2306-12.
17. Verhave JC, Hillege HL, Burgerhof JG, Gansevoort RT, de Zeeuw D, de Jong PE. The association between atherosclerotic risk factors and renal function in the general population. *Kidney Int* 2005; 67:1967-73.
18. Missouris CG, Papavassiliou MB, Khaw K, et al. High prevalence of carotid artery disease in patients with atheromatous renal artery stenosis. *Nephrol Dial Transplant* 1998; 13:945-8.
19. Toprak O. Conflicting and new risk factors for contrast induced nephropathy. *J Urol* 2007; 178:2277-83.
20. Goldenberg I, Matetzky S. Nephropathy induced by contrast media: pathogenesis, risk factors and preventive strategies. *CMAJ* 2005; 172:1461-71.
21. Smith WS, Roberts HC, Chuang NA, et al. Safety and feasibility of a CT protocol for acute stroke: combined CT, CT angiography, and CT perfusion imaging in 53 consecutive patients. *AJNR* 2003; 24:688-90.
22. Nabavi DG, Kloska SP, Nam EM, et al. MOSAIC: Multimodal Stroke Assessment Using Computed Tomography: novel diagnostic approach for the prediction of infarction size and clinical outcome. *Stroke* 2002; 33:2819-26.
23. Haage P, Schmitz-Rode T, Hubner D, Piroth W, Gunther RW. Reduction of contrast material dose and artifacts by a saline flush using a double power injector in helical CT of the thorax. *AJR* 2000; 174:1049-53.
24. Rubin GD, Lane MJ, Bloch DA, Leung AN, Stark P. Optimization of thoracic spiral CT: effects of iodinated contrast medium concentration. *Radiology* 1996; 201:785-91.
25. Loubeyre P, Debard I, Nemoz C, Minh VA. High opacification of hilar pulmonary vessels with a small amount of nonionic contrast medium for general thoracic CT: a prospective study. *AJR* 2002; 178:1377-81.
26. Buskens E, Nederkoorn PJ, Buijs-Van Der Woude T, et al. Imaging of carotid arteries in symptomatic patients: cost-effectiveness of diagnostic strategies. *Radiology* 2004; 233:101-12.
27. Josephson SA, Bryant SO, Mak HK, Johnston SC, Dillon WP, Smith WS. Evaluation of carotid stenosis using CT angiography in the initial evaluation of stroke and TIA. *Neurology* 2004; 63:457-60.
28. Naghavi M, Libby P, Falk E, et al. From vulnerable plaque to vulnerable patient: a call for new definitions and risk assessment strategies: Part II. *Circulation* 2003; 108:1772-8.
29. de Weert TT, Ouhlous M, Meijering E, et al. In vivo characterization and quantification of atherosclerotic carotid plaque components with multidetector computed tomography and histopathological correlation. *Arterioscler Thromb Vasc Biol* 2006; 26:2366-72.
30. de Weert TT, Ouhlous M, Zondervan PE, et al. In vitro characterization of atherosclerotic carotid plaque with multidetector computed tomography and histopathological correlation. *Eur Radiol* 2005; 15:1906-14.
31. van Raamt AF, Mali WP, van Laar PJ, van der Graaf Y. The Fetal Variant of the Circle of Willis and Its Influence on the Cerebral Collateral Circulation. *Cerebrovasc Dis* 2006; 22:217-24.
32. Jongen JC, Franke CL, Soeterboek AA, Versteeg CW, Ramos LM, van Gijn J. Blood supply of the posterior cerebral artery by the carotid system on angiograms. *J Neurol* 2002; 249:455-60.
33. Saeki N, Rhoton AL, Jr. Microsurgical anatomy of the upper basilar artery and the posterior circle of Willis. *J Neurosurg* 1977; 46:563-78.
34. Pedroza A, Dujovny M, Artero JC, et al. Microanatomy of the posterior communicating artery. *Neurosurgery* 1987;20:228-35.
35. Tulleken CA, Luiten ML. The basilar artery bifurcation: microscopical anatomy. *Acta Neurochir (Wien)* 1987;85:50-5.
36. Pessin MS, Kwan ES, Scott RM, Hedges TR, 3rd. Occipital infarction with hemianopsia from carotid occlusive disease. *Stroke* 1989;20:409-11.
37. Kuker W, Mull M, Block F, Thron A. Carotid artery dissections presenting as isolated posterior cerebral artery infarctions. *J Neurol* 1997;244:324-7.
38. Cohen SN. Occipital infarction with hemianopsia from carotid occlusive disease. *Stroke* 1989;20:1433-4.
39. MRC European Carotid Surgery Trial: interim results for symptomatic patients with severe (70-99%) or with mild (0-29%) carotid stenosis. European Carotid Surgery Trialists' Collaborative Group. *Lancet* 1991;337:1235-43.

Chapter 2

Sixteen-Detector Row CT Angiography
of Carotid Arteries: Comparison of
Different Volumes of Contrast Material
with and without a Bolus Chaser

Sixteen-detector row CT angiography of carotid arteries: Comparison of different volumes of contrast material with and without a bolus chaser

Cécile de Monyé, MD
 Filippo Cademartiri, MD
 Thomas T. de Weert, MD
 Dorine A. M. Siepman, MD
 Diederik W. J. Dippel, MD, PhD
 Aad van der Lugt, MD, PhD

Radiology 2005; 237:555–562

Abstract

Purpose: To prospectively compare different volumes of intravenously administered contrast material with and without a bolus chaser at 16-detector row computed tomographic (CT) angiography of the carotid arteries.

Materials and methods: Institutional Review Board approval and informed consent were obtained. Seventy-five consecutive patients (44 men, 31 women; mean age, 63 years; range, 22–85 years) were allocated to one of three protocols: group 1, 80 mL of contrast material; group 2, 80 mL of contrast material followed by 40 mL of saline; and group 3, 60 mL of contrast material followed by 40 mL of saline. Bolus tracking was used to synchronize contrast material injection with CT scanning. The attenuation in Hounsfield units was measured from the ascending aorta to the intracranial arteries at 1-second intervals. Differences were tested with the Student *t*-test.

Results: The maximum attenuation was reached in the proximal internal carotid artery in all groups. The addition of a bolus chaser to 80-mL contrast material resulted in a higher mean attenuation (323 HU \pm 39 vs 351 HU \pm 60, $p = 0.06$), higher maximum attenuation (393 HU \pm 53 vs 425 HU \pm 76, $p = 0.09$), and higher minimum attenuation (240 HU \pm 34 vs 264 HU \pm 48, $p < 0.05$). Group 3 had lower mean, maximum, and minimum attenuation than did groups 1 and 2 ($p < 0.001$).

Conclusion: The addition of a bolus chaser to 80 mL of contrast material results in a slightly higher attenuation. Decreasing the volume of contrast material from 80 to 60 mL results in a significantly lower attenuation.

Introduction

The benefit of carotid endarterectomy in patients with severe symptomatic carotid artery stenosis (>70%) has been established in large randomized trials.^{1,2} The degree of stenosis in these trials was assessed with digital subtraction angiography. The inherent risk of this invasive procedure has led to a noninvasive diagnostic strategy in which patients are screened with duplex ultrasonography (US) followed by a magnetic resonance (MR) angiography in case of abnormal US findings.³

With the introduction of spiral computed tomography (CT), CT angiography entered clinical practice.^{4,5} Evaluation of CT angiography for the assessment of significant stenosis (>70%) in the carotid artery has already revealed a high sensitivity and specificity.^{6–11} However, single-section CT angiography has not gained much popularity in the diagnostic work-up of patients suspected of having symptomatic carotid artery stenosis. This may have been related to limitations in the required volume of contrast material (>100 mL), scan range (<120 mm), section thickness (≥ 2 mm), and available postprocessing techniques.

Multidetector row CT, and in particular, 16-detector row CT, has eliminated several of these limitations.^{12–15} It allows CT angiography of the carotid arteries to be performed with an increased coverage from the aortic arch to the circle of Willis, an improved spatial resolution of less than 1-mm section thickness, shorter acquisition times of less than 15 seconds, and lower doses of contrast material.

The application of a saline bolus chaser after the injection of contrast material may further reduce the volume of contrast material^{16–20}, but an optimal contrast material injection protocol has not yet been established for 16-detector row CT angiography of the carotid arteries. Thus, the purpose of our study was to prospectively compare different volumes of intravenously administered contrast material with and without a bolus chaser at 16-detector row CT angiography of the carotid arteries.

Methods

Study Population

From October 2002 to February 2003, 75 consecutive patients (44 men and 31 women; mean age, 63 years; range, 22–85 years) who underwent CT angiography of the carotid arteries were enrolled in the study (62 outpatients and 13 inpatients). Indication for CT angiography was possible atherosclerotic disease of the carotid or vertebrobasilar vascular system in patients with a transient ischemic attack or minor ischemic stroke. Exclusion criteria were previous allergic reaction to iodinated contrast media, renal insufficiency (serum creatinine level of >100 mmol/L), pregnancy, and age younger than 18 years. Patients with an occlusion of the carotid artery were also excluded. The Institutional Review Board approved the study, and patients provided informed consent.

Each patient was allocated to one of three contrast material administration protocols. The first 25 patients (group 1: 14 men and 11 women; mean age, 60 years; range, 36–81 years) received 80 mL of contrast material without bolus chaser, the next 25 patients (group 2: 17 men and 8 women; mean age, 68 years; range, 27–84 years) received 80 mL of contrast material followed by 40 mL of saline bolus chaser, and the last group of 25 patients (group 3: 13 men and 12 women; mean age, 60 years; range, 22–85 years) received 60 mL of contrast material followed by 40 mL of saline bolus chaser. In case of bolus tracking, which allows synchronization of CT scanning with the passage of contrast material, the amount of contrast material should be equal to or more than the scan time times the injection rate as follows: $\pm 15 \text{ seconds} \times 4 \text{ mL/sec} = 60 \text{ mL}$. As a precaution, we started the study with 80 mL of contrast material and tried to reduce the dose to 60 mL. With an injection rate of 4 mL/sec, 40 mL of saline is a reasonable amount of fluid to flush the vein for injection and to push the tail of the contrast material bolus to the superior vena cava. For each patient, age, sex, and weight were recorded.

Scanning Protocol

Patients underwent CT angiography of the carotid arteries with a 16-detector row CT scanner (Sensation 16; Siemens Medical Solutions, Forchheim, Germany). Patients were positioned supine on the CT table with the arms along the chest. A lateral scout view that included the thorax, neck, and skull was acquired. The scan range reached from the ascending aorta to the intracranial circulation (2 cm above the sella turcica). Scanning parameters were 0.75-mm collimation, 12-mm (pitch of 1) table feed per rotation, 0.5-second rotation time, 120 kV, 180 mAs, caudo-cranial scanning direction, and 10–14-seconds scan time (depending on individual patient's size and anatomy). The entire examination took 15 minutes.

The contrast material iodixanol (320 mg of iodine per milliliter, Visipaque; Amersham Health, Little Chalfont, UK) was injected intravenously through an 18–20-gauge cannula, depending on the size of the vein, into the antecubital vein by using a power injector (EnVision; MedRAD, Pittsburgh, Pa). The right antecubital vein was preferentially used because it provides the shortest path for the contrast material through the venous system and therefore the least dilution. When venous access on the right side could not be achieved, the left antecubital vein was used. The saline bolus chaser was injected immediately after the contrast material injection was completed by using a second power injector (EnVision; MedRAD). Both power injectors were connected to the injection cannula with a T-shaped tube (MedRAD), with an integrated one-way valve attached to the power injector that contained the saline bolus chaser to prevent reflux of the contrast medium. Contrast material and saline bolus chaser injection rates were 4 mL/sec.

Synchronization between the passage of contrast material and data acquisition was achieved with real-time bolus tracking. The arrival of the injected contrast material was monitored in real time by using a series of dynamic transverse low-dose monitoring scans (120 kV, 20–40 mAs) at the level of the ascending aorta at intervals of

1 second. The monitoring sequence started 5 seconds after the initiation of contrast material administration. CT angiography was triggered automatically on the basis of a threshold measured in a region of interest (ROI) in the ascending aorta. The size of the ROI in the ascending aorta for the bolus triggering was adjusted to the size and composition of the ascending aorta but was always greater than 5 mm in diameter. The trigger threshold was set at an increase of 75 HU over the baseline (approximately 150 HU in absolute value). When the threshold was reached, the table was moved to the caudal start position while the patient was instructed not to swallow. Four seconds after the trigger threshold was reached, CT angiographic data acquisition was started automatically. All bolus timing procedures and CT angiographic scans were successfully completed. No adverse reactions to contrast material were observed.

Data Collection and Analysis

Images were reconstructed with an effective section width of 1 mm, reconstruction interval of 0.6 mm, field of view of 100 mm, and a medium-smooth convolution kernel (B30f; Siemens Medical Solutions). The images were transferred to a stand-

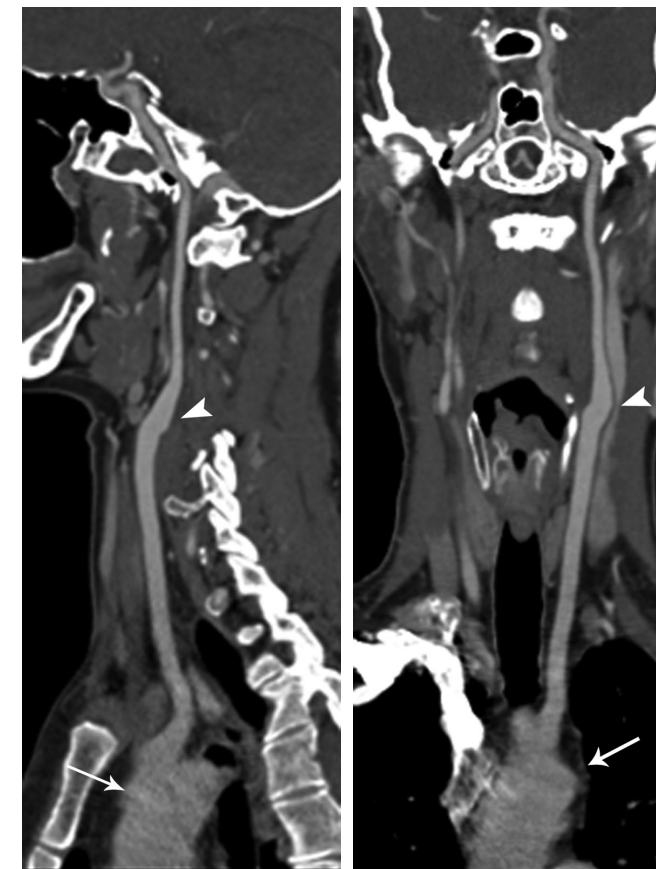


Fig. 1 CT angiograms of left carotid artery. (a) Sagittal and (b) coronal curved planar reformations from the aortic arch to the carotid siphon. The curved planar reformations demonstrate a homogeneous attenuation in the artery from the aortic arch (arrow) through the carotid bifurcation (arrowhead) to the intracranial circulation.

alone workstation and evaluated by using dedicated analysis software (Leonardo; Siemens Medical Solutions). For clinical analysis, two curved planar reformations of each carotid artery from the aortic arch to the carotid siphon were created in perpendicular planes (Fig 1).

In each patient, the site of injection, scan coverage (in millimeters), number of transverse sections, scan delay (in seconds), and scan time (in seconds) were recorded.

Transverse images were used for attenuation measurements. The Digital Imaging and Communications in Medicine layout of the images showed the time at which the scanning was performed. At intervals of 1 second (each 40th section), an ROI was drawn throughout the data sets in two regions: (a) the ascending aorta to the right internal carotid artery (ICA) and (b) the ascending aorta to the left ICA. The location of the measurements was recorded as follows: the ascending aorta, aortic arch, proximal common carotid artery (CCA) (first two measurements in the CCA), distal CCA, proximal ICA (first two measurements in the ICA), distal ICA, carotid siphon, and intracranial part of the ICA; measurements in the brachiocephalic trunk were considered to be measurements in the CCA.

One observer (C.d.M.) with 3 years of experience with CT angiography measured and recorded all data. The attenuation was measured by drawing a circular ROI in the center of the vessel lumen. The ROIs were drawn as large as the anatomic configuration of the lumen allowed in the transverse section.

The mean value of the measurements on the left and right side at each time point was calculated. Time-attenuation curves were generated for each patient. Subsequently, the attenuation at time 0; the mean, minimum, and maximum attenuation; and the time to reach the maximum attenuation were assessed. Because attenuation above 200 HU was considered optimal, the number of measurements below 200 HU was counted.

The aforementioned analysis resulted in one to three measurements per location, depending on the size of the patient. To analyze the attenuation in these locations, the measurements obtained in these locations were averaged. The relationship between the mean attenuation and weight was analyzed in all three groups.

Statistical Analysis

Differences between measurements on the left and right side were analyzed with paired Student *t*-test. Baseline characteristics and attenuation parameters (value at time 0, minimum and maximum attenuation, and time to maximum attenuation) in the three groups were compared with a one-way analysis of variance (ANOVA) test or χ^2 test. In case of a significant difference, a pair-wise comparison was performed with the Student *t*-test. The mean attenuation and the attenuation at different locations in the three groups were compared with repeated-measures ANOVA. In case

of a significant difference, a pair-wise comparison with repeated-measures ANOVA was performed. In addition, a pair-wise comparison of attenuation parameters with adjustment for differences in weight, age, and sex was performed with a linear regression model. The relationship between weight and mean attenuation in the three groups was analyzed with linear regression analysis.

Statistical analysis was performed by using software (SPSS, version 9.0, SPSS, Chicago, Ill; and SAS Proc Mixed, SAS Institute, Cary, NC). $p < 0.05$ was considered to indicate a significant difference.

Results

Patients and Procedures

More patients in group 3 received the contrast material (60 mL) and bolus chaser (40 mL) via the left antecubital vein than patients in groups 1 and 2 (32%, 4%, and 12%, respectively; $p < 0.05$). Patient demographics, weight, scan delay, scan time, scan range, and the number of images were not significantly different in the three groups (Table 1).

Table 1. Patient and Scan Characteristics in Three Groups with Different Volumes of Contrast Material

Parameter	Group 1	Group 2	Group 3
	(80-mL CM)	(80-mL CM plus 40-mL BC)	(60-mL CM plus 40-mL BC)
No. of patients	25	25	25
M/F	14/11	17/8	13/12
Mean age (y)	60 (36-81)	68 (27-84)	60 (22-85)
Mean weight (kg)	75 (58-107)	71 (55-92)	78 (56-103)
Right/left injection side*	24/1	22/3	17/8
Mean scan delay (sec)	18 (12-26)	18 (15-24)	19 (14-27)
Mean scan time (sec)	14 (11-17)	13 (11-16)	13 (11-15)
Mean scan coverage (mm)	331 (275-401)	325 (256-372)	316 (256-368)
Mean no. of sections	553 (459-670)	546 (427-637)	527 (427-621)

Data in parentheses are the range. BC = bolus chaser, CM = contrast material

* = χ^2 test, $p < 0.05$

Left versus Right Injection Side

Combination of data from all 75 patients revealed a slightly higher mean attenuation (2.5 HU \pm 8.8) on the left side in comparison with the right side ($p < 0.05$) (Fig 2). In addition, the time to maximum attenuation was slightly shorter (0.3 second \pm 1.3) on the left side ($p < 0.05$). The maximum and minimum attenuations on the left and right side were not different (Table 2).

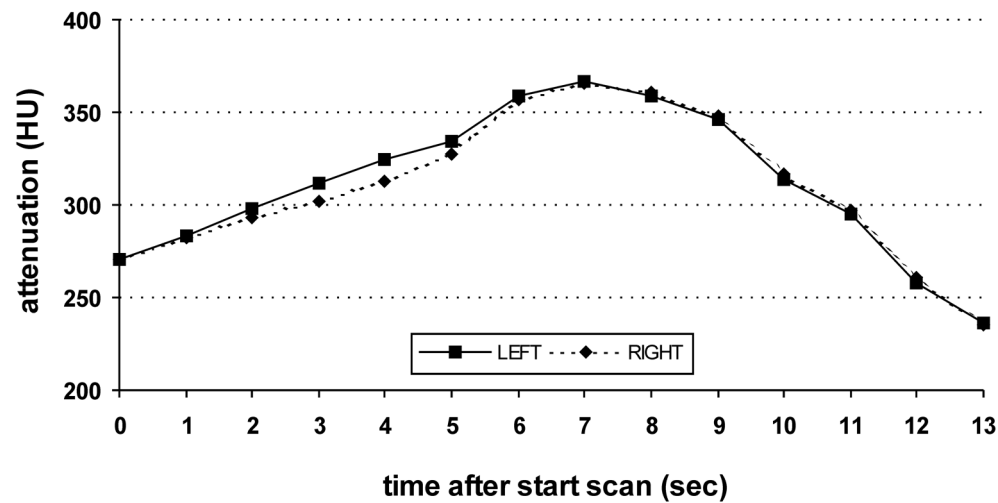


Fig. 2 Time-attenuation curves show the mean intraluminal attenuation in left ($n = 75$) and right ($n = 75$) carotid arteries after start of scanning. There is a slightly higher mean attenuation on the left side in comparison with the right side.

Table 2. Paired Difference of Attenuation Parameters Obtained at the Left and Right Sides in 75 Patients

Parameter	Paired Difference	p Value
Mean attenuation (HU)	2.5 ± 8.8	< 0.05
Minimum attenuation (HU)	3.6 ± 24.9	Not significant
Maximum attenuation (HU)	0.7 ± 17.8	Not significant
Time to maximum attenuation (sec)	-0.3 ± 1.3	< 0.05

Group 1: 80-mL Contrast Material

The mean arterial attenuation was $323 \text{ HU} \pm 39$. The minimum and maximum arterial attenuations were $240 \text{ HU} \pm 34$ and $393 \text{ HU} \pm 53$, respectively. Two measurements in two of the 25 patients (330 measurements) had an attenuation of less than 200 HU. Both measurements were in the intracranial arteries.

Group 2: 80-mL Contrast Material with 40-mL Saline

The mean arterial attenuation per patient was $351 \text{ HU} \pm 60$. The minimum and maximum arterial attenuations per patient were $264 \text{ HU} \pm 48$ and $425 \text{ HU} \pm 76$, respectively. Five measurements in two of the 25 patients (330 measurements) had an attenuation of less than 200 HU. Two of these measurements were in the ascending aorta or aortic arch, and three were in the carotid siphon or intracranial arteries.

Group 3: 60-mL Contrast Material with 40-mL Saline

The mean arterial attenuation per patient was $273 \text{ HU} \pm 53$. The minimum and maximum arterial attenuations per patient were $185 \text{ HU} \pm 43$ and $331 \text{ HU} \pm 64$, respectively. Fifty-three of the attenuation measurements in 16 of the 25 patients (326 measurements) were less than 200 HU. These measurements were obtained in the ascending aorta, CCA, ICA, and intracranial arteries in two, 15, nine, and 27 cases, respectively.

Comparison of Time-Attenuation Curves

The attenuation value at time 0 was significantly higher with the application of 40-mL bolus chaser (group 1 vs group 2); in addition, the maximum attenuation was higher (425 HU in group 2 vs 393 HU in group 1), although not significantly ($p = 0.09$). The minimum attenuation was significantly higher with the bolus chaser ($p < 0.05$). The time to maximum attenuation was shorter (6.9 seconds in group 2 vs 7.8 seconds in group 1, $p < 0.05$) (Table 3, Fig 3).

Table 3. Attenuation Parameters in Three groups with Different Volumes of Contrast Material

Parameter	Group 1 (80-mL CM)	Group 2 (80-mL CM plus 40-mL BC)	Group 3 (60 mL CM plus 40 mL BC)	p Value		
				Group 1 vs 2	Group 2 vs 3	Group 1 vs 3
Value at time 0 (HU) *	258 ± 32	288 ± 42	266 ± 48	< 0.01	NS	NS
Mean attenuation (HU) †	323 ± 39	351 ± 60	273 ± 53	NS	< 0.001	< 0.001
Minimum attenuation (HU) ‡	240 ± 34	264 ± 48	185 ± 43	< 0.05	< 0.001	< 0.001
Maximum attenuation (HU) ‡	393 ± 52	425 ± 76	331 ± 64	NS	< 0.001	< 0.001
Time to maximum attenuation (sec) ‡	7.8 ± 1.4	6.9 ± 1.4	5.0 ± 2.0	< 0.05	< 0.001	< 0.001

Data are the mean \pm standard deviation. BC = bolus chaser, CM = contrast material, NS = not significant

* ANOVA, $p < 0.05$

† Repeated measures ANOVA, $p < 0.001$

‡ ANOVA, $p < 0.001$

The group that received 60 mL of contrast material and 40 mL of bolus chaser had lower mean, maximum, and minimum attenuations and time to maximum attenuation ($p < 0.001$) in comparison to the group that received 80 mL of contrast material without 40 mL of bolus chaser and the group that received 80 mL of contrast material with 40 mL of bolus chaser (Table 3). Adjustment for weight, age, and sex in a regression model showed the same significant differences between the groups.

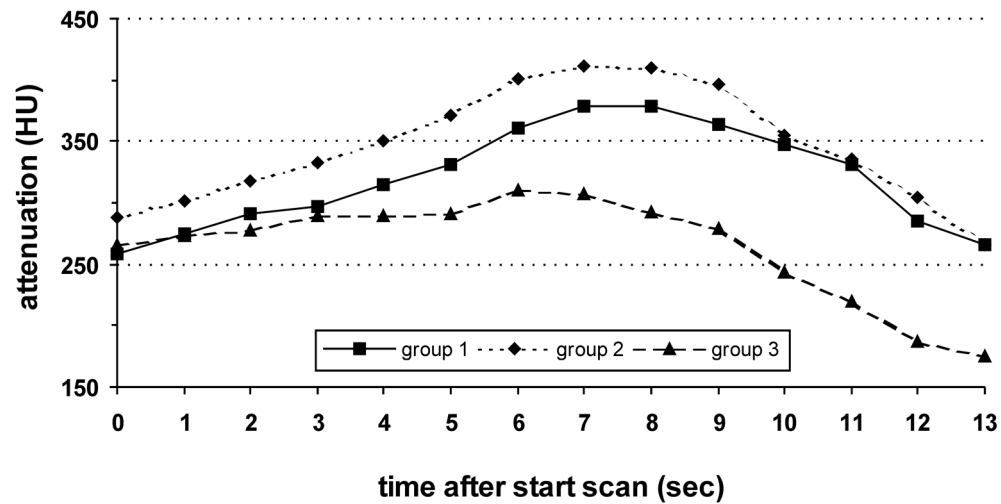


Fig. 3 Time-attenuation curves show intraluminal attenuation after start of scanning in group 1 (80-mL contrast material, $n = 25$), group 2 (80-mL contrast material plus 40-mL saline, $n = 25$), and group 3 (60-mL contrast material plus 40-mL saline, $n = 25$). A lower volume of contrast material resulted in lower attenuation.

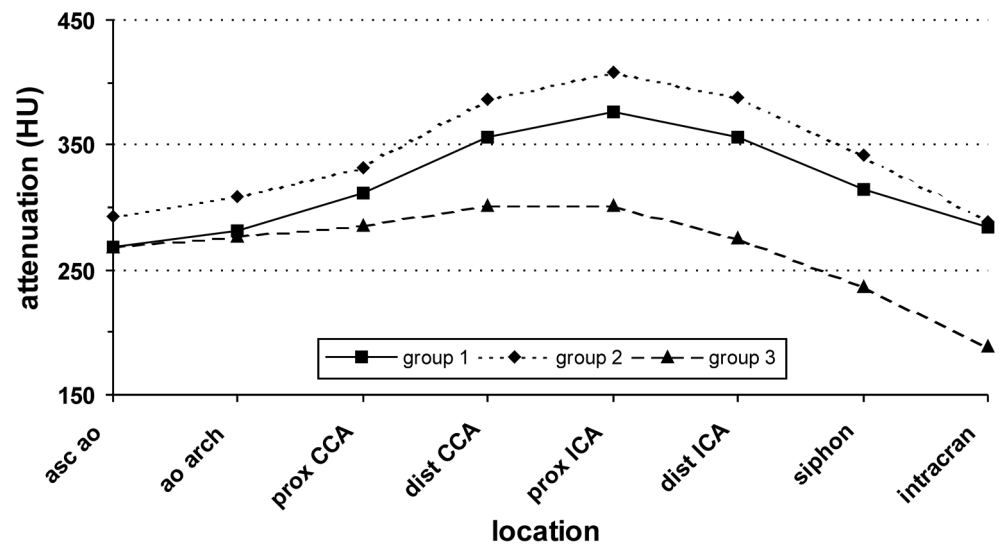


Fig. 4 Intraluminal attenuation in group 1 (80-mL contrast material, $n = 25$), group 2 (80-mL contrast material plus 40-mL saline, $n = 25$), and group 3 (60-mL contrast material plus 40-mL saline, $n = 25$) at different locations, from the ascending aorta to the circle of Willis. The maximum attenuation was reached in the proximal ICA in all three groups. The addition of a bolus chaser resulted in a higher attenuation at all locations, although no significant difference was reached, except for the aortic arch ($p < 0.05$). Group 3 had a lower attenuation at all locations, from the distal CCA to the intracranial arteries, in comparison with that in groups 1 and 2 ($p < 0.01$).

Table 4. Attenuation Measurements at Different Locations in Three Groups with Different Volumes of Contrast Material

Location	Group 1 (80-mL CM)	Group 2 (80-mL CM plus 40-mL BC)	Group 3 (60-mL CM plus 40-mL BC)	p Value		
				Group 1 vs 2	Group 2 vs 3	Group 1 vs 3
Ascending aorta (HU)	268 ± 34	292 ± 40	268 ± 48	NT	NT	NT
Aortic arch (HU) *	281 ± 36	309 ± 43	276 ± 46	< 0.05	< 0.05	NS
Proximal CCA (HU) †	311 ± 41	331 ± 52	286 ± 51	NS	< 0.01	NS
Distal CCA (HU) †	357 ± 53	386 ± 70	301 ± 77	NS	< 0.001	< 0.01
Proximal ICA (HU) †	376 ± 52	409 ± 82	301 ± 70	NS	< 0.001	< 0.001
Distal ICA (HU) †	356 ± 59	387 ± 83	275 ± 65	NS	< 0.001	< 0.001
Carotid siphon (HU) †	314 ± 53	342 ± 71	236 ± 57	NS	< 0.001	< 0.001
Intracranial ICA (HU) †	274 ± 67	289 ± 63	190 ± 44	NS	< 0.001	< 0.001

Data are the mean ± standard deviation. BC = bolus chaser, CM = contrast material, NS = not significant, NT = not tested

* Repeated-measures ANOVA, $p < 0.05$

† Repeated-measures ANOVA, $p < 0.01$

‡ Repeated-measures ANOVA, $p < 0.001$

Comparison of Locations

In all groups, the attenuation first increased to a maximum and then decreased during the course of the CT angiographic examination (Table 4, Fig 4). The maximum attenuation was reached in the proximal ICA in all three groups. The addition of a bolus chaser resulted in a higher attenuation at all locations, although no significant difference was reached except for the aortic arch ($p < 0.05$).

The group that received 60 mL of contrast material and 40 mL of bolus chaser had a lower attenuation ($p < 0.01$) at all locations, from the distal CCA to the intracranial arteries, in comparison to the group that received 80 mL of contrast material without 40 mL of bolus chaser and the group that received 80 mL of contrast material with 40 mL of bolus chaser (Table 4).

Relationship of Weight and Mean Attenuation

In the group that received 80 mL of contrast material, there was a weak, though almost significant, relationship between weight and the mean attenuation (slope, -1.2 ; $p = 0.06$; $R^2 = 0.16$). With the addition of a bolus chaser in groups 2 and 3, this relationship became stronger and more significant, with a slope of -4.4 and -2.6 ($p < 0.01$) and R^2 of 0.56 and 0.42, respectively (Fig 5).

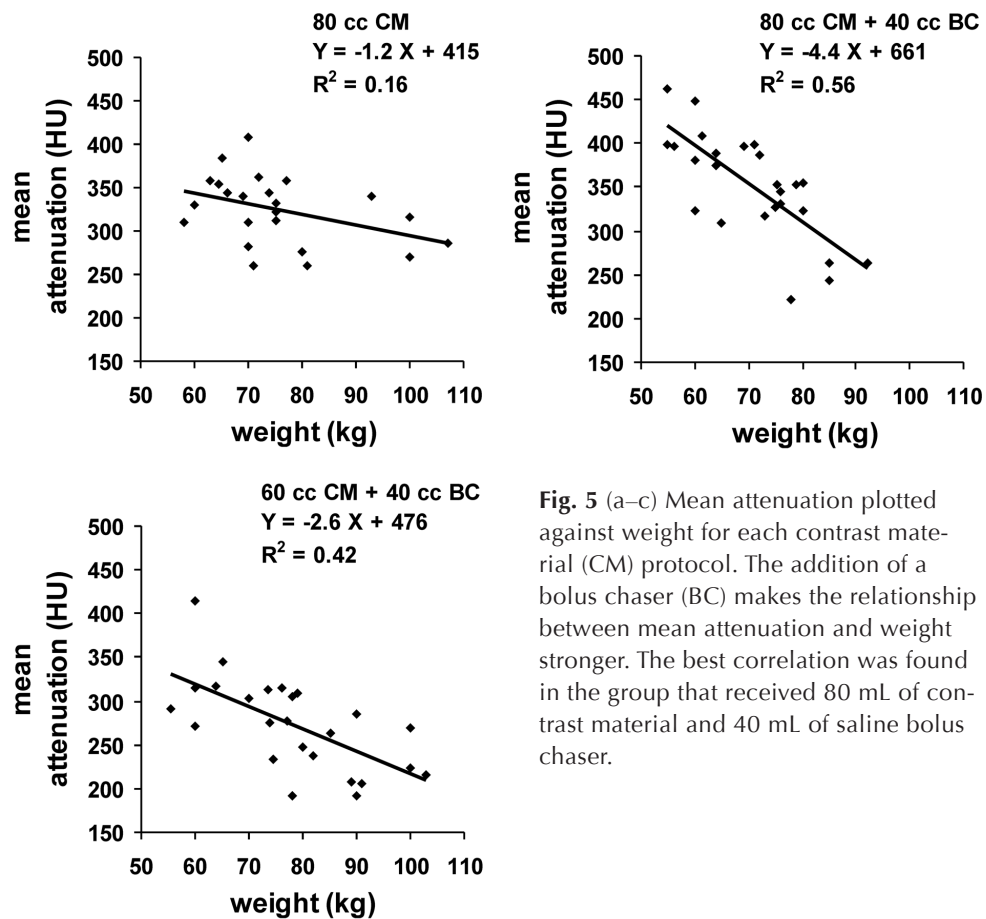


Fig. 5 (a–c) Mean attenuation plotted against weight for each contrast material (CM) protocol. The addition of a bolus chaser (BC) makes the relationship between mean attenuation and weight stronger. The best correlation was found in the group that received 80 mL of contrast material and 40 mL of saline bolus chaser.

In the group that received 80 mL of contrast material and 40 mL of saline, a significant difference was found in the mean attenuation between patients weighing 75 kg or less and those weighing more than 75 kg ($381 \text{ HU} \pm 45$ vs $305 \text{ HU} \pm 52$, $p < 0.001$). In the group that received 60 mL of contrast material and 40 mL of saline, a significant difference was found in the mean attenuation between patients weighing 75 kg or less and those weighing more than 75 kg ($308 \text{ HU} \pm 49$ vs $250 \text{ HU} \pm 43$, $p < 0.01$). There was no significant difference in the mean attenuation between patients weighing 75 kg or less who received 60 mL of contrast material and patients weighing more than 75 kg who received 80 mL of contrast material ($p = 0.90$) (Fig 6).

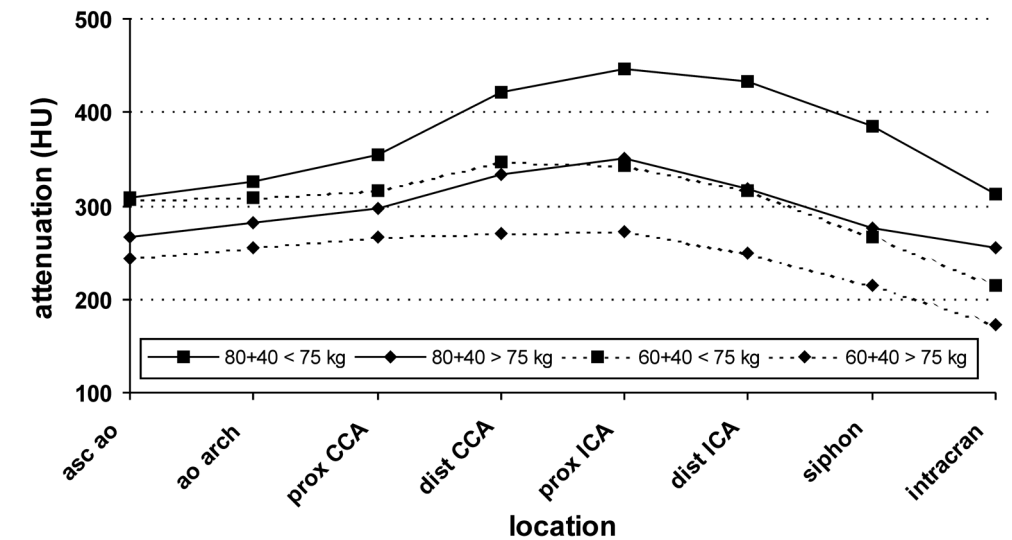


Fig. 6 Intraluminal attenuation in the group that received 80 mL of contrast material and 40 mL of saline bolus chaser and the patient group that received 60 mL of contrast material and 40 mL of saline bolus chaser at different locations, from the ascending aorta (asc ao) to the circle of Willis. Subdivision was made between patients weighing 75 kg or less and patients weighing more than 75 kg. There is no significant difference in the mean attenuation between patients weighing 75 kg or less and who received 60 mL of contrast material and patients weighing more than 75 kg and who received 80 mL of contrast material ($p = 0.9$). ao arch = aortic arch, prox CCA = proximal CCA, dist CCA = distal CCA, prox ICA = proximal ICA, dist ICA = distal ICA, siphon = carotid siphon, intracran = intracranial part of ICA.

Discussion

Multidetector row CT scanners allow performance of CT angiography of the carotid arteries with increased coverage from the aortic arch to the circle of Willis, improved spatial resolution, and shorter acquisition times. The short acquisition time may lead to lower doses of contrast material. It has been reported^{16–20} that a saline bolus chaser after the injection of contrast material may further reduce the volume of contrast material without a subsequent decrease in arterial attenuation. Yet, to our knowledge, no studies have been performed to determine the optimal contrast material administration protocol for CT angiography of the carotid arteries at multidetector row CT.

When the left carotid artery was compared with the right carotid artery, a slightly higher mean attenuation and a shorter time to maximum attenuation were found on the left side. This may be caused by the way the time-attenuation curves were assessed. The time scale does not correspond to the length of the path the contrast material has passed through the vessel: The contrast material reaches the left ca-

rotid artery, which originates directly from the aortic arch, earlier than the right carotid artery, where the contrast material has to follow a longer path through the brachiocephalic trunk to reach the right carotid artery.

Injection of 80 mL of contrast material resulted in an attenuation above 200 HU in all but two measurements. Comparison of the mean time-attenuation curve of 80 mL of contrast material with and without a saline bolus chaser demonstrated higher mean and maximum attenuations along the carotid arteries, although the differences were not significant.

Hopper et al¹⁹ found higher attenuation in the ascending aorta with the addition of a 50-mL saline bolus chaser to 75 or 100 mL of contrast material, although the differences were not significant. The results from their study can be explained by the lack of the analysis of a time-attenuation curve of the aorta, which allows the assessment of maximum and mean attenuations. However, Irie et al¹⁶, who did perform such an analysis, failed to demonstrate a significant increase in the maximum attenuation with the application of a saline bolus chaser. Failure to demonstrate a significant effect of a bolus chaser on attenuation in these two studies and in our study may be explained by the small number of patients ($n = 15-25$) in the groups with different contrast material protocols.

On the basis of the attenuation curves of 80 mL of contrast material with and without a saline bolus chaser, we analyzed whether a decrease in the volume of contrast material was possible without compromising the attenuation. However, 60 mL of contrast material followed by 40 mL of saline bolus chaser resulted in a significantly lower mean and maximum attenuation in comparison to those with 80 mL of contrast material with and without saline bolus chaser.

Previous studies have not revealed such a decrease in attenuation with the replacement of contrast material by a saline bolus chaser. Haage et al¹⁸ found the same attenuation in the ascending aorta by comparing 60 mL of contrast material and 30-mL saline bolus chaser with 75 mL of contrast material alone (240 HU for both). In another study, almost the same attenuation in the ascending aorta was observed by using 75 mL of contrast material with 50-mL saline bolus chaser and 125 mL of contrast material alone (254 vs 225 HU, respectively).¹⁹ In both studies, the attenuation was measured in one region instead of several levels. Irie et al¹⁶, who assessed the time-attenuation curve in the aorta, found the same maximum attenuation with 75 mL of contrast material alone and with 63 mL of contrast material and a 25-mL saline bolus chaser. Cademartiri et al²⁰ found the same mean and maximum attenuations in a time-attenuation curve in the descending aorta with 140 mL of contrast material alone and with 100 mL of contrast material followed by a 40-mL saline bolus chaser. The discrepancy of our results could partly be explained by the difference, although not significant, in weight between the groups in our study, especially between groups 2 and 3. However, adjustment for weight in a regression model still showed a difference in mean and maximum attenuations between group 3 and groups 1 and 2.

Patient weight is inversely correlated with arterial enhancement.^{17,21-23} Our study revealed only a relationship between weight and mean attenuation in the groups with a bolus chaser. The best correlation was found in the group that received 80 mL of contrast material and a 40-mL saline bolus chaser. This could be explained by a better circulation of the contrast material with the addition of a bolus chaser to the contrast material protocol. On the basis of our results, a consideration could be made to adjust for weight; for example, use 60 mL of contrast material followed by a 40-mL saline bolus chaser in patients weighing 75 kg or less and use 80 mL of contrast material followed by a 40-mL saline bolus chaser in patients weighing more than 75 kg to establish the mean and minimum attenuations of more than 250 and 200 HU, respectively.

The search for the lowest volume of contrast material necessary for optimal analysis has several motives. First, the high cost of contrast material forces the radiologist to search for ways to further decrease contrast material volume. However, one should realize that replacement of contrast material by saline necessitates the purchase of a dual-head power injector or an additional single-head power injector and the extra use of saline, a T connector, and a syringe. Schoellnast et al²⁴ showed that by taking these extra costs into account there is still a cost reduction. Second, the risk of nephrotoxicity is related to the volume of contrast material, and decreasing the volume of contrast material may influence the risk of subsequent nephrotoxicity.²⁵⁻²⁷ Third, in patients with acute stroke, CT angiography of the carotid artery has been combined with CT perfusion of the brain, which required an additional injection of 50 mL of contrast material.^{28,29} In such studies, the total volume of contrast material should be restricted to what is necessary for optimal analysis. Finally, it may be possible that, in comparison to what is commonly thought, the best contrast material protocol is not the one with the highest intraluminal attenuation. Which attenuation in CT angiography allows the best evaluation of the presence and severity of vessel disease is not well studied. Attenuation levels obtained with 60 mL of contrast material followed by 40 mL of saline may be high enough for an excellent interpretation of the vessel, owing to a better contrast with calcifications in the vessel wall or atherosclerotic plaque. This may have an effect on both visual analysis and semiquantitative analysis of the vessel dimensions.

Our study had several limitations. First, the patients were not randomly assigned to the groups. However, baseline characteristics were not substantially different except for the injection side. The higher frequency of the left-sided injection in group 3 may have led to a lower mean attenuation, because the longer path of the contrast material through the venous system may have diluted the contrast material. Second, the groups may be too small to lead to a significant result. Third, we analyzed attenuation from the aortic arch to the circle of Willis. Ideally, a single-level dynamic CT study will result in a more precise analysis of the contrast media dynamics.³⁰ Such a study will cause extra radiation exposure to the patients, and we were reluctant to do this. Nevertheless, in clinical practice we are dealing with attenuation along the supra-aortic arteries, which reflects the way contrast material passes through the vessels.

In conclusion, of the protocols we tested the integration of a saline bolus chaser in the contrast material protocol for evaluation of the carotid artery with 16-detector row CT leads to optimization of the attenuation but does not allow decrease in contrast material volume from 80 to 60 mL in all patients. Future studies may focus on a less strong reduction in contrast material volume, weight-adjusted dose of contrast material, or adjustment of the scanning protocol; increase in pitch will shift the maximum attenuation distally.

Acknowledgment:

We thank Theo Stijnen, PhD, professor of biostatistics, Department of Epidemiology and Biostatistics, Erasmus MC, University Medical Center, Rotterdam, for his help with the statistical analysis.

References

1. Beneficial effect of carotid endarterectomy in symptomatic patients with high-grade carotid stenosis. North American Symptomatic Carotid Endarterectomy Trial Collaborators. *N Engl J Med* 1991; 325:445–453.
2. MRC European Carotid Surgery Trial: interim results for symptomatic patients with severe (70–99%) or with mild (0–29%) carotid stenosis. European Carotid Surgery Trialists' Collaborative Group. *Lancet* 1991; 337:1235–1243.
3. Nederkoorn PJ, Mali WP, Eikelboom BC, et al. Preoperative diagnosis of carotid artery stenosis: accuracy of noninvasive testing. *Stroke* 2002; 33:2003–2008.
4. Napel S, Marks MP, Rubin GD, et al. CT angiography with spiral CT and maximum intensity projection. *Radiology* 1992; 185:607–610.
5. Katz DA, Marks MP, Napel SA, Bracci PM, Roberts SL. Circle of Willis: evaluation with spiral CT angiography, MR angiography, and conventional angiography. *Radiology* 1995; 195:445–449.
6. Hollingworth W, Nathens AB, Kanne JP, et al. The diagnostic accuracy of computed tomography angiography for traumatic or atherosclerotic lesions of the carotid and vertebral arteries: a systematic review. *Eur J Radiol* 2003; 48:88–102.
7. Dillon EH, van Leeuwen MS, Fernandez MA, Eikelboom BC, Mali WP. CT angiography: application to the evaluation of carotid artery stenosis. *Radiology* 1993; 189:211–219.
8. Cumming MJ, Morrow IM. Carotid artery stenosis: a prospective comparison of CT angiography and conventional angiography. *Am J Roentgenol* 1994; 163:517–523.
9. Link J, Brossmann J, Grabener M, et al. Spiral CT angiography and selective digital subtraction angiography of internal carotid artery stenosis. *Am J Neuroradiol* 1996; 17:89–94.
10. Marcus CD, Ladam-Marcus VJ, Bigot JL, Clement C, Baehrel B, Menanteau BP. Carotid arterial stenosis: evaluation at CT angiography with the volume-rendering technique. *Radiology* 1999; 211:775–780.
11. Leclerc X, Godefroy O, Lucas C, et al. Internal carotid arterial stenosis: CT angiography with volume rendering. *Radiology* 1999; 210:673–682.
12. Lell M, Wildberger JE, Heuschmid M, et al. CT-angiographie der A. carotis: erste erfahrungen mit einem 16-schicht-spiral-CT. *Rofo* 2002; 174:1165–1169.
13. Ertl-Wagner B, Hoffmann RT, Bruning R, Dichgans M, Reiser MF. Supraaortale gefassdiagnostik mit dem 16-zeilen-multidetektor-spiral-CT: untersuchungsprotokoll und erste erfahrungen. *Radiologe* 2002; 42:728–732.
14. Fleischmann D. Present and future trends in multiple detector-row CT applications: CT angiography. *Eur Radiol* 2002; 12(suppl 2): S11–S15.
15. Fleischmann D. Use of high concentration contrast media: principles and rationale - vascular district. *Eur J Radiol* 2003; 45(suppl 1): S88–S93.
16. Irie T, Kajitani M, Yamaguchi M, Itai Y. Contrast-enhanced CT with saline flush technique using two automated injectors: how much contrast medium does it save? *J Comput Assist Tomogr* 2002; 26:287–291.
17. Cademartiri F, van der Lugt A, Luccichenti G, Pavone P, Krestin GP. Parameters affecting bolus geometry in CTA: a review. *J Comput Assist Tomogr* 2002; 26:598–607.

18. Haage P, Schmitz-Rode T, Hubner D, Piroth W, Gunther RW. Reduction of contrast material dose and artifacts by a saline flush using a double power injector in helical CT of the thorax. *Am J Roentgenol* 2000; 174:1049–1053.
19. Hopper KD, Mosher TJ, Kasales CJ, Ten-Have TR, Tully DA, Weaver JS. Thoracic spiral CT: delivery of contrast material pushed with injectable saline solution in a power injector. *Radiology* 1997; 205:269–271.
20. Cademartiri F, Mollet N, van der Lugt A, et al. Non-invasive 16-row multislice CT coronary angiography: usefulness of saline chaser. *Eur Radiol* 2004; 14:178–183.
21. Platt JF, Reige KA, Ellis JH. Aortic enhancement during abdominal CT angiography: correlation with test injections, flow rates, and patient demographics. *Am J Roentgenol* 1999; 172:53–56.
22. Fleischmann D, Rubin GD, Bankier AA, Hittmair K. Improved uniformity of aortic enhancement with customized contrast medium injection protocols at CT angiography. *Radiology* 2000; 214:363–371.
23. Bae KT, Heiken JP, Brink JA. Aortic and hepatic contrast medium enhancement at CT. I. Prediction with a computer model. *Radiology* 1998; 207:647–655.
24. Schoellnast H, Tillich M, Deutschmann HA, et al. Abdominal multidetector row computed tomography: reduction of cost and contrast material dose using saline flush. *J Comput Assist Tomogr* 2003; 27:847–853.
25. Rudnick MR, Goldfarb S, Wexler L, et al. Nephrotoxicity of ionic and nonionic contrast media in 1196 patients: a randomized trial. The Iohexol Cooperative Study. *Kidney Int* 1995; 47:254–261.
26. Manske CL, Sprafka JM, Strony JT, Wang Y. Contrast nephropathy in azotemic diabetic patients undergoing coronary angiography. *Am J Med* 1990; 89:615–620.
27. Rosovsky MA, Rusinek H, Berenstein A, Basak S, Setton A, Nelson PK. High-dose administration of nonionic contrast media: a retrospective review. *Radiology* 1996; 200:119–122.
28. Smith WS, Roberts HC, Chuang NA, et al. Safety and feasibility of a CT protocol for acute stroke: combined CT, CT angiography, and CT perfusion imaging in 53 consecutive patients. *Am J Neuroradiol* 2003; 24:688–690.
29. Nabavi DG, Kloska SP, Nam EM, et al. MOSAIC: Multimodal Stroke Assessment Using Computed Tomography—novel diagnostic approach for the prediction of infarction size and clinical outcome. *Stroke* 2002; 33:2819–2826.
30. Bae KT, Heiken JP, Brink JA. Aortic and hepatic contrast medium enhancement at CT. II. Effect of reduced cardiac output in a porcine model. *Radiology* 1998; 207:657–662.

Chapter 3

Optimization of CT Angiography of
the Carotid Artery with a 16-MDCT
Scanner: Craniocaudal Scan Direction
Reduces Contrast Material-Related
Perivenous Artifacts

Optimization of CT angiography of the carotid artery with a 16-MDCT scanner: Craniocaudal scan direction reduces contrast material-related perivenous artifacts

Cécile de Monyé, MD
 Thomas T. de Weert, MD
 William Zaalberg, MSc
 Filippo Cademartiri, MD, PhD
 Dorine A. M. Siepman, MD
 Diederik W. J. Dippel, MD, PhD
 Aad van der Lugt, MD, PhD

AJR 2006; 186:1737–1745

Abstract

Objective: The objective of our study was to compare the effect of a caudocranial scan direction versus a craniocaudal scan direction on arterial enhancement and perivenous artifacts in 16-MDCT angiography of the supra-aortic arteries.

Subjects and methods: Eighty consecutive patients (51 men; mean age, 62 years; age range, 28–89 years) underwent scanning in the caudocranial direction (group 1; $n = 40$) or the craniocaudal direction (group 2; $n = 40$). All patients received 80 mL of contrast material followed by a 40-mL saline chaser bolus, both administered IV at 4 mL/sec. Bolus tracking was used. Attenuation inside the arterial lumen was measured at intervals of 1 sec throughout the data set. Attenuation in the superior vena cava (SVC) was measured. Contrast material-related perivenous artifacts were graded on a scale of 0–3 (none to extensive).

Results: Attenuation in the ascending aorta, carotid bifurcation, and intracranial arteries was slightly lower in group 2 versus group 1 ($231 \text{ HU} \pm 64$, $348 \text{ HU} \pm 52$, and $258 \text{ HU} \pm 48$ vs $282 \text{ HU} \pm 43$, $381 \text{ HU} \pm 73$, and $291 \text{ HU} \pm 77$, respectively; $p < 0.05$). Maximum and mean arterial attenuations were slightly lower in group 2 versus group 1 ($369 \text{ HU} \pm 58$ and $303 \text{ HU} \pm 48$ vs $401 \text{ HU} \pm 71$ and $334 \text{ HU} \pm 58$; $p < 0.05$). Attenuation in the SVC was much lower in group 2 versus group 1 ($169 \text{ HU} \pm 39$ vs $783 \text{ HU} \pm 330$; $p < 0.001$). Mean streak artifact score was much lower in group 2 versus group 1 (1.3 ± 0.9 vs 2.5 ± 0.6 ; $p < 0.001$).

Conclusion: Use of a craniocaudal scan direction results in slightly lower attenuation of the carotid artery and much lower attenuation of the SVC. Streak artifacts are significantly reduced. This technique allows better evaluation of the ascending aorta and supra-aortic arteries.

Introduction

Acute ischemic neurologic symptoms are related to small-vessel disease of the intracranial perforating arteries, thromboembolism from atherosclerotic disease in the supra-aortic arteries, and cardiac embolism.¹ The most common source of thromboembolism is atherosclerotic disease of the carotid bifurcation. However, atherosclerotic lesions in the aorta, the origin of the supra-aortic arteries, the common carotid artery (CCA), the internal carotid artery (ICA) distal to the bifurcation, and the vertebrobasilar circulation can cause transient ischemic attack or ischemic stroke due to thromboembolism.^{2,3} In the evaluation of patients with cerebrovascular disease, complete vascular imaging from the aorta to the circle of Willis must be performed before therapeutic decision making can be undertaken.

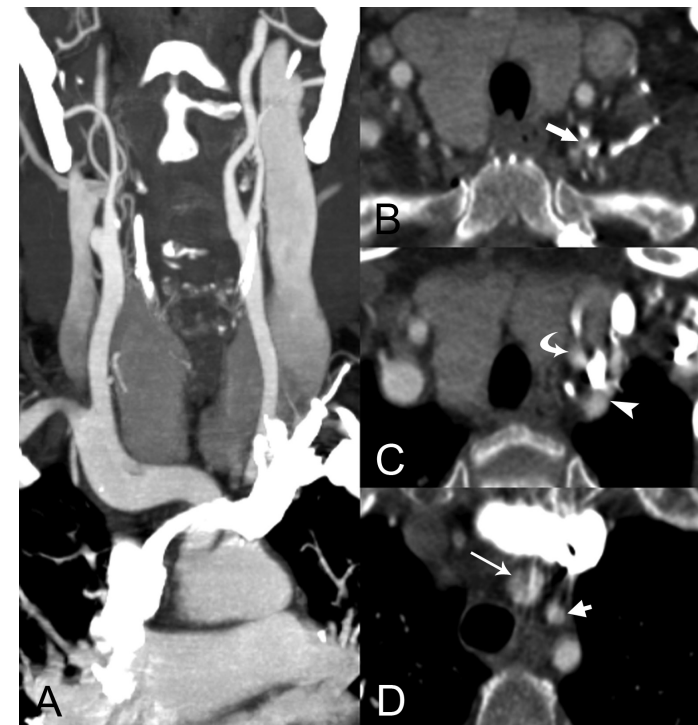


Fig. 1 CT angiograms of supra-aortic arteries in 74-year-old woman scanned in caudocranial direction with left-sided injection of contrast material.

A, Coronal maximum intensity projection (15 mm). High-density contrast material in left subclavian vein and reflux of contrast material in neck veins give rise to artifacts over origin of supra-aortic vessels.

B, Axial image at level of origin of left vertebral artery (arrow).

C, Axial image at level of proximal part of left common carotid artery (arrow) and left subclavian artery (arrowhead).

D, Axial image at level of first 1 cm of brachiocephalic trunk (long arrow) and left common carotid artery (short arrow). Evaluation of atherosclerotic disease is hampered by streak artifacts.

With the introduction of MDCT, particularly 16-MDCT scanners, CT angiography (CTA) has become an attractive diagnostic method in the care of patients with cerebrovascular symptoms.⁴ With bolus tracking, CTA scanning can be optimally synchronized with the passage of contrast material in the arteries.⁵ The CTA scanning usually starts before the injection of contrast material ends. With this method, the presence of undiluted contrast material in the subclavian vein, brachiocephalic vein, and superior vena cava (SVC) produces artifacts that project over the ascending aorta and the origin of the supra-aortic arteries.^{6,7} Such artifacts can obscure adjacent structures and thus hide or suggest stenosis or occlusion of the proximal supra-aortic arteries (Fig 1). Addition of a chaser bolus to the main contrast bolus may reduce the frequency of these artifacts by clearing the veins of contrast material. However, the timing of the CTA scan is not altered by the addition of a chaser bolus, and artifacts do occur. Use of a craniocaudal scan direction, opposite to the direction of blood flow, may reduce the number of artifacts caused by delayed scanning of the apex of the thorax (Fig 2).

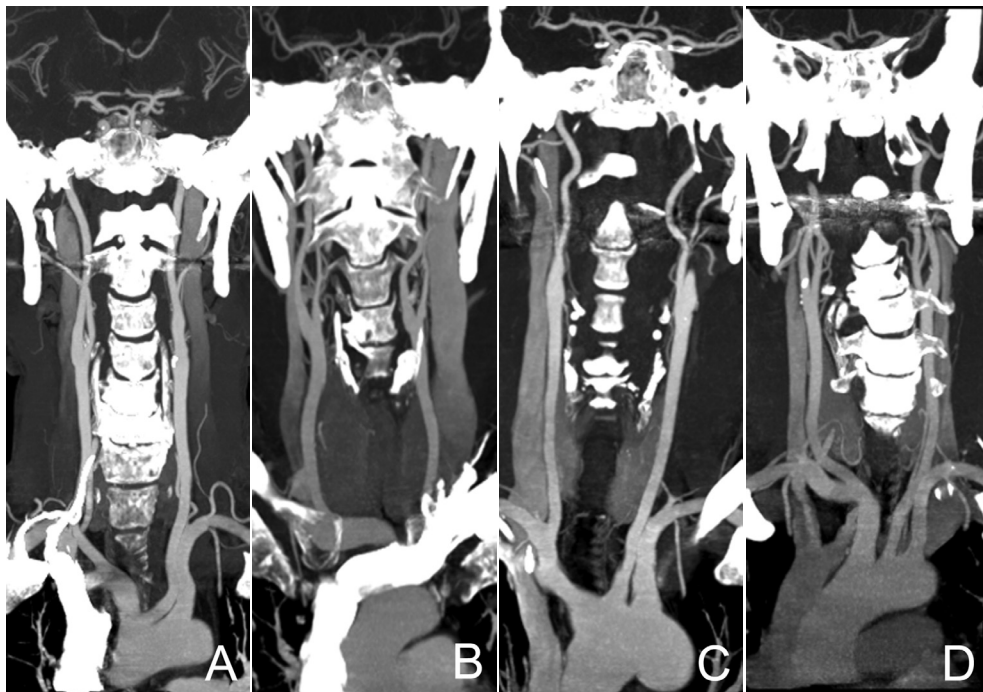


Fig. 2 CT angiograms of supra-aortic arteries. Four maximum intensity projections (30 mm) in coronal plane in four patients.

A and B, CT angiographic scans in caudocranial direction with right-sided (72-year-old man, A) and left-sided (74-year-old woman, B) injection of contrast material. Very high density of contrast material in subclavian vein and superior vena cava hides origin of supra-aortic arteries.

C and D, CT angiographic scans in craniocaudal direction with right-sided (48-year-old man, C) and left-sided (54-year-old man, D) injection of contrast material. High density of contrast material is not left in veins, and all arteries are clearly depicted.

The purpose of this study was to compare the effects of a caudocranial scan direction versus a craniocaudal scan direction on enhancement of the carotid artery and on the presence of perivenous artifacts in CTA with a 16-MDCT scanner.

Methods

Study Population

Between November 2002 and August 2003, 80 consecutive patients (51 men and 29 women; mean age, 62 years; age range, 28–89 years) who underwent CTA of the carotid artery were enrolled in the study. The indication for CTA was suspected atherosclerotic disease of the carotid or vertebrobasilar vascular system in patients who had had a transient ischemic attack or minor ischemic stroke. Exclusion criteria were previous allergic reaction to iodine contrast medium, renal insufficiency (serum creatinine concentration >100 mmol/L), pregnancy, and age less than 18 years. Patients with occlusion of the carotid artery also were excluded. The institutional review board approved the study, and patients gave informed consent in writing. Each patient was allocated to one of two groups with different scan protocols. The first 40 patients (group 1) underwent scanning in the caudal to cranial direction, the second 40 patients (group 2) underwent scanning in the cranial to caudal direction. Age, sex, and body weight were recorded for each patient.

Scan Protocol

The patients underwent CTA of the carotid artery with a 16-MDCT scanner (Sensation 16, Siemens Medical Solutions). Patients were positioned supine on the CT table with the arms along the chest. A lateral scout view including the thorax, neck, and skull was acquired. The CTA scan range reached from the ascending aorta to the intracranial blood vessels (2 cm above the sella turcica). Scan parameters were as follows: number of detectors, 16; individual detector width, 0.75 mm; table feed per rotation, 12 mm (pitch of 1); gantry rotation time, 0.5 sec; 120 kV; 180 mAs; and scanning time, 10–14 sec, depending on patient's size and anatomic features. The entire examination took approximately 15 min.

Contrast material (iodixanol 320 mg I/mL [Visipaque, Amersham Health]) was injected with a double-head power injector (Stellant, Medrad) through an 18- to 20-gauge IV cannula (depending on the size of the vein) in an antecubital vein. The right antecubital vein was preferentially used because it provides the shortest path for contrast material through the venous system and therefore the least dilution. When venous access could not be achieved on the right side, the left antecubital vein was used. The saline chaser bolus was injected through the second head of the power injector immediately after injection of contrast material was completed. All patients received 80 mL of contrast material and a 40-mL saline chaser bolus, both at an injection rate of 4 mL/sec.

Synchronization between the passage of contrast material and data acquisition was achieved with real-time bolus tracking. The arrival of the injected contrast material was monitored in real time with a series of dynamic axial low-dose monitoring scans (120 kV, 20–40 mAs) at the level of the ascending aorta at intervals of 1 sec. The monitoring sequence started 5 sec after initiation of administration of contrast material. The CTA scan was triggered automatically by means of a threshold measured in a region of interest (ROI) set in the ascending aorta. The size of the ROI in the ascending aorta for the bolus triggering was adjusted to the size and composition of the ascending aorta but was always greater than 5 mm in diameter. The trigger threshold was set at an increase in attenuation of 75 HU above baseline attenuation (≈ 150 HU in absolute HU value). When the threshold was reached, the table was moved to the start position while the patient was instructed not to swallow. Breath-hold instructions were not given to the patient. CTA data acquisition was started automatically 4 sec (caudocranial scan direction) or 6 sec (craniocaudal scan direction) after the trigger threshold was reached. All bolus timing procedures and CTA scans were successfully completed. No significant adverse reactions to contrast material or other side effects occurred.

Data Collection and Analysis

Images were reconstructed with an effective slice width of 1 mm, reconstruction interval of 0.6 mm, field of view of 100 mm, and convolution kernel B30f (medium smooth). The images were transferred to a stand-alone workstation and evaluated with dedicated analysis software (Leonardo, Siemens Medical Solutions).

For each patient, site of injection and scan delay (in seconds) were recorded. Axial images were used for the attenuation measurements. On each 40th slice (1-sec interval), beginning with the most caudal slice, an ROI was drawn throughout the data sets in two regions: the ascending aorta to the right ICA and the ascending aorta to the left ICA. Measurements were recorded at the following locations: ascending aorta, aortic arch, proximal CCA (first two measurements in the CCA), distal CCA, proximal ICA (first two measurements in the ICA), distal ICA, carotid siphon, and intracranial part of the ICA. Measurements in the brachiocephalic trunk were considered measurements in the CCA.

Two observers measured and recorded all data. Attenuation was measured by drawing a circular ROI in the center of the vessel lumen. The ROI was drawn as large as the anatomic configuration of the lumen allowed in the axial slice. The mean value of the measurements on the left and the right side at each time point was calculated. Time-attenuation curves were generated for each patient, and mean, minimum, and maximum attenuations were assessed. Because attenuation greater than 200 HU was considered optimal, the number of measurements less than 200 HU was counted. The analysis resulted in one to three measurements per location depending on the size of the patient. For analysis of attenuation, the measurements obtained in these locations were averaged.

Contrast material-related perivenous artifacts were graded on a four-point scale adjusted from Rubin et al⁶ and Vogel et al⁸ (Fig 3). A score of 0 indicated no streak artifacts and clear anatomic detail; 1, minimal streak artifacts without notable obscuration of adjacent arteries; 2, moderate streak artifacts partially obscuring adjacent arteries; and 3, extensive streak artifacts completely obscuring adjacent arteries. The artifact score was assessed by two observers blinded to scan protocol. In case of a lack of congruence, consensus was reached. Attenuation in the SVC was measured in the most caudal slice. Reflux of contrast material in the veins of the neck was measured in centimeters on a coronal maximum-intensity-projection image.

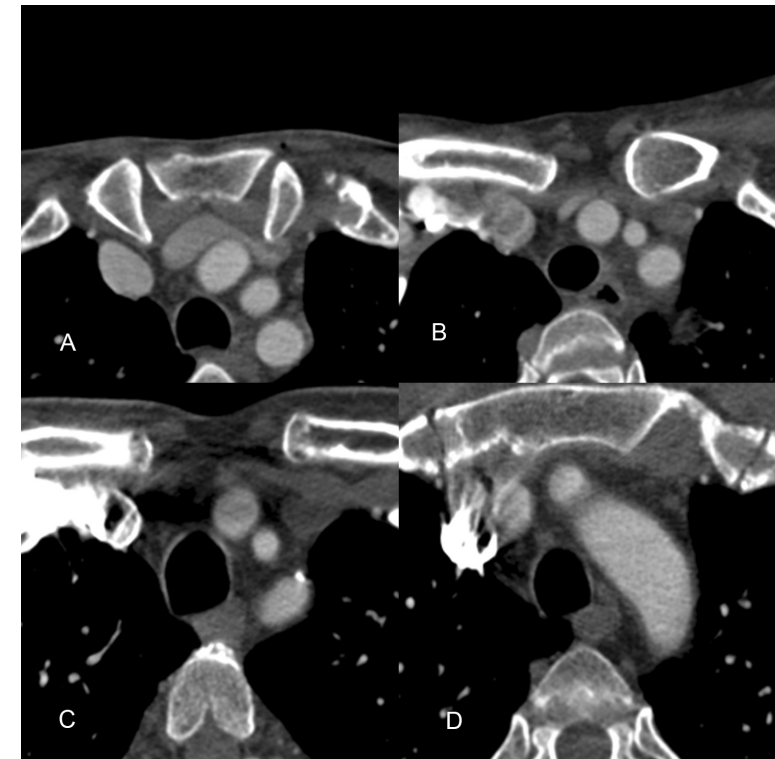


Fig. 3 Contrast material-related perivenous artifacts graded on four-point scale in four different patients.

- A**, Score of 0 indicates no streak artifacts and clear anatomic detail in 39-year-old man.
- B**, Score of 1 indicates minimal streak artifacts without notable obscuration of adjacent arteries in 40-year-old woman.
- C**, Score of 2 indicates moderate streak artifacts partially obscuring adjacent arteries in 59-year-old man.
- D**, Score of 3 indicates extensive streak artifacts completely obscuring adjacent arteries in 63-year-old man.

Statistical Analysis

Baseline characteristics, attenuation parameters, and artifact parameters in the two groups were compared using Student's *t*-test, chi-square test, or MannWhitney test. In the pair-wise comparison of attenuation parameters, a linear regression model was used to adjust for weight and age. The Spearman's rank correlation test was used for assessment of the relation between artifact parameters. The software used for statistical analysis was SPSS 11.5 (SPSS). A *p* value of < 0.05 was considered statistically significant.

Results

Patients and Procedures

Patient demographics were not significantly different in the two groups (Table 1). Scan delay was significantly higher in group 2 ($p < 0.01$) because of the extra 2 sec necessary after the threshold was reached for the table to move to a cranial start position in comparison with a caudal start position. After correction for those 2 sec, there was no significant difference in scan delay between the two groups.

Table 1. Patient and Scan Characteristics

Characteristic	Caudocranial Scan Direction (Group 1)	Craniocaudal Scan Direction (Group 2)
No. of patients	40	40
Sex (male/female)	26/14	25/15
Age (yr)		
Mean	65	59
Range	28-85	32-89
Weight (kg)		
Mean	74	75
Range	55-97	54-96
Injection side (right/left)	34/6	29/11
Scan delay (sec) ^a		
Mean	18	20
Range	14-22	14-30
No. of slices ^b		
Mean	532	500
Range	427-637	430-564

^aStudent's *t*-test: $p < 0.01$

^bStudent's *t*-test: $p < 0.001$

Caudocranial Scan Direction

Mean arterial attenuation for the caudocranial scan direction was $334 \text{ HU} \pm 58$ (Table 2). The minimum and maximum arterial attenuations were $255 \text{ HU} \pm 50$ and $401 \text{ HU} \pm 71$. Fifteen measurements in five of the 40 patients (513 measurements) had an attenuation less than 200 HU. These measurements were obtained in the ascending aorta ($n = 2$), aortic arch ($n = 2$), CCA ($n = 3$), ICA ($n = 1$), carotid siphon ($n = 2$), and intracranial arteries ($n = 5$).

Table 2: Attenuation Levels

Parameter	Attenuation (HU)		<i>p</i> ^a	<i>p</i> ^b After Adjustment for Age and Weight
	Caudocranial scan direction (Group 1)	Craniocaudal scan direction (Group 2)		
Mean	334 ± 58	303 ± 48	< 0.05	NS
Maximum	401 ± 71	369 ± 58	< 0.05	NS
Minimum	255 ± 50	212 ± 49	< 0.001	< 0.01

NS = not significant

^aStudent's *t*-test

^bMultiple linear regression

Craniocaudal Scan Direction

The mean arterial attenuation per patient was $303 \text{ HU} \pm 48$ (Table 2). The minimum and maximum arterial attenuations per patient were $212 \text{ HU} \pm 49$ and $369 \text{ HU} \pm 58$. Sixty-nine of the measurements in 16 of the 40 patients (493 measurements) had an attenuation less than 200 HU. These measurements were obtained in the ascending aorta ($n = 23$), aortic arch ($n = 12$), CCA ($n = 15$), ICA ($n = 8$), carotid siphon ($n = 5$), and intracranial arteries ($n = 6$).

Comparison of Attenuation Curves

Group 2, in whom the craniocaudal scan direction was used, had lower mean, maximum, and minimum attenuations ($p < 0.05$) than group 1, in whom the caudocranial scan direction was used (Tables 2 and 3, Figs 4 and 5). After adjustment for age and weight, no significant difference was found in mean ($p = 0.07$) or maximum ($p = 0.26$) attenuation. Minimum attenuation remained significantly different ($p < 0.01$). In both patient groups, maximum attenuation was reached in the proximal ICA.

The craniocaudal scan direction resulted in significantly lower attenuation in all locations ($p < 0.05$), except for the proximal CCA ($p = 0.39$). After adjustment for age and weight, no significant difference was found for the aortic arch ($p = 0.07$),

proximal CCA ($p = 0.87$), distal CCA ($p = 0.17$), proximal ICA ($p = 0.21$), or distal ICA ($p = 0.16$). Attenuation in the ascending aorta, carotid siphon, and intracranial arteries remained significantly different ($p < 0.05$).

TABLE 3: Attenuation by Location

Location	Mean Attenuation \pm SD (HU)		p^a	p^b After Adjustment for Age and Weight
	Caudocranial Scan Direction (Group 1)	Craniocaudal Scan Direction (Group 2)		
Ascending aorta	282 \pm 43	231 \pm 64	<0.001	<0.01
Aortic arch	293 \pm 44	259 \pm 62	<0.01	NS
Proximal CCA	310 \pm 52	299 \pm 64	NS	NS
Distal CCA	363 \pm 65	334 \pm 59	<0.05	NS
Proximal ICA	381 \pm 73	348 \pm 52	<0.05	NS
Distal ICA	368 \pm 75	331 \pm 50	<0.05	NS
Carotid siphon	333 \pm 71	288 \pm 46	<0.01	<0.01
Intracranial ICA	291 \pm 77	258 \pm 48	<0.05	<0.05

NS = not significant, CCA = common carotid artery, ICA = internal carotid artery

^aStudent's *t*-test

^bMultiple linear regression

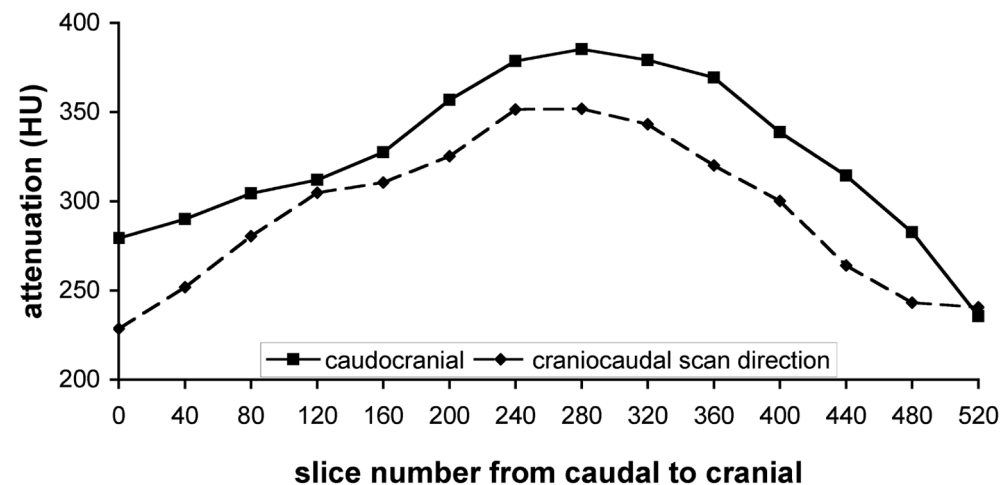


Fig. 4 Time-attenuation curves show intraluminal attenuation at slice number from caudal to cranial. Slightly lower attenuation is evident for craniocaudal scan direction in comparison with caudocranial scan direction.

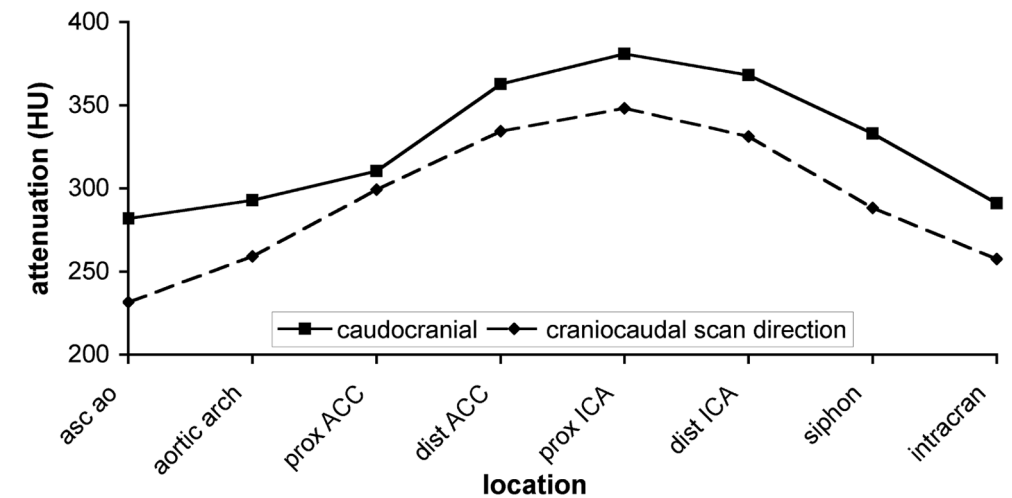


Fig. 5 Intraluminal attenuation of group 1 (caudocranial scan direction) and group 2 (craniocaudal scan direction) at different locations from ascending aorta (asc ao) to circle of Willis. Maximum attenuation was reached in proximal internal carotid artery (ICA) in both groups. Prox = proximal, CCA = common carotid artery, Dist = distal, Intracran = intracranial arteries.

Comparison of Artifacts

Attenuation in the SVC was much higher in group 1 (caudocranial) than in group 2 (craniocaudal): 782 HU \pm 330 (range, 183–2,083 HU) and 169 HU \pm 39 (range, 102–288 HU) ($p < 0.001$) (Table 4). The mean artifact scores were 2.5 \pm 0.6 and 1.3 \pm 0.9 for groups 1 and 2, respectively ($p < 0.001$). All but one of the patients in group 1 had an artifact score of 2 or more. Extensive streak artifacts completely obscuring adjacent arteries (score of 3) were seen in 21 (53%) of the patients in group 1 and in three (8%) of the patients in group 2. Reflux of contrast material in the neck veins measured 2.9 cm \pm 2.4 (range, 0–14.4 cm) and 1.2 cm \pm 1.5 (range, 0–5.1 cm) in groups 1 and 2 ($p < 0.001$). Reflux of contrast material in the neck veins measuring more than 2 cm was seen in group 1 in 24 (60%) of the patients and in group 2 in 11 (28%) of the patients ($p < 0.001$).

Table 4: Attenuation in Relation to Artifacts

Parameter	Mean \pm SD		p
	Caudocranial Scan Direction (Group 1)	Craniocaudal Scan Direction (Group 2)	
Attenuation of superior vena cava (HU)	782 \pm 330	169 \pm 39	<0.001
Streak artifact score	2.5 \pm 0.6	1.3 \pm 0.9	<0.001
Neck vein reflux (cm)	2.9 \pm 2.4	1.2 \pm 1.5	<0.001

Comparison of Left and Right Injection Sides

In group 2 (craniocaudal scan direction) there was more reflux and a higher artifact score with left-sided injection than with right-sided injection, although the difference was significant only for reflux ($p < 0.01$) and almost significant for artifact score ($p = 0.08$) (Table 5). Attenuation of the SVC was higher in patients who received a right-sided injection, although the difference was not significant ($p = 0.19$).

Table 5: Artifact Parameters According to Injection Side

Parameter	Mean \pm SD		<i>p</i>
	Left Injection (n=17)	Right Injection (n=63)	
Caudocranial scan direction (group 1)			
SVC (HU)	732 \pm 265	791 \pm 343	NS
Artifact score	2.7 \pm 0.5	2.4 \pm 0.7	NS
Reflux (cm)	2.9 \pm 1.6	2.9 \pm 2.6	NS
Craniocaudal scan direction (group 2)			
SVC (HU)	167 \pm 56	170 \pm 32	NS
Artifact score	1.7 \pm 1.0	1.2 \pm 0.8	NS
Reflux (cm)	2.2 \pm 1.9	0.8 \pm 1.1	<0.01

SVC = superior vena cava, NS = not significant

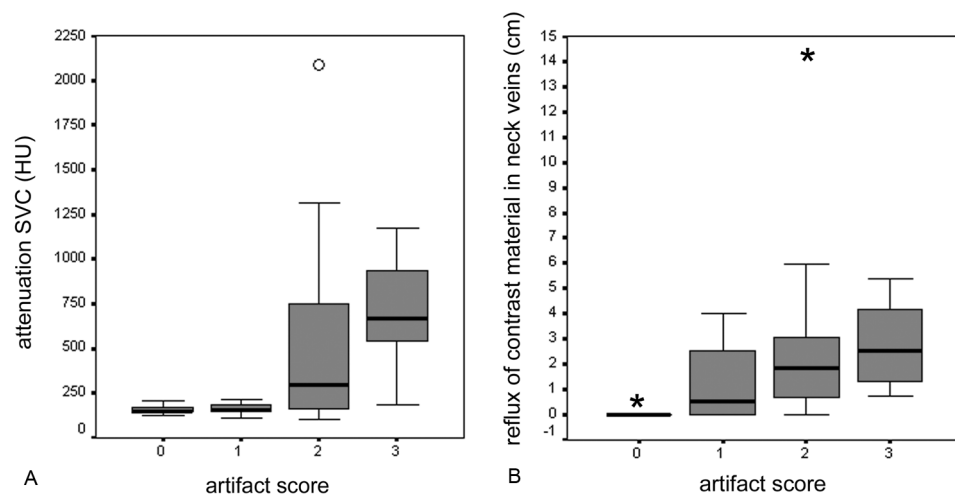


Fig. 6 Box and whisker plots of attenuation in superior vena cava (SVC) and of reflux of contrast material in neck veins according to artifact score.

A, Plot shows clear cutoff point at ± 200 HU attenuation of SVC. Above this level artifacts interfered with evaluation of arteries. Circle indicates outlier.

B, Plot shows greater amount of reflux is associated with higher artifact score. Stars indicate extremes.

Relationships Among Artifact Parameters

There was a significant relation between attenuation of the SVC and artifact score (Spearman's $r = 0.62$, $p < 0.001$) (Fig. 6). A clear cutoff point was seen at an attenuation of the SVC of ± 200 HU. Above this level, artifacts interfered with evaluation of the arteries. There was also a significant relation between reflux in the neck veins and artifact score (Spearman's $r = 0.52$, $p < 0.001$).

Discussion

Artifacts caused by the inflow of undiluted high-density contrast material in the SVC during thoracic helical CT have been described.^{5-7,9} These artifacts can cause obscuration of enlarged lymph nodes, incomplete characterization of axillary and mediastinal masses, and obscuration of vascular lesions. During CTA, artifacts can especially obscure the ascending aorta and proximal supra-aortic arteries and thus hide or suggest stenosis or occlusion of the origin of the supra-aortic arteries. Perivenous artifacts are frequently seen when the start of a CT scan occurs before injection of contrast material ends. In case of delayed start of data acquisition, after the end of contrast material injection, stasis of contrast material in the major thoracic veins can cause artifacts.

Rubin et al⁶, who performed helical CT with an injection duration of 40 sec and a scan delay of 25 sec, found that 3:1 dilution of contrast material resulted in diminished perivenous artifacts. To keep the same total injected iodine dose with a 3:1 dilution, the total injected volume and the injection rate have to be increased four times. In CTA, however, dilution of contrast material is not an option because the already high injection rate should be increased to more than 10 mL/sec in maintaining the injected iodine dose.

Haage et al⁵ tested the effect of the addition of a chaser bolus to the main contrast material bolus and subsequent reduction of contrast material. They found a reduction in perivenous artifacts. This result can be explained by the reduction in total iodine concentration and shorter contrast material injection time rather than use of a chaser bolus after the main bolus.

In theory, to prevent perivenous artifacts, a chaser bolus is useful in CTA only when the scan starts after injection of contrast material ends. In our study, the optimal scan delay was within the injection period of 20 sec in most of the patients. Although use of a chaser bolus in CTA of the supra-aortic arteries leads to optimal use of contrast material⁴, it does not decrease perivenous artifacts.

To synchronize data acquisition relative to optimal arterial enhancement, the scan direction in CTA usually is in the direction of blood flow.¹⁰ With 16-MDCT, scanning time in CTA of the supra-aortic arteries has decreased to less than 15 sec. This change may allow reversal of the scan direction without a compromise in vascular attenuation. In addition, perivenous artifacts may decrease because of the delay in scanning of the apex of the thorax when a craniocaudal scan direction is used.

Our study showed that a craniocaudal scan direction resulted in slightly lower attenuation of the carotid artery, although attenuation remained high enough for good evaluation, in comparison with a caudocranial scan direction. With both scan directions, peak attenuation was at the level of the proximal ICA, which is the most relevant site. After adjustment for age and weight, no significant difference in mean or maximum attenuation was found for the two scan directions. Minimum attenuation, however, was significantly lower for the craniocaudal scan direction. The explanation is that the scan direction is the opposite of the direction of blood flow, and to have maximal enhancement at the halfway point (the level of the proximal ICA), the scan is at the cranial level a little too early and at the caudal part a little too late for optimal enhancement. Therefore, attenuation at the beginning and at the end of the craniocaudal scan, and thus minimum attenuation, is lower than for a caudocranial scan. This factor is also reflected in the significantly lower attenuation, after adjustment for age and weight, at the ascending aorta, carotid siphon, and intracranial arteries and the lack of difference in attenuation at locations in between.

We found that a craniocaudal scan direction resulted in much lower attenuation of the SVC, which resulted in fewer perivenous artifacts. By the time the craniocaudal scan reaches the apex of the thorax, injection of contrast material has ended, and contrast material has been flushed from the veins by the chaser bolus.

There was a tendency to increased artifacts with left-sided injection compared with right-sided injection, although this difference was not significant ($p = 0.08$ for the craniocaudal scan direction). The explanation is that venous return in the left subclavian vein, because of its transverse course into the SVC, may be more likely to be affected by changes in intrathoracic pressure and to be compressed by normal structures, such as the aorta. These effects can cause more pooling of contrast material in the subclavian vein and more reflux in the neck veins with left-sided injection than occurs with right-sided injection.¹¹ We found more reflux in patients in the craniocaudal scan direction group who received a left-sided injection ($p < 0.01$) and a significant relation between reflux and artifacts ($p < 0.01$).

A limitation of our study was that the groups were not randomly allocated. Baseline characteristics, however, were not significantly different. Another limitation was that our results probably will not apply when bolus triggering is not used to optimize the timing of data acquisition. The timing for a craniocaudal scan direction has to be more precise than for a caudocranial scan direction. Without bolus triggering, data acquisition may be too early for good arterial attenuation in the intracranial arteries and too late for good attenuation in the aorta.

In conclusion, we advocate the use of a craniocaudal scan direction in 16-MDCT angiography of the supra-aortic arteries. Right-sided injection is preferred over left-sided injection. This protocol results in good arterial attenuation, low attenuation of the SVC, and few perivenous artifacts and facilitates evaluation of the ascending aorta and supra-aortic arteries.

References

1. Warlow C, Sudlow C, Dennis M, Wardlaw J, Sandercock P. Stroke. *Lancet* 2003; 362:1211–1224
2. Ersoy H, Watts R, Sanelli P, et al. Atherosclerotic disease distribution in carotid and vertebrobasilar arteries: clinical experience in 100 patients undergoing fluorotriggered 3D Gd-MRA. *J Magn Reson Imaging* 2003; 17:545–558
3. Rouleau PA, Huston J 3rd, Gilbertson J, Brown RD Jr, Meyer FB, Bower TC. Carotid artery tandem lesions: frequency of angiographic detection and consequences for endarterectomy. *AJNR* 1999; 20:621–625
4. de Monyé C, Cademartiri F, de Weert TT, Siepmann DA, Dippel DW, van der Lugt A. CT angiography of the carotid artery with a 16-multidetector-row CT scanner: comparison of different volumes of contrast material with and without bolus chaser. *Radiology* 2005; 237:555–562
5. Haage P, Schmitz-Rode T, Hubner D, Piroth W, Gunther RW. Reduction of contrast material dose and artifacts by a saline flush using a double power injector in helical CT of the thorax. *AJR* 2000; 174:1049–1053
6. Rubin GD, Lane MJ, Bloch DA, Leung AN, Stark P. Optimization of thoracic spiral CT: effects of iodinated contrast medium concentration. *Radiology* 1996; 201:785–791
7. Loubeyre P, Debard I, Nemoz C, Minh VA. High opacification of hilar pulmonary vessels with a small amount of nonionic contrast medium for general thoracic CT: a prospective study. *AJR* 2002; 178:1377–1381
8. Vogel N, Kauczor HU, Heussel CP, Ries BG, Thelen M. Artefact reducing in diagnosis of lung embolism using spiral CT with saline bolus [in German]. *Rofo* 2001; 173:460–465
9. Nakayama M, Yamashita Y, Oyama Y, Ando M, Kadota M, Takahashi M. Hand exercise during contrast medium delivery at thoracic helical CT: a simple method to minimize perivenous artifact. *J Comput Assist Tomogr* 2000; 24:432–436
10. Fleischmann D. Use of high concentration contrast media: principles and rationale—vascular district. *Eur J Radiol* 2003; 45[suppl 1]:S88–S93
11. Sakai O, Nakashima N, Shibayama C, Shinozaki T, Furuse M. Asymmetrical or heterogeneous enhancement of the internal jugular veins in contrast-enhanced CT of the head and neck. *Neuroradiology* 1997; 39:292–295

Chapter 4

High Iodine Concentration Contrast
Material for Noninvasive Multislice
Computed Tomography Coronary
Angiography: Iopromide 370 Versus
Iomeprol 400

High iodine concentration contrast material for noninvasive multislice computed tomography coronary angiography: iopromide 370 versus iomeprol 400

Filippo Cademartiri, MD, PhD
 Cécile de Monyé, MD
 Francesca Pugliese, MD
 Nico R. Mollet, MD
 Giuseppe Runza, MD
 Aad van der Lugt, MD, PhD
 Massimo Midiri, MD
 Pim J. de Feyter, MD, PhD
 Roberto Lagalla, MD
 Gabriel P. Krestin, MD, PhD

Invest Radiol 2006; 41:349-353

Abstract

Objective: The objective of this study was to compare intracoronary attenuation on 16-row multislice computed tomography (16-MSCT) coronary angiography using 2 contrast materials (CM) with high iodine concentration.

Material and Methods: Forty consecutive patients (29 male, 11 female; mean age, 61 ± 11 years) with suspected coronary artery disease were randomized to 2 groups to receive 100 mL of either iopromide 370 (group 1: Ultravist 370, 370 mg iodine/mL; Schering AG, Berlin, Germany) or iomeprol 400 (group 2: Iomeron 400, 400 mg iodine/mL; Bracco Imaging SpA, Milan, Italy). Both CM were administered at a rate of 4 mL/s. All patients underwent 16-MSCT coronary angiography (Sensation 16; Siemens, Germany) with collimation 16×0.75 mm and rotation time 375 ms. The attenuation in Hounsfield units (HU) achieved after each CM was determined at regions of interest (ROIs) placed at the origin of coronary arteries and on the ascending aorta, descending aorta, and pulmonary artery. Differences in mean attenuation in the coronary arteries and on the ascending aorta, descending aorta, and pulmonary artery were evaluated using Student's *t*-test.

Results: The mean attenuation achieved at each anatomic site was consistently greater after iomeprol 400 than after iopromide 370. At the origin of coronary arteries, the mean attenuation after iomeprol 400 (340 ± 53 HU) was greater ($p < 0.05$) than that after iopromide 370 (313 ± 42 HU). Similar findings were noted for the mean attenuation in the ascending aorta, descending aorta, and pulmonary artery.

Conclusion: The intravenous administration of iomeprol 400 provides higher attenuation of the coronary arteries and of the great arteries of the thorax as compared with iopromide 370 using the same injection parameters.

Introduction

Current data suggest that significant coronary artery stenosis can be detected with 16-row multidetector computed tomography (16-MDCT) angiography.¹⁻⁷ The increased number of detector rows and faster gantry rotation with 16-MDCT compared with the previous 4-MDCT generation have improved the diagnostic performance of the technique and reduced the time needed to cover the entire heart to approximately 20 seconds.³ The type and iodine concentration of contrast media (CM) used in CT angiography (CTA) have assumed increasing importance because the attenuation that can be achieved in vessels greatly affects image quality and thus diagnostic yield.⁸⁻¹⁰ These considerations are even more important for imaging the coronary arteries because of the small caliber and tortuous anatomy of these vessels, and because of the presence of often extensive vessel wall disease.

The attenuation achievable in vessels can be improved by optimizing synchronization between the arterial passage of the CM and CT data acquisition and by modifying the injection parameters for intravenous (IV) administration of CM.⁸ Whereas various bolus-tracking techniques are available to improve synchronization,¹¹ modification of the injection parameters to increase vascular attenuation might involve altering the rate of CM injection, the volume injected, and/or the iodine concentration of the CM used.⁸ Recently, we have demonstrated that CM with higher iodine concentrations yields significantly higher attenuation in the coronary arteries and descending aorta.¹² Although several iodinated CM are available on the market, very few are formulated to contain a high or very high concentration of iodine (ie, >350 mgI/mL). The purpose of the present study was to prospectively compare 2 different CM, one with a high concentration of iodine (iopromide 370 mgI/mL) and one with a very high concentration of iodine (iomeprol 400 mgI/mL), in terms of the attenuation obtained in an extended territory comprising the coronary arteries as well as the ascending and descending thoracic aorta and pulmonary arteries.

Methods

Patient Population

A total of 40 patients (29 men, 11 women; mean age, 61 ± 11 years; age range, 34–79 years) referred for noninvasive MSCT coronary angiography for suspected coronary artery disease were enrolled prospectively. Exclusion criteria for coronary CTA were irregular heart rate, previous allergic reaction to iodine contrast media, renal insufficiency (serum creatinine >120 mmol/L), pregnancy, respiratory impairment, unstable clinical status, or marked heart failure. Institutional Review Board approval was received and all patients gave informed consent to participate in the study.

Patients were assigned randomly to 2 groups to receive either 100 mL of iopromide 370 (Ultravist 370; Schering AG, Berlin, Germany; 370 mg iodine/mL) (group 1) or 100 mL of iomeprol 400 (Iomeron 400; Bracco Imaging SpA, Milan Italy; 400 mg

iodine/mL) (group 2). Patients with a preexamination heart rate equal to or greater than 65 beats per minute (bpm) were given 100 mg of metoprolol orally 1 hour before the scan. The heart rate during the examination was recorded continuously.

Multislice Computed Tomography Examination Protocol

MSCT coronary angiography was performed on a 16-row detector system (Sensation 16; Siemens, Forchheim, Germany) in the craniocaudal direction. The scan parameters were as follows: number of detector rows: 16, individual detector width: 0.75 mm, gantry rotation time: 375 ms, tube voltage: 120 kV, tube current: 600–700 mAs, feed/rotation: 3.0 mm, scan range: 120–140 mm.

CM administration was performed intravenously (antecubital vein) using a prototype double-head power injector (Stellant; MedRAD, Pittsburgh, PA) through an 18-G Venflon needle. All CM administrations were performed intravenously at a rate of 4 mL/s and were followed by 40 mL of saline flush at the same rate. The resulting iodine administration rate was 1.48 g iodine/s for group 1 and 1.6 g iodine/s for group 2.

Synchronization between the passage of contrast material and data acquisition was achieved with real-time bolus tracking (CARE bolus; Siemens, Forchheim, Germany) using a region of interest (ROI) positioned on the ascending aorta. Automatic triggering of the scan acquisition occurred at a threshold attenuation of +100 Hounsfield units (HU) above baseline average attenuation.

Data Collection

Data collection and analysis was performed using previously reported methodology with some modifications.¹³ Two datasets were reconstructed using retrospective electrocardiographic gating with a time window beginning 400 ms before the next R wave. The first dataset was reconstructed for the purpose of coronary artery attenuation assessment. Reconstruction of this dataset was performed with the following parameters: effective slice width: 1 mm, reconstruction interval: 0.5 mm (50% overlap), field of view (FOV): 160 mm, and convolution filter: medium-smooth (Siemens Medical Solutions; factory filter: B30f). The second dataset was reconstructed to assess the vessels of the thorax. Reconstruction of this dataset was performed with the following parameters: effective slice width: 3 mm, reconstruction interval: 3 mm, FOV: 200 mm, and convolution filter: medium-smooth.

Measurements of Attenuation

Coronary Arteries

Axial slices in the first dataset were scrolled to find the best location to measure the attenuation (HU) at the origin of the 4 main coronary arteries (right coronary artery [RCA], left main artery [LM], left anterior descending artery [LAD], circumflex [CX]) (Fig. 1). The ROIs were drawn as large as possible on the vessels with care taken to avoid calcifications, plaques, and stenoses.

Great Vessels

The attenuation was determined at ROIs positioned on consecutive slices (at intervals of approximately 1 second) on the ascending aorta through to the left ventricle (ROI1), the descending aorta (ROI2), and the pulmonary artery through to the right ventricle (ROI3). A fourth ROI (ROI4) was positioned on the superior vena cava (Fig. 2). The attenuation after each CM and the bolus geometry of the CM in each vessel were determined.

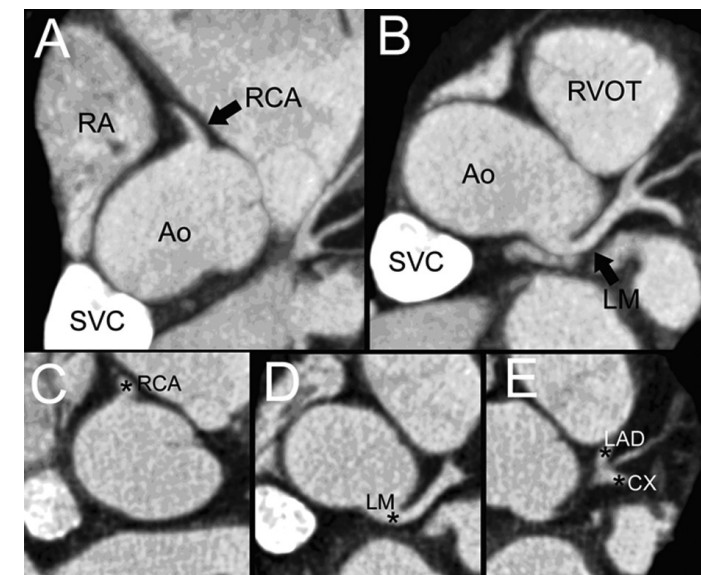


Figure 1. Assessment of attenuation at the origin of coronary vessels. In A and B, 2 oblique para-axial maximum intensity projection reconstructions show the ascending aorta (Ao) and the origin of the right coronary artery (RCA) and left main coronary artery (LM). The superior vena cava (SVC) is also shown with very high attenuation. The assessments of attenuation at the origin of the main coronary arteries are performed for RCA, for LM, for the left anterior descending (LAD) artery and for the circumflex (CX), as shown in C, D, and E, respectively.

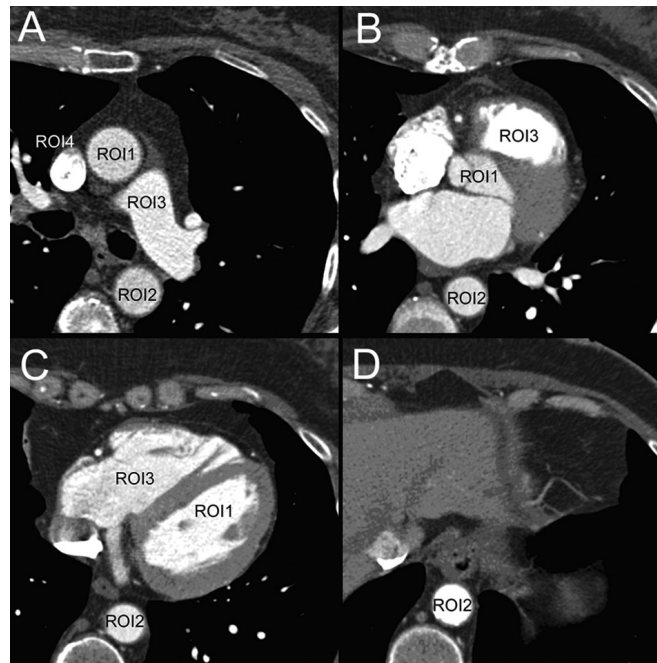


Figure 2. Assessment of bolus geometry through the dataset. The assessment of bolus geometry in the great vessels of the thorax was performed using regions of interest (ROI) positioned on each vessel on consecutive slices. ROIs on the ascending aorta (ROI1) were positioned at the beginning of the scan (A and B) and at the point of entry of contrast material into the left ventricle (C). ROIs on the descending aorta (ROI2) were positioned on consecutive slices throughout the dataset (A–D). ROIs on the pulmonary artery (ROI3) were positioned at the beginning of the scan (A), at the right ventricle outflow tract (B), and in the right ventricle (C). A fourth (ROI4) was positioned on the superior vena cava at the beginning of the scan (A).

Data Analysis

The attenuation values of the 4 coronary arteries were averaged for all patients in each group, and the overall average was used to compare the 2 groups.

The attenuation values obtained from the ROIs positioned on the ascending and descending aorta and pulmonary artery in each patient were averaged at each time point to generate average time/density curves. The average vascular attenuation in these vessels indicated quantitatively the amount of CM present in the vessel during the scan. Two additional parameters were considered descriptive of vascular attenuation in the great vessels of the thorax: the attenuation at the beginning of the scan (time 0) and the maximum enhancement value (MEV; peak of attenuation) determined from the time/density curve.

Significant differences between the 2 groups were assessed using a Student's *t*-test. A *p* value of < 0.05 was considered significant.

Results

The mean (\pm standard deviation) age, body weight, and heart rate (HR) of patients in each group are shown in Table 1 along with the mean scan delay and mean scan time of the MSCT examinations. No significant differences ($p > 0.05$) in any parameter were apparent between the groups. Of the 40 patients enrolled for the study, 22 (55%) were already on long-term beta-blockers. A total of 28 of 40 (70%) patients received additional oral beta-blockers before the scan. The average heart rate at patient presentation for the scan was 69 ± 11 bpm, which dropped to 57 ± 8 bpm after beta-blocker administration.

Table 1. Demographic Data

	Group 1	Group 2
No. patients	20	20
Male/female	15/5	14/6
Age (yrs)	59 ± 12	63 ± 10
Weight (kg)	73 ± 9	75 ± 11
Heart rate (beats/min)	61 ± 7	60 ± 8
Mean scan delay (sec)	21.7 ± 1.9	20.6 ± 2.3
Mean scan time (sec)	18.0 ± 2.1	18.5 ± 2.4

Values are expressed as mean \pm standard deviation.

No significant differences ($p > 0.05$) were noted between the 2 groups for any parameter.

All examinations and bolus timing procedures were successfully completed in all patients. No significant adverse reactions to contrast material were observed in any patient and no changes in heart rate were noted either during the administration of contrast material or during the MSCT examination itself.

Table 2. Attenuation at Origin of Coronary Arteries

Vessel	Group 1	Group 2	Δ
RCA (HU)	315 ± 58	357 ± 66	+42
LM (HU)	322 ± 45	350 ± 52	+28
LAD (HU)	295 ± 57	321 ± 65	+34
CX (HU)	287 ± 46	331 ± 60	+44
Average*	313 ± 42	340 ± 53	+27

*The average attenuation at the origin of coronary arteries was significantly lower for group 1 (Ultravist 370) compared with group 2 (Iomeron 400) ($p < 0.05$).

SD, standard deviation; Δ , relative difference (group 2 average HU – group 1 average HU).

Table 3. Bolus Geometry in the Great Vessels of the Thorax

	Group 1	Group 2	Δ	p
Ascending Aorta				
Average (HU)	312±47	353±59	+41	<0.05
Time 0 (HU)	309±45	348±55	+39	<0.05
MEV (HU)	339±48	390±70	+51	<0.05
Descending Aorta				
Average (HU)	307±48	350±55	+43	<0.05
Time 0 (HU)	292±47	330±53	+38	<0.05
MEV (HU)	341±49	408±73	+67	<0.05
Pulmonary Artery				
Average (HU)	282±52	317±72	+35	<0.05
Time 0 (HU)	330±85	405±109	+75	<0.05
MEV (HU)	317±52	352±100	+35	0.17

Measurements of vascular attenuation for the main vessels of the thorax are displayed for group 1 (Ultravist 370) and group 2 (Iomeron 400).

Δ , relative difference (group 2 average HU – group 1 average HU).

Coronary Artery Attenuation

The mean attenuation at the origin of the 4 coronary arteries was always higher after Iomeron 400 (340 ± 53 HU) than after Iopromide 370 (313 ± 42 HU) (Table 2; Fig. 3). Comparison of the mean overall difference between the 2 groups revealed significantly ($p < 0.05$) higher mean attenuation after Iomeron 400 than after Iopromide 370.

Great Vessel Attenuation

The average attenuation was in all cases significantly ($p < 0.05$) higher after Iomeron 400 than after Iopromide 370 (ascending aorta: 353 ± 59 HU vs 312 ± 47 HU; descending aorta: 350 ± 55 HU vs 307 ± 48 HU; pulmonary artery: 317 ± 72 HU vs 282 ± 52 HU, respectively) (Table 3; Fig. 3). Similar findings were obtained for the attenuation at time zero. Determinations of the MEV revealed significantly ($p < 0.05$) greater attenuation with Iomeron 400 in the ascending and descending aorta but not in the pulmonary artery.

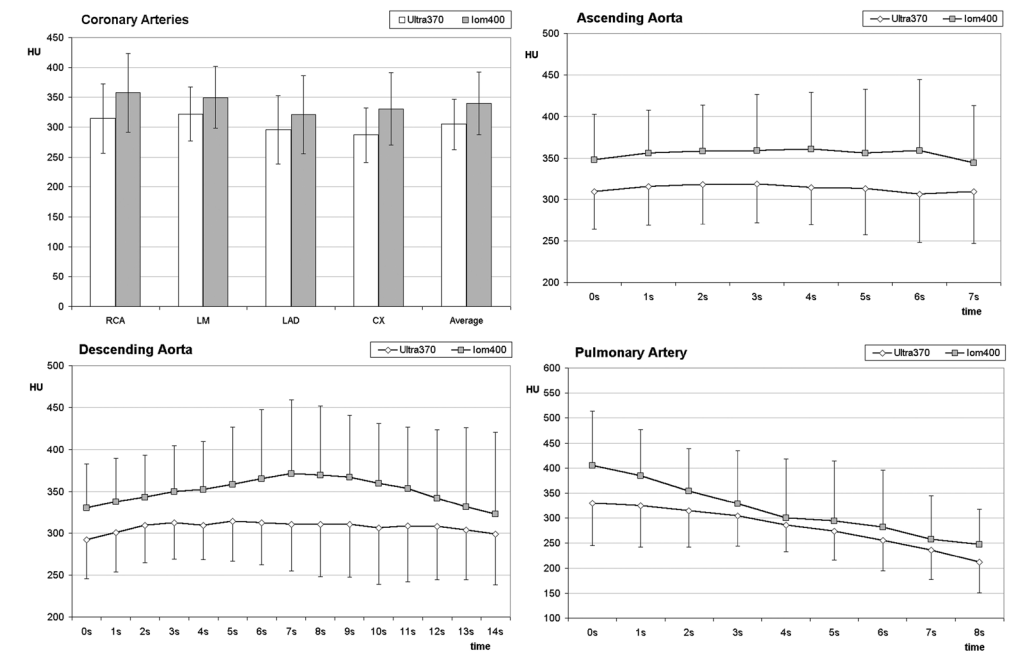


Figure 3. Results of attenuation assessment of coronary arteries and great thoracic vessels. The results of the attenuation assessment at the level of coronary arteries show slightly lower values for group 1 but not significantly different in all 4 sample regions (A). The average time/density curves in the ascending aorta and descending aorta are almost identical for groups 1 and group 2 (B and C). For the pulmonary artery, instead, group 1 shows more “pooling” of contrast material in the right chambers of the heart (D).

Discussion

Imaging of the coronary arteries is hampered by their small size and tortuous course and, when a stenosis or obstruction is present, by reduced blood flow. Improved visualization of these vessels can be achieved by increasing the iodine administration rate either by increasing the injection rate to provide a progressively higher vascular attenuation or by increasing the iodine concentration of the administered CM.¹⁴ Although increasing the injection rate is possibly a more readily feasible approach than increasing the iodine concentration of the CM, the injection rates used in routine clinical practice for coronary artery imaging are already typically 4 to 5 mL/s. To increase the injection rate further would require larger needles and larger veins and more time to set the intravenous supply. Moreover, the risk of CM extravasation would also increase. The use of a CM with higher iodine concentration may thus be an attractive alternative, particularly for the improved visualization of vessels that contain a smaller volume of blood.^{9,10}

A number of reports have discussed the role of CM with high iodine concentration for CT angiography.^{12,14,15} In a recent study comparing several contrast agents with differing iodine concentrations (iohexol 300 mgI/mL, iodixanol 320 mgI/mL, iohexol 350 mgI/mL, iomeprol 350 mgI/mL, and iomeprol 400 mgI/mL) for MSCT of

the coronary arteries, we have shown that significantly higher vascular attenuation is achieved with the highest iodine concentration and that significantly lower attenuation is achieved with the lowest iodine concentration.¹² Our findings support the findings of an earlier study by Becker et al¹⁶ in which 2 different iodine concentrations (iomeprol 300 and 400 mgI/mL) were compared at 2 different injection rates (2.5 and 3.5 mL/s) for 4-MSCT angiography of coronary arteries. Their conclusion was that the vascular attenuation achieved with 400 mgI/mL and 3.5 mL/s was significantly higher than the other protocols and that 300 mgI/mL and 2.5 mL/s provides significantly lower attenuation. More recently, a study by Rist et al has shown that 63 mL of a CM with high iodine concentration (Iomeron 400) injected at a rate of 2.5 mL/s provides equivalent attenuation to that achieved after injection of 83 mL of a CM with standard iodine concentration (Iomeron 300) at a rate of 3.3 mL/s (Rist, personal communication).

Our prospective study was aimed at further defining the benefits of CM with high iodine concentration by comparing the attenuation achieved in the coronary arteries and great vessels of the thorax after administration of 2 CM with high iodine concentration (iopromide 370 and Iomeron 400). Along with Iopamidol 370 (Isovue 370; Bracco Diagnostics, Princeton, NJ), these 2 CM contain the highest concentrations of iodine of any CM currently available on the market. With all other injection variables (volume, injection rate) and examination parameters kept constant, significantly higher attenuation was found in all vessels with the CM with the highest concentration of iodine (400 mgI/mL). These findings suggest that modest increases in the concentration of iodine can lead to significant increases in the attenuation observed and thereby improve the visualization of the vessels of interest.

With the advent of newer, faster 16- and 64-slice CT scanners with considerably more rapid acquisition times, there is a greater need to achieve high attenuation in a shorter period time without a concomitant increase in CM volume. Although one way to achieve this is by modifying the iodine administration rate through alteration of the CM injection rate, a more practical way might entail the use of a CM with higher iodine concentration. Given the greater attenuation seen in the present study with Iomeron 400, and the fact that no differences were observed in either the incidence of adverse events or the heart rate before and after injection, the CM with the highest concentration of iodine can be recommended for CT angiography of small arteries.

In conclusion, our study has demonstrated that the use of CM with higher iodine concentration provides higher vascular attenuation in the coronary arteries as well as in the ascending and descending thoracic aorta and pulmonary arteries.

References

1. Nieman K, Cademartiri F, Lemos PA, et al. Reliable noninvasive coronary angiography with fast submillimeter multislice spiral computed tomography. *Circulation* 2002; 106:2051–2054
2. Ropers D, Baum U, Pohle K, et al. Detection of coronary artery stenoses with thin-slice multi-detector row spiral computed tomography and multiplanar reconstruction. *Circulation* 2003; 107:664–666
3. Heuschmid M, Kuttner A, Flohr T, et al. Visualization of coronary arteries in CT as assessed by a new 16 slice technology and reduced gantry rotation time: first experiences. *Rofo* 2002; 174:721–724
4. Flohr T, Stierstorfer K, Bruder H, et al. New technical developments in multislice CT—part 1: approaching isotropic resolution with sub-millimeter 16-slice scanning. *Rofo* 2002; 174:839–845
5. Flohr T, Bruder H, Stierstorfer K, et al. New technical developments in multislice CT—part 2: sub-millimeter 16-slice scanning and increased gantry rotation speed for cardiac imaging. *Rofo* 2002; 174:1022–1027
6. Gerber TC, Stratman BP, Kuzo RS, et al. Effect of acquisition technique on radiation dose and image quality in multidetector row computed tomography coronary angiography with sub-millimeter collimation. *Invest Radiol* 2005; 40:556–563
7. Sanz J, Rius T, Kuschnir, et al. The importance of end-systole for optimal reconstruction protocol of coronary angiography with 16-slice multidetector computed tomography. *Invest Radiol* 2005; 40:155–163
8. Cademartiri F, van der Lugt A, Luccichenti G, et al. Parameters affecting bolus geometry in CTA: a review. *J Comput Assist Tomogr* 2002; 26:596–607
9. Bae KT, Heiken JP, Brink JA. Aortic and hepatic peak enhancement at CT: effect of contrast medium injection rate—pharmacokinetic analysis and experimental porcine model. *Radiology* 1998; 206:455–464
10. Fleischmann D, Rubin GD, Bankier AA, et al. Improved uniformity of aortic enhancement with customized contrast medium injection protocols at CT angiography. *Radiology* 2000; 214:363–371
11. Cademartiri F, Nieman K, van der Lugt A, et al. Intravenous contrast material administration at helical 16-multidetector-row helical CT: test bolus vs bolus tracking. *Radiology* 2004; 233:817–823
12. Cademartiri F, Mollet NR, van der Lugt A, et al. Intravenous contrast material administration at helical 16-detector row CT coronary angiography: effect of iodine concentration on vascular attenuation. *Radiology* 2005; 236:661–665
13. Cademartiri F, Mollet N, van der Lugt A, et al. Non-invasive 16-row multislice CT coronary angiography: usefulness of saline chaser. *Eur Radiol* 2004; 14:178–183
14. Fleischmann D. Use of high concentration contrast media: principles and rationale—vascular district. *Eur J Radiol* 2003; 45(suppl 1):S88–S93
15. Brink JA. Use of high concentration contrast media (HCCM): principles and rationale—body CT. *Eur J Radiol* 2003; 45(suppl 1):S53–S58
16. Becker CR, Hong C, Knez A, et al. Optimal contrast application for cardiac 4-detector-row computed tomography. *Invest Radiol* 2003; 38:690–694

Chapter 5

Diagnostic Accuracy of CT Angiography
and Duplex Ultrasound for the
Detection of Carotid Artery Stenosis in
TIA or Minor Stroke Patients

Diagnostic accuracy of CT angiography and duplex ultrasound for the detection of carotid artery stenosis in TIA or minor stroke patients

Cécile de Monyé, MD
 Hervé L.J. Tanghe, MD
 M.G.Myriam Hunink, MD, PhD
 Diederik W. J. Dippel, MD, PhD
 Aad van der Lugt, MD, PhD

Submitted

Abstract

Purpose: To determine the diagnostic accuracy of multidetector CTA and DUS in the assessment of carotid stenosis.

Materials and methods: 351 patients with amaurosis fugax, TIA or minor ischemic stroke underwent DUS and CTA of the symptomatic carotid artery. If one or both modalities showed a stenosis of 50-99%, or if one of the modalities was uninterpretable, DSA was performed as reference standard. If both CTA and DUS demonstrated a stenosis of <50%, or both showed an occlusion, DUS and CTA were used as the reference standard. If both CTA and DUS showed a stenosis of 80-99% and DSA was not performed to prevent treatment delay, DUS and CTA were used as the reference standard.

Results: CTA resulted in a sensitivity of 91% (95%CI, 71-99%) and a specificity of 99% (95%CI, 98-100%) in identifying stenoses of 70-99% and a sensitivity of 100% (95%CI, 88-100%) and a specificity of 98% (95%CI, 96-99%) in identifying stenoses of 50-99%. DUS resulted in a sensitivity of 59% (95%CI, 36-79%) and a specificity of 99% (95%CI, 97-100%) in identifying stenoses of 70-99% and a sensitivity of 79% (95%CI, 59-92%) and a specificity of 98% (95%CI, 96-99%) in identifying stenoses of 50-99%.

Conclusion: CTA can replace DUS and DSA in providing an accurate and fast diagnosis in patients suspected of a symptomatic carotid stenosis.

Introduction

The benefit of carotid endarterectomy (CEA) in patients with severe symptomatic carotid artery stenosis ($\geq 70\%$) has been established in large randomized trials.¹⁻³ The degree of stenosis in these trials was assessed with digital subtraction angiography. The inherent risk of this invasive procedure led to a less invasive diagnostic strategy in which patients were screened with duplex ultrasound (DUS). If a stenosis was found by DUS, digital subtraction angiography (DSA) was performed to confirm the stenosis and assess the severity of stenosis. Since then, multiple studies have been performed to demonstrate that magnetic resonance angiography (MRA) and computed tomography angiography (CTA) can replace DSA as a confirmative study and is as accurate as DSA in the assessment of the severity of stenosis.⁴⁻⁷

Although DUS as the only modality in the workup of stroke patients proved to be a cost-effective strategy⁸, most clinicians like to confirm a stenosis diagnosed on DUS with a second angiographic modality. In practice, this two-step strategy can be time-consuming due to logistic problems. Moreover, apart from the degree of carotid stenosis and vascular risk factors, the benefit of CEA also depends on the timing of surgery after the ischemic event. For symptomatic stenoses the benefit from surgery falls rapidly with increasing delay.⁹

We therefore propose CTA as the initial and only diagnostic modality in the evaluation of symptomatic carotid arteries.¹⁰ Since CT of the brain is recommended in the diagnostic work-up of patients with TIA or minor ischemic stroke CTA can easily be added to the CT protocol. The purpose of our study was to determine the diagnostic accuracy of multidetector CTA and DUS in a consecutive cohort of patients with TIA or minor stroke symptoms. The study was reported according to the STARD criteria.¹¹

Materials and methods

Study Population

The study was approved by the Institutional Review Board, and all patients gave written informed consent. Consecutive patients with cerebrovascular symptoms in the territory of the carotid artery were included in a prospective diagnostic study. Inclusion criteria were: symptoms of carotid artery disease in the preceding 6 months (amaurosis fugax, TIA or minor ischemic stroke with a Rankin score ≤ 3) and age ≥ 18 years. Exclusion criteria were: contraindication for iodinated intravenous contrast material which includes impaired renal function (creatinin > 150 mmol/l), allergy for iodinated contrast material, thyroid carcinoma, pregnancy, and no informed consent.

Patients underwent complete neurological examination on admission. Medical history was recorded for all patients. Clinical measures and information on risk factors and medication were obtained on admission to the hospital. Patients underwent DUS and CTA of the carotid arteries preferably on the same day. If both

DUS and CTA agreed on a stenosis of <50% or an occlusion of the symptomatic artery, no DSA was performed. If either DUS and/or CTA showed a stenosis of 50-99% of the symptomatic artery or one of the modalities was uninterpretable, DSA was performed. However, if both DUS and CTA showed a stenosis of $\geq 80\%$ of the symptomatic artery, DSA was not mandatory, in order to prevent unnecessary risks of invasive testing and treatment delay.

Diagnostic Tests

DUS

DUS was performed with HDI 3000 or HDI 5000 ultrasound machine and a 12 MHz transducer (Advanced Technology Laboratories, Bothell, Wash). DUS examinations were performed by dedicated vascular technologists with more than 5 years of experience blinded to the results of the other tests.

The degree of stenosis on DUS was determined on the basis of the peak systolic velocity (PSV) in the proximal part of the internal carotid artery (ICA).¹² Cutoff criteria for the PSV for different stenosis categories in our laboratory were defined using data from a previously performed study.¹³ DUS PSV thresholds for 50%, 70% and 80% stenosis were 189 cm/s, 262 cm/s and 308 cm/s, respectively. Slow flow in combination with a visualized severe stenosis was categorized as 80%-99% stenosis.

CTA

CTA of the carotid artery was performed on a 16-row MDCT scanner (Siemens Medical Solutions, Forchheim, Germany). The CTA scan range reached from the ascending aorta to the intracranial circulation. All patients received 80 mL of contrast material (320 mg/ml) and 40 mL saline bolus chaser, both with an injection rate of 4 mL/sec. Images were reconstructed with effective slice width 1 mm, reconstruction interval 0.6 mm, FOV 100 mm and convolution kernel B30f (= medium smooth).¹⁴ The radiation exposure was 2.6 mSv.

The level of maximum stenosis was determined on the axial images. Manual measurements using calipers were performed on Multi Planar Reformat (MPR) images created parallel to the axis of the carotid artery at the level of maximum stenosis and reference segment distal to the stenosis. One reader (C.M.) with 3 years of general radiology training and 3 years of experience in vascular radiology evaluated all CTA examinations, blinded to clinical information and the results of the other tests.

The grade of stenosis on CTA was measured according to the North American Symptomatic Carotid Endarterectomy Trial (NASCET) criteria and categorized into 0-49%, 50-69%, 70-99% and 100%. The degree of stenosis (in percentage) was defined as 100 minus the minimal lumen diameter (mean of three measurements) at

the site of the stenosis as percentage of the normal lumen diameter (mean of three measurements) distal to the stenosis.

DSA

DSA was performed using an Integris V3000 angiographic unit (Philips Medical Systems, Best, the Netherlands) with an image intensifier matrix of 1024 x 1024. An intra-arterial catheter was selectively placed in both common carotid arteries. From each carotid bifurcation 3 projections (lateral, posteroanterior, and oblique) were acquired.

The DSA was read on printed hard copies or on the PACS station by a neuroradiologist (A.L.) with more than 4 years experience in interpreting DSA examinations, blinded to clinical information and the results of the other tests.

Manual measurements using calipers were performed. The grade of stenosis on DSA was measured and categorized in the same manner as for CTA.

Data Analysis

The test result of CTA and DUS were compared with the reference standard. We included for each patient only the stenosis of the carotid artery on the symptomatic side in the analysis.¹⁵ In case of agreement between CTA and DUS on a stenosis of <50% or an occlusion, DUS and CTA were used as the reference standard. If both CTA and DUS showed a stenosis of 80-99% and DSA was not performed to prevent treatment delay, DUS and CTA were used as the reference standard. In all other cases the reference standard was DSA. Sensitivity and specificity (and their 95% confidence intervals) were calculated for CTA and DUS for a stenosis of 70%-99% and for a stenosis of 50%-99% as these are the relevant categories for surgical or interventional treatment.

We performed complete case analyses and sensitivity analyses adjusted for the 18/351 missing values of the reference standard. Two adjustment methods were explored. The first method used inverse-probability weighting with weights equal to the probability of verification with the reference standard.¹⁶ The probability of verification was calculated in a logistic regression model using the non-invasive test results, age, gender, and symptoms at presentation as predictors. Each patient with known reference standard result was subsequently weighed in the analysis with the inverse of the probability that he/she would be verified conditional on his/her predictors.¹² In the second method we performed conditional mean single imputation of the percentage stenosis on DSA assuming missingness at random using the non-invasive test results, age, gender, and symptoms at presentation as predictors to estimate the degree of stenosis.¹⁷⁻¹⁹

The analyses were performed with SPSS version 14.0 (SPSS Inc., Chicago, Illinois USA) and STATA version 10 (StataCorp, College Station, Texas USA).

Results

Study Population

In 2 years and 3 months 541 patients with amaurosis fugax, TIA or minor stroke visited our outpatient clinic or neurology ward (Fig 1). Sixty patients were not asked to participate due to logistic reasons. One hundred eighteen patients were excluded because they refused to participate ($n=107$), were not capable of giving informed consent ($n=5$) or had a contraindication for iodinated contrast material ($n=9$). In 8 patients the CTA was not successfully performed because of CT scan failure ($n=1$), restlessness of the patient ($n=1$), contrast extravasation ($n=1$) or venous access could not be achieved ($n=5$). In 4 patients DUS was not performed because of logistic reasons. This resulted in 351 patients with both DUS and CTA of the carotid arteries. Baseline characteristics and relevant medical history are listed in Table 1. No adverse events related to CTA were registered. CTA was performed on the first day of the hospital visit in 74% of the patients, within 1-7 days in 14%, within 8-14 days in 5% and with a delay of more than 14 days in 7% of the patients. CTA and DUS were performed on the same day in 298 patients (85%), within 1-7 days in 33 patients (9%) and with a delay of more than 7 days in 20 patients (6%).

According to protocol DSA was not performed in 296 of the 351 patients: DUS and CTA showed a stenosis of $<50\%$ ($n=286$) or a total occlusion ($n=10$). In 4 patients both DUS and CTA showed a stenosis of $\geq 80\%$. One of these patients received a carotid endarterectomy without prior diagnostic DSA to prevent therapeutic delay and one patient refused surgical treatment, which made the risk of DSA unjustified. The other two patients underwent carotid stent placement and DSA prior to intervention confirmed the presence of a stenosis $> 70\%$. In the remaining 51 patients DUS and CTA were discordant ($n=28$), the carotid artery could not be analyzed

Table 1. Baseline Characteristics of the Study Population

Characteristic	Men ($n=212$)	Women ($n=139$)	Total ($n=351$)
Age (years)	62 (22 – 88)	61 (19 – 90)	62 (19 – 90)
Symptoms *			
Amarosis Fugax (%)	51 (24%)	33 (24%)	84 (24%)
TIA (%)	56 (26%)	43 (31%)	99 (28%)
Minor Stroke (%)	105 (50%)	63 (45%)	168 (48%)
Hypertension (%)	153 (72%)	90 (65%)	243 (69%)
Hypercholesterolemia (%)	154 (73%)	119 (86%)	273 (78%)
Diabetes mellitus (%)	36 (17%)	22 (16%)	58 (17%)
Smoking			
Currently (%)	81 (38%)	39 (28%)	120 (34%)
Past (%)	34 (16%)	11 (8%)	45 (13%)
Never (%)	97 (46%)	89 (64%)	186 (53%)
Previous Cardiac disease (%)	63 (30%)	27(19%)	90 (26%)
Previous Cerebrovascular disease (%)	64 (30%)	34 (24%)	98 (28%)

* 0 - 6 months prior to inclusion

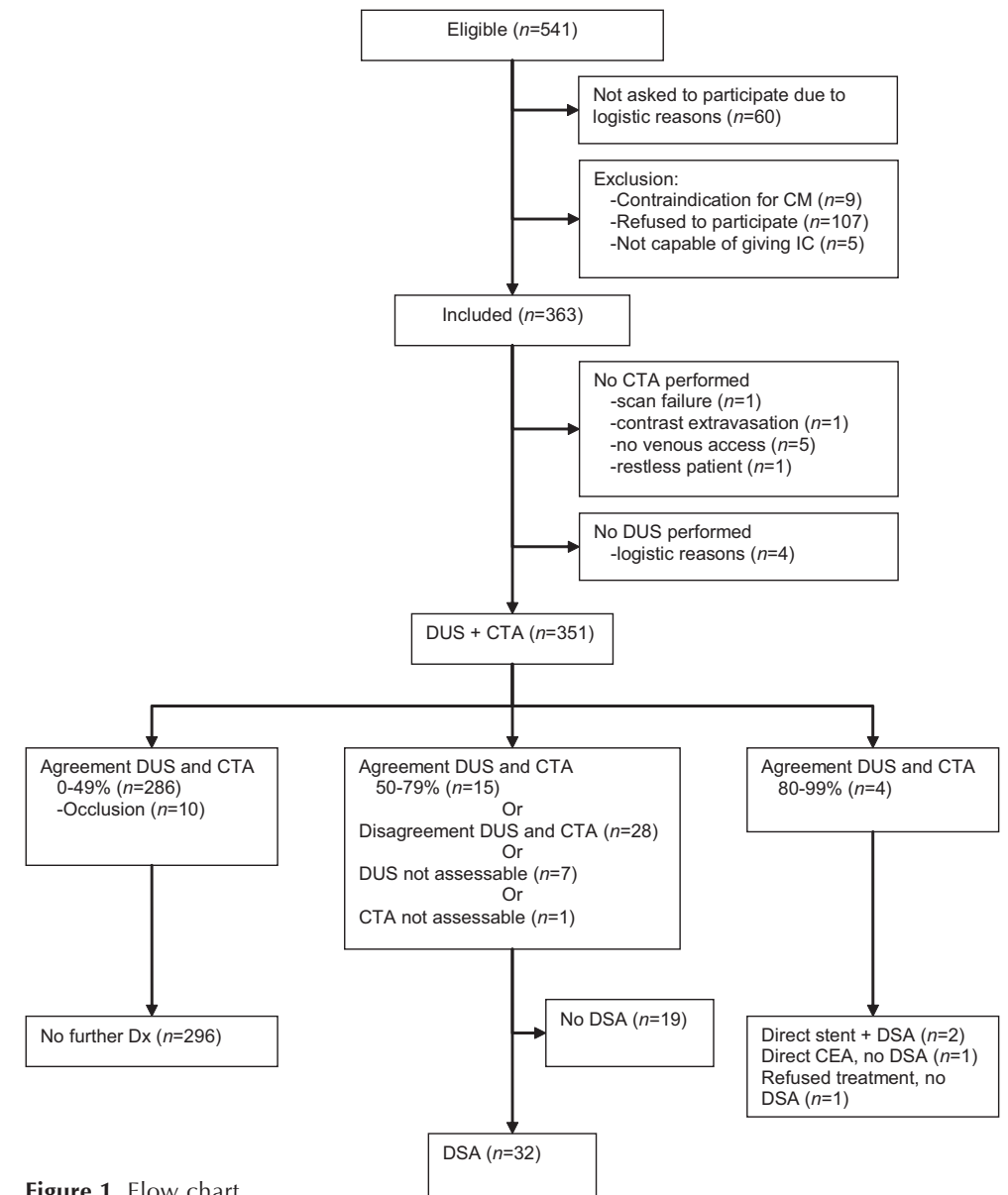


Figure 1. Flow chart.

with DUS ($n=7$), CTA could not be analyzed due to dental streak artefacts ($n=1$) or DUS and CTA showed both a stenosis between 50% and 80% ($n=15$). In 32 of these 51 patients DSA was performed according to protocol. In 1 patient the operation report recorded a subtotal occlusion and this was used as the reference standard instead of a DSA result. 18 cases remained unverified: In 16 patients DSA was not performed because the neurologist already decided that no treatment would follow for the following reasons: CTA showed no atherosclerotic disease and no stenosis at all ($n=4$), CTA showed abnormalities of the symptomatic carotid artery that were not treatable, i.e. dissection, fibromuscular dysplasia, very long stenosis or radiation arteriitis ($n=4$), the patients clinical condition was a contraindication

for treatment ($n=5$), the patient refused treatment ($n=2$) or DUS showed a stenosis of <50% and CTA showed a stenosis slightly over 50% ($n=1$). In 2 patients CTA showed a subtotal stenosis and DUS showed a stenosis between 70% and 80%. They were treated with endarterectomy without prior DSA to prevent treatment delay. No adverse events related to DSA were registered. Median time delay between the first day of the hospital visit and DSA was 29 days (range 6-93 days).

Diagnostic Test Results

In Table 2a and 2b the test results of CTA and DUS according to category of stenosis degree are presented compared to the reference standard. Table 3a and 3b show the accuracy of CTA and DUS. For the baseline analysis the unverified cases were not included in the analysis. CTA resulted in a sensitivity of 91% (95%CI, 71-99%) and a specificity of 99% (95%CI, 98-100%) in identifying severe ICA stenosis (70%-99%). CTA resulted in a sensitivity of 100% (95%CI, 88-100%) and a specificity of 98% (95%CI, 96-99%) in identifying moderate and severe ICA stenosis (50%-99%). DUS resulted in a sensitivity of 59% (95%CI, 36-79%) and a specificity of 99% (95%CI, 97-100%) in identifying severe ICA stenosis (70%-99%). DUS resulted in a sensitivity of 79% (95%CI, 59-92%) and a specificity of 98% (95%CI, 96-99%) in identifying moderate and severe ICA stenosis (50%-99%). The correction for

Table 2a. Categorized Stenosis Measurements of Symptomatic ICA: CTA versus Reference Standard

CTA stenosis categories	Reference standard stenosis categories					Total
	0%-49%	50%-69%	70%-99%	100%	Unverified	
0%-49%	289	0	0	0	4	293
50%-69%	5	4	2	0	5	16
70%-99%	0	2	19	0	8	29
100%	0	0	0	11	1	12
NA*	0	0	1	0	0	1
Total	294	6	22	11	18	351

* NA = not accessible

Table 2b. Categorized Stenosis Measurements of Symptomatic ICA: DUS versus Reference Standard

DUS stenosis categories	Reference standard stenosis categories					Total
	0%-49%	50%-69%	70%-99%	100%	Unverified	
0%-49%	289	1	4	1	9	304
50%-69%	2	4	4	0	0	10
70%-99%	1	1	13	0	3	18
100%	0	0	1	10	1	12
NA*	2	0	0	0	5	7
Total	294	6	22	11	18	351

* NA = not accessible

Table 3a. Accuracy of CTA Compared with the Reference Standard in Diagnosing Symptomatic ICA Stenosis. Results of the complete case analysis and two sensitivity analyses are presented. In the sensitivity analyses adjustments were made for the 18 unverified cases (See text for details).

CTA		Sensitivity analysis		
		Complete Case analysis	Inverse probability weighting	Imputation
Sensitivity	70%-99%	91% (71%-99%)	93% (83%-100%)	93% (82%-100%)
	50%-99%	100% (88%-100%)	100% (88%-100%)	100% (100%-100%)
Specificity	70%-99%	99% (98%-100%)	99% (97%-100%)	98% (97%-100%)
	50%-99%	98% (96%-99%)	98% (96%-100%)	98% (97%-100%)

Data in parentheses are 95%CIs.

Table 3b. Accuracy of DUS Compared with the Reference Standard in Diagnosing Symptomatic ICA Stenosis. Results of the complete case analysis and two sensitivity analyses are presented. In the sensitivity analyses adjustments were made for the 18 unverified cases (See text for details).

DUS		Sensitivity analysis		
		Complete Case analysis	Inverse probability weighting	Imputation
Sensitivity	70%-99%	59% (36%-79%)	52% (29%-76%)	63% (43%-82%)
	50%-99%	79% (59%-92%)	71% (51%-91%)	66% (51%-81%)
Specificity	70%-99%	99% (97%-100%)	99% (98%-100%)	98% (96%-99%)
	50%-99%	98% (96%-99%)	98% (97%-99%)	97% (96%-99%)

Data in parentheses are 95%CIs.

missing values of the unverified cases with probability of verification analysis and imputation analysis resulted in very small changes in sensitivity and specificity for both CTA and DUS.

Discussion

We performed a study in the setting of routine clinical practice to determine the accuracy of CTA and DUS in detecting a significant stenosis of the symptomatic internal carotid artery in the diagnostic work-up of patients with amaurosis fugax, TIA or minor stroke. The results of this study show a very high sensitivity and specificity of CTA for both 70%-99% and 50%-99% stenoses. The sensitivity of DUS on the contrary is much lower for both 70%-99% and 50%-99% stenoses, while the specificity of DUS is comparable to the specificity of CTA.

This study was designed to test CTA as a first-line investigation. The major strength of this study is the inclusion of a large group of consecutive patients with amaurosis

fugax, TIA or minor ischemic stroke. Thus, CTA was performed in a patient population without selection based on prior imaging, which was commonly the case in previous studies.^{7,20,21} Secondly, only the symptomatic artery is included in the analysis. This approach is recently advocated²² based on differences in accuracy of CTA and DUS in assessing the severity of stenosis in symptomatic and contralateral asymptomatic carotid arteries.^{15,23}

Stenosis of more than 70% was present in the symptomatic artery of 7-8% of the patients with amaurosis fugax, TIA or minor stroke. This prevalence is much lower than the prevalence of 24-46% reported in previous studies.^{4,20,21} This large difference can be explained by the fact that in these validation studies CTA, MRA or DSA were performed based on prior DUS, while this selection bias does not play a role in our study.

Two meta-analyses reported lower sensitivities and specificities of CTA for the diagnosis of 70%-99% stenosis.^{5,7} Both meta-analyses included CTA studies, which were performed on a single slice CT scanner and mostly used post-processing techniques like Shaded Surface Display (SSD), Volume Rendering (VR) and Maximum Intension Projections (MIP) for grading of the stenosis. Our study shows a higher sensitivity of 91%. This might be explained by the fact that our study was performed on a 16-slice MDCT-scanner resulting in images with a higher spatial resolution and that grading of stenosis was done using MPR images. The accuracy of CTA data analysed with MPR images instead of MIP is higher.²⁴ Other large studies on the accuracy of multidetector CTA have not been performed yet.

It is important to diagnose moderate stenoses ($\geq 50\%$) accurately. When treated very quickly after the ischemic event, both patients with a severe stenosis of 70%-99% and those with a stenosis of 50%-69% benefit from CEA (9). Our study demonstrated a high sensitivity in detecting stenoses of more than 50% with CTA. There are very limited data available on the detection of 50%-99% symptomatic stenoses with CTA. Alvarez et al²⁵ found a sensitivity of 93% (95%CI 81-98%) for the detection of stenoses of 50%-99%, which is comparable to our results. A meta-analysis reported on the sensitivity of CTA to detect stenoses of 50%-69%, which was 67% (95%CI 30-90%).⁷ However, assessment of the accuracy in detecting stenoses of 50%-69% has little clinical relevance because if they are treated they will have the same treatment and same prognosis as 70%-99% stenoses. Misclassification of a moderate stenosis (50%-69%) as severe stenosis (70%-99%) is then a non-relevant false negative result.

The sensitivity of DUS in our study was relatively low (59%, 95%CI 36%-79% for 70%-99% stenosis) compared to other studies.⁷ Validation studies of DUS of symptomatic arteries have frequently performed a reference test in case DUS revealed an abnormal PSV.²⁶⁻²⁸ In these studies normal DUS examinations in symptomatic arteries were not verified systematically. In most studies, verification was performed on normal DUS findings in asymptomatic arteries, contralateral to the symptomatic artery. Based on our study one might conclude that if DUS is used as a screening modality, a considerable number of patients will be erroneously not scheduled for further diagnostic evaluation and consequently receive no treatment.

One important reason to suggest CTA as the initial and only diagnostic modality is to prevent treatment delay with an increased risk on recurrent stroke. The benefit from surgery falls rapidly with increasing delay between presentation of the symptoms and treatment.⁹ Since all patients with symptoms of TIA or stroke receive a CT scan of the brain, it only takes less than 15 minutes to add CTA to the scan protocol. A complete diagnostic workup with recommendation for treatment can be made on the day of the visit to the hospital. CTA has an additional advantage over DUS as screening modality. Although the severity of stenosis caused by atherosclerosis in the carotid bifurcation is the most important risk factor for (recurrent) stroke and is used to decide which patients could benefit from carotid endarterectomy, pathological studies have shown that other atherosclerotic plaque features play a role in an acute ischemic event. Atherosclerotic plaque volume, composition and morphology could be parameters, which may help in a better risk prediction and selection of patients who could benefit from surgical intervention.²⁹ CTA is better equipped to assess these plaque features than DUS. Additionally, CTA provides information on the presence of atherosclerotic plaque and stenosis at other locations in the vascular tree, i.e. the ascending aorta, and proximal common carotid arteries, as well as intracranially.

A drawback of performing CTA in all patients suspected of having an ICA stenosis is radiation exposure and the risk of contrast-induced nephropathy. However, the majority of these patients are relatively old and radiation exposure is for this reason of less importance.³⁰ Contrast induced nephropathy can be reduced by exclusion of patients with impaired renal function. MRA could also replace DUS and/or DSA, but is less suitable as a first-line investigation because of lower availability, higher costs and higher percentage of contraindications. Also, the longer duration of the examination can be a problem in acute patients.

Our study has several limitations: verification bias may exist if the decision to perform the reference standard procedure depends on the result of the test under investigation.¹⁶ In our study no DSA was performed if DUS and CTA agreed on a stenosis of less than 50% or an occlusion. Although not expected it could still be that DSA would have yielded a different result. It was however not ethical to perform DSA in all patients because of the risks of DSA.⁸ When DUS and CTA agreed on a stenosis of $>80\%$, DSA was not performed in order to prevent treatment delay which was extremely important in these tight stenoses.⁹

Another limitation is that 18 of the 51 moderate to severe stenoses remained unverified. In the setting of clinical practice this is a problem that cannot be avoided. If there were reasons for the neurologist to decide that no treatment would follow, it was no longer ethical to perform a DSA. This decision was sometimes patient-related but also sometimes based on the CTA result. However, sensitivity analyses revealed no important differences in sensitivity and specificity.

In conclusion, our study demonstrated that CTA can provide an accurate and fast diagnosis in patients suspected of having a carotid stenosis in the setting of routine clinical practice.

References

1. Beneficial effect of carotid endarterectomy in symptomatic patients with high-grade carotid stenosis. North American Symptomatic Carotid Endarterectomy Trial Collaborators. *N Engl J Med* 1991; 325:445-453.
2. MRC European Carotid Surgery Trial: interim results for symptomatic patients with severe (70-99%) or with mild (0-29%) carotid stenosis. European Carotid Surgery Trialists' Collaborative Group. *Lancet* 1991; 337:1235-1243.
3. Rothwell PM, Eliasziw M, Gutnikov SA, et al. Analysis of pooled data from the randomised controlled trials of endarterectomy for symptomatic carotid stenosis. *Lancet* 2003; 361:107-116.
4. Nederkoorn PJ, Mali WP, Eikelboom BC, et al. Preoperative diagnosis of carotid artery stenosis: accuracy of noninvasive testing. *Stroke* 2002; 33:2003-2008.
5. Koelemay MJ, Nederkoorn PJ, Reitsma JB, Majoie CB. Systematic review of computed tomographic angiography for assessment of carotid artery disease. *Stroke* 2004; 35:2306-2312.
6. Nonent M, Serfaty JM, Nighoghossian N, et al. Concordance rate differences of 3 noninvasive imaging techniques to measure carotid stenosis in clinical routine practice: results of the CARMEDAS multicenter study. *Stroke* 2004; 35:682-686.
7. Wardlaw JM, Chappell FM, Best JJ, Wartolowska K, Berry E. Non-invasive imaging compared with intra-arterial angiography in the diagnosis of symptomatic carotid stenosis: a meta-analysis. *Lancet* 2006; 367:1503-1512.
8. Buskens E, Nederkoorn PJ, Buijs-Van Der Woude T, et al. Imaging of carotid arteries in symptomatic patients: cost-effectiveness of diagnostic strategies. *Radiology* 2004; 233:101-112.
9. Rothwell PM, Eliasziw M, Gutnikov SA, Warlow CP, Barnett HJ. Endarterectomy for symptomatic carotid stenosis in relation to clinical subgroups and timing of surgery. *Lancet* 2004; 363:915-924.
10. Josephson SA, Bryant SO, Mak HK, Johnston SC, Dillon WP, Smith WS. Evaluation of carotid stenosis using CT angiography in the initial evaluation of stroke and TIA. *Neurology* 2004; 63:457-460.
11. Bossuyt PM, Reitsma JB, Bruns DE, et al. Towards complete and accurate reporting of studies of diagnostic accuracy: the STARD initiative. *AJR* 2003; 181:51-55.
12. Hunink MG, Polak JF, Barlan MM, O'Leary DH. Detection and quantification of carotid artery stenosis: efficacy of various Doppler velocity parameters. *AJR* 1993; 160:619-625.
13. Heijenbrok-Kal MH, Buskens E, Nederkoorn PJ, van der Graaf Y, Hunink MG. Optimal peak systolic velocity threshold at duplex us for determining the need for carotid endarterectomy: a decision analytic approach. *Radiology* 2006; 238:480-488.
14. de Monye C, Cademartiri F, de Weert TT, Siepman DA, Dippel DW, van Der Lugt A. Sixteen-detector row CT angiography of carotid arteries: comparison of different volumes of contrast material with and without a bolus chaser. *Radiology* 2005; 237:555-562.
15. Chappell FM, Wardlaw JM, Young GR, et al. Carotid artery stenosis: accuracy of noninvasive tests--individual patient data meta-analysis. *Radiology* 2009; 251:493-502.
16. Begg CB, Greenes RA. Assessment of diagnostic tests when disease verification is subject to selection bias. *Biometrics* 1983; 39:207-215.
17. van der Heijden GJ, Donders AR, Stijnen T, Moons KG. Imputation of missing values is superior to complete case analysis and the missing-indicator method in multivariable diagnostic research: a clinical example. *J Clin Epidemiol* 2006; 59:1102-1109.
18. Donders AR, van der Heijden GJ, Stijnen T, Moons KG. Review: a gentle introduction to imputation of missing values. *J Clin Epidemiol* 2006; 59:1087-1091.
19. Schafer J. Analysis of incomplete multivariate data. Bury St. Edmunds, Suffolk: Chapman & Hall, 1997.
20. Cumming MJ, Morrow IM. Carotid artery stenosis: a prospective comparison of CT angiography and conventional angiography. *AJR* 1994; 163:517-523.
21. Link J, Brossmann J, Grabener M, et al. Spiral CT angiography and selective digital subtraction angiography of internal carotid artery stenosis. *AJNR* 1996; 17:89-94.
22. Kallmes DF. Noninvasive carotid artery imaging: caution ahead. *Radiology* 2009; 251:311-312.
23. Heijenbrok-Kal MH, Nederkoorn PJ, Buskens E, van der Graaf Y, Hunink MG. Diagnostic performance of duplex ultrasound in patients suspected of carotid artery disease: the ipsilateral versus contralateral artery. *Stroke* 2005; 36:2105-2109.
24. Hacklander T, Wegner H, Hoppe S, et al. Agreement of multislice CT angiography and MR angiography in assessing the degree of carotid artery stenosis in consideration of different methods of postprocessing. *J Comput Assist Tomogr* 2006; 30:433-442.
25. Alvarez-Linera J, Benito-Leon J, Escibano J, Campollo J, Gesto R. Prospective evaluation of carotid artery stenosis: elliptic centric contrast-enhanced MR angiography and spiral CT angiography compared with digital subtraction angiography. *AJNR* 2003; 24:1012-1019.
26. Grant EG, Duerinckx AJ, El Saden S, et al. Doppler sonographic parameters for detection of carotid stenosis: is there an optimum method for their selection? *AJR* 1999; 172:1123-1129.
27. Grant EG, Benson CB, Moneta GL, et al. Carotid artery stenosis: gray-scale and Doppler US diagnosis--Society of Radiologists in Ultrasound Consensus Conference. *Radiology* 2003; 229:340-346.
28. Huston J, 3rd, James EM, Brown RD, Jr., et al. Redefined duplex ultrasonographic criteria for diagnosis of carotid artery stenosis. *Mayo Clin Proc* 2000; 75:1133-1140.
29. de Weert TT, Cretier S, Groen HC, et al. Atherosclerotic plaque surface morphology in the carotid bifurcation assessed with multidetector computed tomography angiography. *Stroke* 2009; 40:1334-1340.
30. Einstein AJ, Hanzlova MJ, Rajagopalan S. Estimating risk of cancer associated with radiation exposure from 64-slice computed tomography coronary angiography. *JAMA* 2007; 298:317-323.

Chapter 6

Suspected Carotid Artery Stenosis: Cost-Effectiveness of CT Angiography in Work-up of Patients with Recent TIA or Minor Ischemic Stroke

Suspected carotid artery stenosis: Cost-effectiveness of CT angiography in work-up of patients with recent TIA or minor ischemic stroke

Aletta T. R. Tholen, MSc
 Cécile de Monyé, MD
 Tessa S. S. Genders, MSc
 Erik Buskens, MD, PhD
 Diederik W. J. Dippel, MD, PhD
 Aad van der Lugt, MD, PhD
 M. G. Myriam Hunink, MD, PhD

Radiology 2010; 256:585–597

Abstract

Purpose: To assess the effectiveness and cost-effectiveness of state-of-the-art non-invasive diagnostic imaging strategies in patients with a transient ischemic attack (TIA) or minor stroke who are suspected of having carotid artery stenosis (CAS).

Materials and methods: All prospectively evaluated patients provided informed consent, and the local ethics committee approved this study. Diagnostic performance, treatment, long-term events, quality of life, and costs resulting from strategies employing duplex ultrasonography (US), computed tomographic (CT) angiography, contrast material-enhanced magnetic resonance (MR) angiography, and combinations of these modalities were modelled in a decision tree and Markov model. Data sources included a prospective diagnostic cohort study, a meta-analysis, and a review of the literature. Outcomes were costs, quality-adjusted life-years (QALYs), incremental cost-effectiveness ratios, and net health benefits (QALY-equivalents), with a willingness-to-pay threshold of €50000 per QALY and a societal perspective. The strategy with the highest net health benefit was considered the most cost effective. Extensive one-way, two-way, and probabilistic sensitivity analyses to explore the effect of varying parameter values were performed. The reference case analysis assumed that patients underwent surgery 2–4 weeks after the first symptoms, and the effect of earlier intervention was explored.

Results: The reference case analysis showed that duplex US combined with CT angiography and surgery for 70%–99% stenoses was the most cost-effective strategy, with a net health benefit of 13.587 and 15.542 QALY-equivalents in men and women, respectively. In men, the CT angiography strategy with a 70%–99% cut off yielded slightly more QALYs, at an incremental cost of €71 419 per QALY, compared with duplex US combined with CT angiography. In patients with a high-risk profile, in patients with a high prior probability of disease, and when patients could be treated within 2 weeks after the first symptoms, the CT angiography strategy with surgery for 50%–99% stenoses was the most cost-effective strategy.

Conclusion: In diagnosing CAS, duplex US should be the initial test, and, if its results are positive, CT angiography should be performed; patients with 70%–99% stenoses should then undergo carotid endarterectomy. In patients with a high-risk profile, a high probability of CAS, or who can undergo surgery without delay, immediate CT angiography and surgery for 50%–99% stenoses is indicated.

Introduction

In 10%–30% of patients with a transient ischemic attack (TIA) or stroke, the cause is a carotid artery stenosis (CAS) of 70% or greater.^{1,2} Detection of a CAS is essential to reduce the probability of a (recurrent) stroke. Carotid endarterectomy reduces the absolute risk of ipsilateral ischemic stroke by 18% in patients with 70%–99% symptomatic CAS and by 8% in patients with a stenosis of 50%–69%, as documented in the North American Symptomatic Carotid Endarterectomy Trial (NASCET).^{3,4} The benefit of carotid endarterectomy, however, depends on the delay between the first symptoms of ischemia and surgery: The benefit from surgery decreases rapidly with an increasing delay.⁵

Digital subtraction angiography (DSA) remains the reference standard for diagnosing a CAS, according to several large randomized trials, such as NASCET and the European Carotid Surgery Trial.^{1,4,6} Because DSA is both invasive and expensive,³ the question arises as to whether alternatives exist that overall would yield better outcomes. Although this question has been studied before, results of an analysis of the effectiveness and cost-effectiveness of, in particular, multidetector computed tomographic (CT) angiography alone and in comparison to duplex ultrasonography (US) and contrast material enhanced magnetic resonance (MR) angiography have, to our knowledge, not yet been published.^{3,7–10}

The purpose of this study was to assess the effectiveness and cost-effectiveness of state-of-the-art noninvasive diagnostic imaging strategies in patients with a TIA or a minor stroke who are suspected of having CAS. Particular attention was paid to the time window between the first ischemic symptoms and carotid endarterectomy and the cut-off value chosen as an indication for surgery (70%–99% vs 50%–99% stenosis).

Materials and methods

Study Population

The target patient population was patients with a TIA or minor stroke who were suspected of having CAS.

Decision Model

A decision model was developed to evaluate and compare various diagnostic strategies by using decision-analytical software (TreeAge Pro, version 3.5, 2009; TreeAge, Williamstown, Mass). We assessed all feasible strategies in normal practice, all tests separately, and CT angiography or contrast-enhanced MR angiography combined with duplex US. In the combination strategies, if duplex US results appeared positive or uninterpretable, a CT angiography or contrast-enhanced MR

angiography examination followed. A noninvasive test with uninterpretable results was followed by a DSA examination in single noninvasive test strategies and if the results of the second test in a combination strategy were uninterpretable. We considered two cutoff values for the indication for carotid endarterectomy: 70%–99% or 50%–99% stenosis. These cutoff values were also the positivity criteria used in interpreting test results. In combination strategies, we considered additional strategies by using the 50%–99% positivity criterion in interpreting the duplex US results if the indication for endarterectomy was 70%–99%, to maximize sensitivity (Fig 1). Both the advantages and the disadvantages of diagnostic tests and of treatment with endarterectomy were modeled.

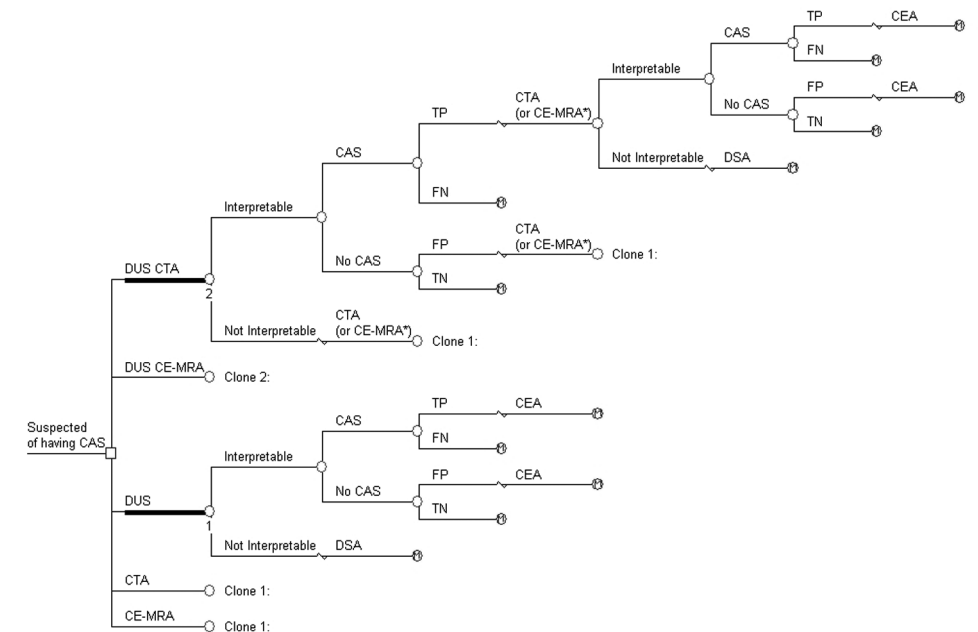


Figure 1: Schematic representation of decision tree. □ = Decision node, ○ = chance node, M = Markov node. After a positive result, carotid endarterectomy (CEA) is performed. DSA has the same structure as a single-test strategy. Clone = the structure of the tree at that point is identical to that of another subtree, which is marked with a black line and a corresponding number. Only one combination strategy (duplex US [DUS] plus CT angiography [CTA]) and one solo strategy (duplex US) have been expanded to limit the size of this figure. The other strategies have a similar structure, however, when combined with another test. * = For the other combination strategy, (duplex US plus contrast-enhanced MR angiography [CE-MRA]), the second test would be contrast-enhanced MR angiography instead of CT angiography. FN = false-negative, FP = false-positive, TN = true-negative, TP = true-positive.

A Markov model with a 1-year cycle length was developed to extrapolate and evaluate long-term outcomes of diagnostic work-up and subsequent treatment. More details about the decision model and Markov model are given in the Appendix and Figure E1 (Appendix).

Table 1. Prevalence, Diagnostic Tests and Procedures: Parameter Estimates, Reported Ranges and Data Sources

Parameter	Point Estimate*	Source
Prevalence of CAS		
0%-49% Stenosis	0.88 (0.84, 0.92)	Prospective diagnostic cohort study
Men	0.84 (0.78, 0.88)	Prospective diagnostic cohort study
Women	0.95 (0.90, 0.98)	Prospective diagnostic cohort study
50%-69% Stenosis	0.02 (0.01, 0.04)	Prospective diagnostic cohort study
Men	0.02 (0.00, 0.05)	Prospective diagnostic cohort study
Women	0.01 (0.00, 0.05)	Prospective diagnostic cohort study
70%-99% Stenosis	0.07 (0.04, 0.10)	Prospective diagnostic cohort study
Men	0.10 (0.06, 0.15)	Prospective diagnostic cohort study
Women	0.02 (0.00, 0.06)	Prospective diagnostic cohort study
100% Stenosis	0.03 (0.02, 0.06)	Prospective diagnostic cohort study
Men	0.05 (0.02, 0.09)	Prospective diagnostic cohort study
Women	0.01 (0.00, 0.05)	Prospective diagnostic cohort study
Carotid endarterectomy		
Risk of stroke in men	0.055 (0.015, 0.15)	Reference 3
Risk of stroke in women	0.070 (0.02, 0.26)	References 3, 11
Mortality	0.0106 (0.003, 0.03)	Reference 3
Costs [†]	4535 (3402, 5669)	Cost analysis
Time cost for patients (min)	4320 (3240, 5400)	Cost analysis
Contrast enhanced MR angiography		
Sensitivity for 70%-99% stenosis	0.94 (0.88, 0.97)	Reference 8
Specificity for 70%-99% stenosis	0.93 (0.89, 0.96)	Reference 8
Sensitivity for 50%-99% stenosis	0.96 (0.90, 0.99)	Reference 8
Specificity for 50%-99% stenosis	0.96 (0.90, 0.99)	Reference 8
Uninterpretable (%)	0.114 (0.09, 0.143)	Reference 3
Mortality due to contrast agent allergy	0.0000007 (0, 0.000016)	Reference 12
Costs [†]	384 (288, 480)	Cost analysis
Time cost for patients (min)	120 (90, 150)	Cost analysis
CT angiography		
Sensitivity for 70%-99% stenosis	0.91 (0.71, 0.99)	Prospective diagnostic cohort study
Specificity for 70%-99% stenosis	0.99 (0.98, 1.00)	Prospective diagnostic cohort study
Sensitivity for 50%-99% stenosis	1.00 (0.88, 1.00)	Prospective diagnostic cohort study
Specificity for 50%-99% stenosis	0.98 (0.96, 0.99)	Prospective diagnostic cohort study
Uninterpretable (%)	0.003 (0, 0.02)	Prospective diagnostic cohort study
Mortality due to contrast agent allergy	0.0000007 (0, 0.000016)	Reference 12
Costs [†]	198 (146, 247)	Cost analysis
Time cost for patients (min)	90 (67.5, 112.5)	Cost analysis

DSA

Sensitivity	1	Assumption
Specificity	1	Assumption
Risk of stroke	0.05 (0.003, 0.008)	Reference 13
Mortality due to contrast agent allergy	0.0000007 (0, 0.000016)	Reference 12
Mortality	0.001 (0.0003, 0.003)	Reference 13
Costs [†]	906 (680, 1133)	Cost analysis
Time cost for patients (min)	285 (214, 356)	Cost analysis
Duplex US		
Sensitivity for 70%-99% stenosis	0.89 (0.85, 0.92)	Prospective diagnostic cohort study
Specificity for 70%-99% stenosis	0.84 (0.77, 0.89)	Prospective diagnostic cohort study
Sensitivity for 50%-99% stenosis	0.84 (0.62, 0.95)	Prospective diagnostic cohort study
Specificity for 50%-99% stenosis	0.83 (0.73, 0.90)	Prospective diagnostic cohort study
Uninterpretable (%)	0.02 (0.008, 0.04)	Prospective diagnostic cohort study
Costs [†]	42 (32, 53)	Cost analysis
Time cost for patients (min)	80 (60, 100)	Cost analysis

*Data in parentheses are 95% confidence intervals (CIs).

[†]All costs were converted to 2007 euros

Data Sources and Assumptions

Prior probability. The prior probability of CAS was based on results of a cross-sectional prospective diagnostic cohort study of 351 patients with a TIA or minor stroke who were admitted between November 2002 and January 2005 to Erasmus University Medical Center, Rotterdam, the Netherlands. Percentage stenosis was categorized by using the NASCET method.¹ Data in 194 male and 139 female patients who had a TIA or minor stroke were included in the study. Nineteen (9.8%) male patients and three female patients (2.2%) had a severe stenosis (70%–99%), and four (2.1%) male patients and two female patients (1.4%) had a moderately severe stenosis (50%–69%). To keep the input data consistent, we derived the prior probability from the same study from which we derived the accuracy of CT angiography. Nevertheless, we performed sensitivity analysis by using a wide range of possible prior probabilities to explore the effect of this variable on the decision. On average, male patients were 62 years of age and female patients were 61 years of age. The age range of the entire population was 19–90 years, with an average age of 62 years. All patients underwent duplex US and multidetector CT angiography of the carotid arteries. If one of the examinations showed a stenosis of 50%–99%, a DSA examination of the carotid arteries followed in the context of the prospective diagnostic cohort study. If neither duplex US nor CT angiography showed a stenosis of greater than 50%, or if both examinations showed a stenosis of greater than 80%, DSA was not performed, to avoid unnecessary risk to the patient. Results of duplex US and CT angiography were interpreted independently. In the model, we used sex-specific prior probabilities of CAS (Table 1).

Diagnostic test performance. Data on the performance of CT angiography were derived from the same cross-sectional study mentioned above. The sensitivity and specificity of CT angiography at a cutoff point of 70%–99% stenosis were 0.91 (95% CI: 0.71, 0.99) and 0.99 (95% CI: 0.98, 1.00), respectively. Sensitivity and specificity at a cutoff point of 50%–99% stenosis were 1.00 (95% CI: 0.88, 1.00) and 0.98 (95% CI: 0.96, 0.99), respectively.

Written informed consent for the prospective diagnostic cohort study was obtained from all 351 patients, and the local ethics committee approved the study.

The diagnostic performances of duplex US and contrast-enhanced MR angiography were based on results of a meta-analysis⁸ that included 41 studies (2541 patients, 4876 arteries) published between January 1987 and April 2004. All studies included in the meta-analysis compared noninvasive imaging with intra-arterial angiography and met Standards for Reporting of Diagnostic Accuracy criteria; this ensured that only good-quality studies were included.¹⁴ Percentage stenosis was categorized by using the NASCET method.⁴ The sensitivity and specificity, respectively, of duplex US were 0.89 (95% CI: 0.85, 0.92) and 0.84 (95% CI: 0.77, 0.89) at a cutoff point of 70%–99% stenosis and 0.84 (95% CI: 0.62, 0.95) and 0.83 (95% CI: 0.73, 0.90) at a cutoff point of 50%–99% stenosis (Table 1). The sensitivity and specificity, respectively, of contrast-enhanced MR angiography were 0.94 (95% CI: 0.88, 0.97) and 0.93 (95% CI: 0.89, 0.96) at a cutoff point of 70%–99% stenosis and 0.96 (95% CI: 0.90, 0.99) and 0.96 (95% CI: 0.90, 0.99) at a cutoff point of 50%–99% stenosis (Table 1).

Information on the disadvantages of the tests was obtained from the prospective diagnostic cohort study and from the literature.^{13,15} The percentage of uninterpretable test results with duplex US was based on findings from the prospective diagnostic cohort study and was 1.99% (seven of 351 patients). Contrast-enhanced MR angiography cannot be performed in patients who are claustrophobic; this applied to 40 (11.4%) of 350 patients.³ Allergy to contrast medium confers a very small probability of dying (5.9×10^{-6})¹², which applies to contrast-enhanced MR angiography, CT angiography, and DSA. DSA as such imposes a risk of inducing a major stroke or death; this risk was modelled (Table 1).¹³

Treatment results. According to the latest publications on the treatment of CAS, carotid endarterectomy is still reported to be the best treatment.^{16–18} Consequently, we modelled carotid endarterectomy as the treatment for CAS. The periprocedural probability of stroke was modelled in a sex-specific fashion (Table 1).¹¹ Long-term outcomes were calculated in the same fashion as in the previous cost-effectiveness study by Buskens et al.³ (Table 2). Buskens et al. combined published clinical NASCET trial data with expert opinion and age- and sex-specific national survival statistics. The benefit of surgical treatment as compared with medical treatment was calculated. From the same national survival statistics, we calculated the risk of dying of a noncerebrovascular accident.

Prognosis and patient risk profile. In addition, we estimated the hazard rate ratios (HRRs) for stroke and death in patients with high-risk profiles compared with pa-

Table 2 HRRs and Event Rates: Parameter Estimates and Data Sources

Parameter	Year 0	Year 1	Year 2	Year 3	Long Term
HRR of CVA-related mortality after carotid endarterectomy	1.01	1.01	1.01	1.01	1.01
HRR of CVA-related mortality with 100% stenosis	1.175	1.09	1.04	1.03	1.03
HRR of CVA-related mortality with 70%-99% stenosis	1.14	1.07	1.03	1.02	1.02
HRR of CVA-related mortality with 50%-69% stenosis	1.06	1.03	1.015	1.015	1.015
HRR of CVA-related mortality with 0%-49% stenosis	1.02	1.01	1.01	1.01	1.01
Probability of stroke after carotid endarterectomy	0.02	0.02	0.02	0.02	0.02
Probability of stroke with 100% stenosis	0	0	0	0	0
Probability of stroke with 70%-99% stenosis	0.14	0.07	0.03	0.02	0.02
Probability of stroke with 50%-69% stenosis	0.08	0.04	0.02	0.02	0.02
Probability of stroke with 0%-49% stenosis	0.04	0.02	0.02	0.02	0.02
Probability of TIA after carotid endarterectomy	0.01	0.01	0.01	0.01	0.01
Probability of TIA with 100% stenosis	0	0	0	0	0
Probability of TIA with 70%-99% stenosis	0.07	0.04	0.02	0.01	0.01
Probability of TIA with 50%-69% stenosis	0.04	0.02	0.02	0.01	0.01
Probability of TIA with 0%-49% stenosis	0.02	0.01	0.01	0.01	0.01

Age- and sex-specific annual non-cerebrovascular accident (CVA)-related mortality data (in Appendix) were obtained from reference 19; all other data were obtained from reference 3.

tients with low-risk profiles and explored their effect on the decision (Table 3).²⁰ A high-risk profile was defined as either unilateral weakness or a symptom duration of 60 minutes or longer or at least two of the following: age 60 years or greater, blood pressure 140/90 mm Hg or higher, speech impairment without weakness, a symptom duration of 10–59 minutes, and diabetes. High risk was associated with an HRR of 2.0 or greater. Finally, we explored the effect of time between first symptoms and treatment (Table 3).^{1,3,5}

Quality of Life

Scores on a utility scale for quality of life after a TIA, after a minor stroke, and after a major stroke were estimated from several published studies.^{3,7,23} After a TIA or carotid endarterectomy, we assumed that patients had a utility of 0.88, which is similar to the mean utility in the general population of the same age.²⁶ We estimated the utility after a minor stroke (0.71) from the literature, and we used a utility of 0.31 for after a major stroke (Table 3).^{7,22,23} We also included disutilities for the events: For a TIA, we used a disutility of 0.0017, which we calculated in the same way as Buskens et al.³ For a minor or major stroke, we used a disutility of 0.0524—a value we found in the literature.²²

Table 3 Quality of Life and Costs: Parameter Estimates, Reported Ranges, and Data Sources

Parameter	Point Estimate*	Source
HRRs for stroke		
Low- to high-risk profile	1.0 (1, 10.6)	Reference 20
Early or late treatment after first symptoms	1.0 (0.5, 2.0)	Reference 21
Quality-of-life weights		
After TIA	0.88 (0.84, 0.92)	Reference 7, 22, 23
After minor stroke	0.71 (0.68, 0.74)	Reference 23
After major stroke	0.31 (0.28, 0.34)	Reference 23
Disutility for TIA	0.0017 (0.0015, 0.0019)	Reference 3
Disutility for minor stroke	0.0524 (0.0523, 0.0525)	Reference 22
Disutility for major stroke	0.0524 (0.0523, 0.0525)	Reference 22
Costs [†]		
Medication per year	20 (15, 25)	Reference 24
Minor stroke during 1st year	7654 (5740, 9567)	Reference 3
Minor stroke subsequent year	1310 (982, 1637)	Reference 3
Major stroke during 1st year	43650 (32737, 54562)	Reference 3
Major stroke subsequent year	25487 (19116, 31859)	Reference 3
Travel cost per visit	5 (4, 6)	Estimation
Time cost per hour	18 (13,22)	Estimation
Friction period (wk)	22	Reference 25
Friction cost per hour		
Men	51 (38, 63)	Reference 25
Women	39 (29, 48)	Reference 25

*Data in parentheses are 95% CIs

[†]All costs were converted to 2007 euros

Costs

We estimated the costs of duplex US, CT angiography, and DSA, including hospitalization, if applicable, in 2007 euros. Current costs, which included expenditures for personnel, equipment, materials, maintenance, housing, cleaning, administration, and overhead, were determined at the Erasmus Medical Center. Additional estimates of costs associated with hospitalization and stroke in the Dutch setting were obtained from the study of Buskens et al.³ For assessment of the costs of contrast-enhanced MR angiography and carotid endarterectomy, we performed a systematic review of the published literature (Table 1).²⁷

Data Analysis

The reference-case analysis was performed for a 60-year-old man. We assumed that the average patient had a low-risk profile and underwent surgery between 2 and 4 weeks after the first symptoms.^{3,28} Diagnostic strategies were compared in terms of costs, effects (in quality-adjusted life-years [QALYs]), incremental cost-effectiveness ratios (ICERs), and net health benefit (NHB) by using a threshold willingness-to-pay (WTP) of €50000 per QALY. NHB is a multiattribute outcome that combines effectiveness and costs in one measure, with $NHB = QALYs - (costs/WTP)$. A strategy with the highest NHB was considered to be the most cost effective, which was equivalent to the highest QALYs at an ICER of less than the WTP of €50000 per QALY. The reference case analysis was performed by using cost estimates and recommendations for cost-effectiveness analyses from the Netherlands that took productivity losses (friction costs) into account and discounted future costs and effectiveness at 4% and 1.5%, respectively.²⁵ Also, a second WTP threshold of €80000 per QALY was considered, as recommended by the Dutch Council for Public Health.²⁹

Subsequently, we performed the cost-effectiveness analysis from the societal perspective according to United States recommendations, considering QALYs, health care costs, and direct non-health care costs (patient time and travel costs), and we discounted both future costs and effectiveness at 3%.^{30–32} Finally, we performed an analysis according to United Kingdom recommendations, discounting both future costs and effectiveness at 3.5%.^{33,34}

We performed extensive sensitivity analyses in which we explored varying assumptions about the risk profile of the patient, the timing of surgery after the first symptoms, and the prior probability of CAS. In addition, we performed a probabilistic sensitivity analysis by using 1000 Monte Carlo simulations in which we sampled from distributions of all uncertain variable values. We calculated the probability that a certain strategy was cost effective compared with other strategies with varying WTP thresholds and present acceptability curves. The expected value of perfect information (EVPI) (simulation with 1000 samples) was calculated to assess the value of performing further research.³⁵ The population EVPI was calculated for the European Union by assuming an annual absolute stroke incidence of 1 million among women and 1 million among men and considering 5 years.^{36,37}

Results

Reference Case Analysis

All strategies that used CT angiography or contrast-enhanced MR angiography, either as a solo strategy or in combination with an initial duplex US examination, demonstrated similar costs and effectiveness, presuming a 2–4 week delay in surgery. In men in similar conditions, the combination strategy of duplex US followed by CT angiography with a cutoff of 70%–99% stenosis dominated all other

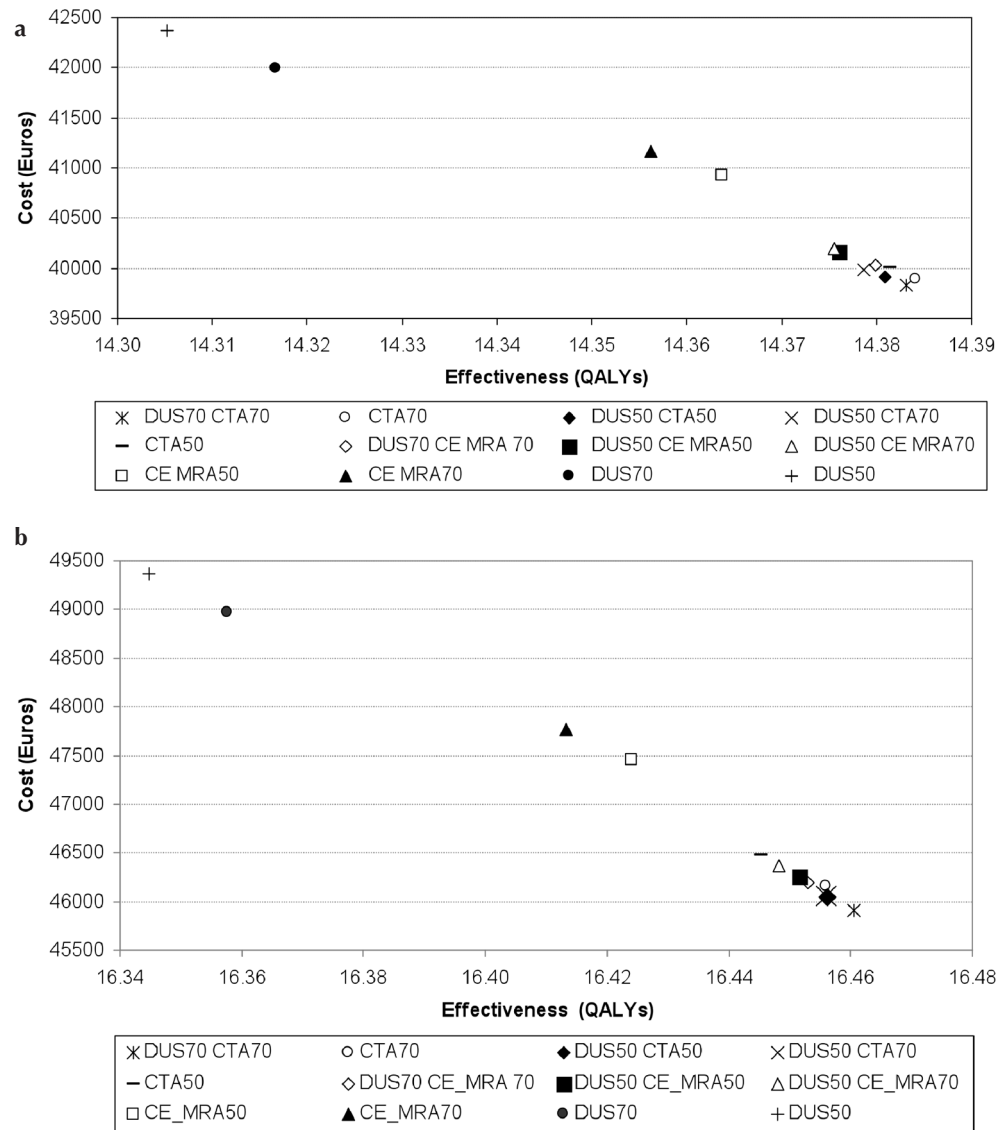


Figure 2: Cost-effectiveness graphs obtained by using the Dutch recommendations for cost-effectiveness analyses in (a) men and (b) women show expected lifetime cost versus QALYs for the various strategies. (a) In men, the combination strategy of duplex US (DUS) and CT angiography (CTA) with a cutoff of 70%–99% stenosis (70) yielded the highest effectiveness at the lowest costs compared with all other strategies except the solo CT angiography strategy with a cutoff of 70%–99% stenosis, which yielded slightly more QALYs, for €71 419 per QALY gained. (b) In women, the combination strategy of duplex US and CT angiography with a cutoff of 70%–99% stenosis yielded the highest effectiveness at the lowest costs compared with all other strategies. 50 = 50%–99% Stenosis, CE MRA = contrast-enhanced MR angiography.

Table 4 Reference Case Analysis Results

Patient and Strategy	Costs (€)	QALYs	ICER	NHB for WTP of €50000 per QALY	NHB for WTP of €80000 per QALY
60-Year-old man					
Duplex US and CT angiography for 70%-99% stenosis (reference strategy)	39826	14.3832		13.587	13.885
CT angiography for 70%-99% stenosis	39893	14.3841	€71419	13.586	13.885
Duplex US and CT angiography for 50%-99% stenosis	39914	14.3809	Dominated	13.583	13.882
Duplex US for 50%-99% stenosis and CT angiography for 70%-99% stenosis	39986	14.3787	Dominated	13.579	13.879
CT angiography for 50%-99% stenosis	40004	14.3815	Dominated	13.581	13.881
Duplex US and contrast-enhanced MR angiography for 70%-99% stenosis	40028	14.3799	Dominated	13.579	13.880
Duplex US and contrast-enhanced MR angiography for 50%-99% stenosis	40162	14.3761	Dominated	13.573	13.874
Duplex US for 50%-99% stenosis and MR angiography for 70%-99% stenosis	40193	14.3755	Dominated	13.572	13.873
Contrast-enhanced MR angiography for 50%-99% stenosis	40924	14.3637	Dominated	13.545	13.852
Contrast-enhanced MR angiography for 70%-99% stenosis	41166	14.3562	Dominated	13.533	13.842
Duplex US for 70%-99% stenosis	41997	14.3167	Dominated	13.477	13.792
Duplex US for 50%-99% stenosis	42368	14.3052	Dominated	13.458	13.776
60-Year-old woman					
Duplex US and CT angiography for 70%-99% stenosis (reference strategy)	45911	16.4605		15.542	15.887
Duplex US and CT angiography for 50%-99% stenosis	46046	16.4562	Dominated	15.535	15.881
Duplex US for 50%-99% stenosis and CT angiography for 70%-99% stenosis	46057	16.4559	Dominated	15.535	15.880
CT angiography for 70%-99% stenosis	46153	16.4559	Dominated	15.533	15.879
Duplex US and contrast-enhanced MR angiography for 70%-99% stenosis	46199	16.4531	Dominated	15.529	15.876
Duplex US and contrast-enhanced MR angiography for 50%-99% stenosis	46256	16.4517	Dominated	15.527	15.873
Duplex US for 50%-99% stenosis and MR angiography for 70%-99% stenosis	46362	16.4482	Dominated	15.521	15.869
CT angiography for 50%-99% stenosis	46475	16.4452	Dominated	15.516	15.864

Contrast-enhanced MR angiography for 50%-99% stenosis	47454	16.4239	Dominated	15.475	15.831
Contrast-enhanced MR angiography for 70%-99% stenosis	47772	16.4133	Dominated	15.458	15.816
Duplex US for 70%-99% stenosis	48965	16.3577	Dominated	15.378	15.746
Duplex US for 50%-99% stenosis	49362	16.3448	Dominated	15.358	15.728

The cost-effectiveness analysis was performed by using recommendations from the Netherlands. Note that all strategies are dominated by the combination strategy of duplex US and CT angiography for 70%-99% stenosis (ie, this strategy is more or equally effective and less costly) except for CT angiography of 70%-99% stenosis in men, which had an ICER that was higher than the chosen threshold WTP. The percentages refer to the degree of stenosis that was considered a positive test result.

strategies, except the solo CT angiography strategy with a cutoff of 70%–99% stenosis, which yielded slightly more QALYs, for €71419 per QALY gained (Fig 2a, Table 4). Likewise, in women, the duplex US–CT angiography combination strategy with a cutoff of 70%–99% stenosis dominated all other strategies (Fig 2b, Table 4). With a WTP of €50000 per QALY, the duplex US–CT angiography strategy yielded the highest NHB in both men and women, whereas with a higher WTP of €80000 per QALY, the solo CT angiography strategy would be preferable in men (Table 4). In both men and women, the least cost-effective strategy was duplex US performed as a solo test. Furthermore, all strategies employing contrast-enhanced MR angiography were dominated by the corresponding strategies employing CT angiography (Table 4).

Probabilistic Sensitivity Analysis

In men, the acceptability curve of the combination strategy of duplex US and CT angiography with a cutoff of 70%–99% stenosis was highest (33%–48%) for all WTP values of less than €100000 per QALY (Fig 3a). The solo CT angiography strategy showed an increasing chance of being most cost effective with increasing WTP values. The value-of-information analysis demonstrated an EVPI for further research of €318 per male patient, which implies a population EVPI of €1.5 billion for the European Union.

In women, the acceptability curve showed that the duplex US–CT angiography combination strategy with a cutoff of 70%–99% stenosis was most cost effective, with an 80% probability, irrespective of the WTP (Fig 3b). The value-of-information analysis demonstrated an EVPI for further research of €40 per female patient, which implies a population EVPI of €193 million for the European Union.

Sensitivity Analysis

United Kingdom and United States recommendations. Analyses performed by using United Kingdom

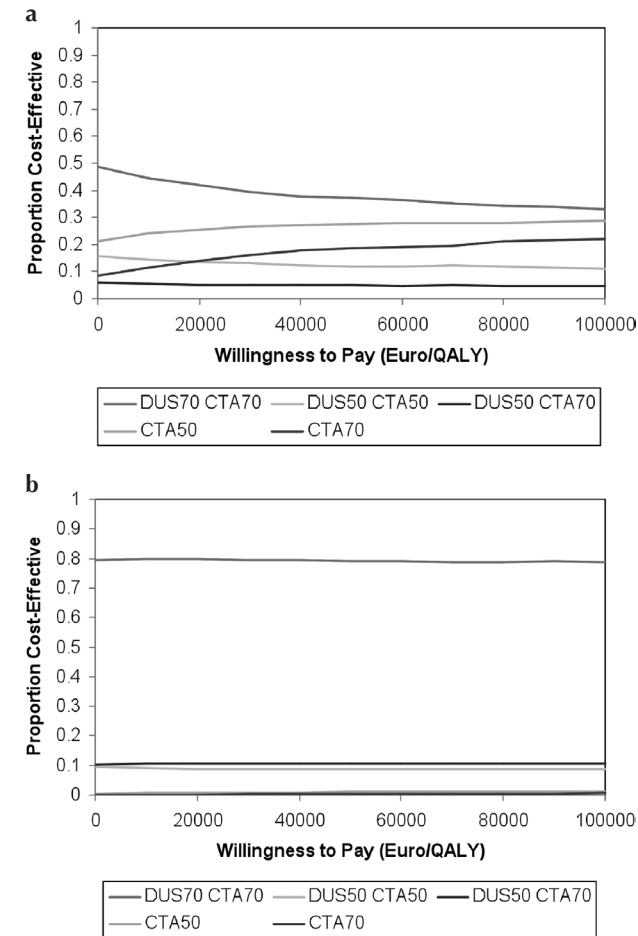


Figure 3: Acceptability curves with the five most competitive strategies for (a) men and (b) women. The graphs plot the proportion of simulated scenarios in the probabilistic sensitivity analysis for which each of the strategies is the most cost effective for varying thresholds of WTP. The probabilistic sensitivity analysis included all strategies. Strategies with a very low probability of being cost effective are not shown. 50 = 50%–99% Stenosis, 70 = 70%–99% stenosis, CTA = CT angiography, DUS = duplex US.

and United States recommendations yielded the same results as the analysis performed by using the Dutch recommendations.

Patient risk profile. For men, if the HRR for the risk profile was 1.03, indicating a low-risk profile, the duplex US–CT angiography combination strategy with a cutoff of 70%–99% stenosis yielded the highest NHB. For HRRs that were slightly higher but still close to 1.03, the solo CT angiography strategy with a cutoff of 70%–99% stenosis was the most cost effective. For HRRs that were clearly greater than 1.11, the CT angiography solo strategy with a cutoff for surgery of 50%–99% stenosis yielded a higher NHB (Fig 4). For women, the duplex US–CT angiography combination strategy with a cutoff of 70%–99% stenosis was most cost effective for an HRR of 1.47 or less; above this threshold, the duplex US–CT angiography combination strategy with a cutoff of 50%–99% stenosis had a higher NHB. If the HRR was greater than 2.34, the solo CT angiography strategy with a cutoff of 50%–99% stenosis was the most cost effective (Fig 4).

Prior probability. The prior probability of CAS was derived from the prospective diagnostic cohort study and was clearly lower than that in the study of Buskens

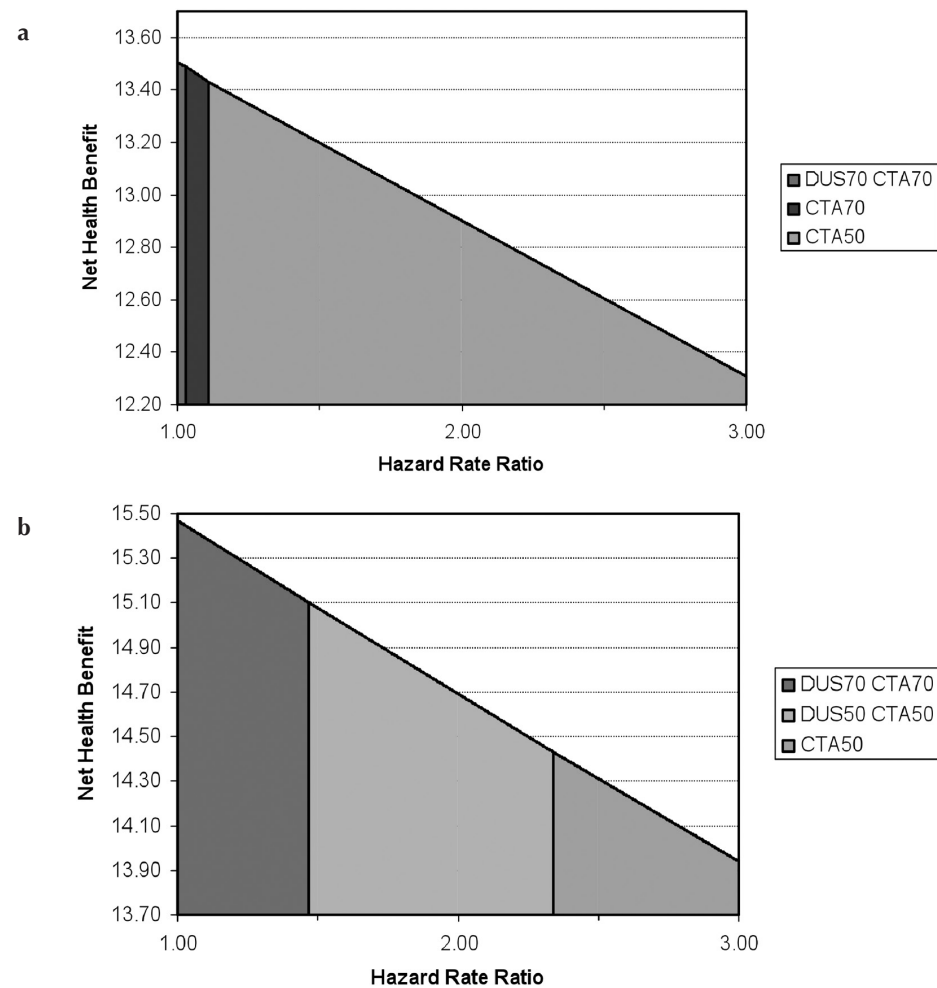


Figure 4: Graphs show results of sensitivity analysis exploring the effect of different patient risk profiles in (a) men and (b) women. Higher-risk profiles are represented with increasing HRRs on the x-axis. The outcome is expressed in NHB on the y-axis with a WTP of €50 000 per QALY. Shading = optimal strategy. 50 = 50%–99% Stenosis, 70 = 70%–99% stenosis, CTA = CT angiography, DUS = duplex US.

et al.³ For men with a low prior probability of disease, the duplex US–CT angiography combination strategy with a cutoff of 70%–99% stenosis had the highest NHB. When the prior probability was greater than 0.20, the solo CT angiography strategy had the highest NHB, and when the prior probability was greater than 0.30, CT angiography with a cutoff of 50%–99% stenosis was optimal (Fig 5a). For women, the solo CT angiography strategy with a cutoff of 70%–99% stenosis had the highest NHB when the prior probability increased above 0.30; with a lower prior probability, the duplex US–CT angiography combination strategy with a cutoff of 70%–99% stenosis had the highest NHB (Fig 5b).

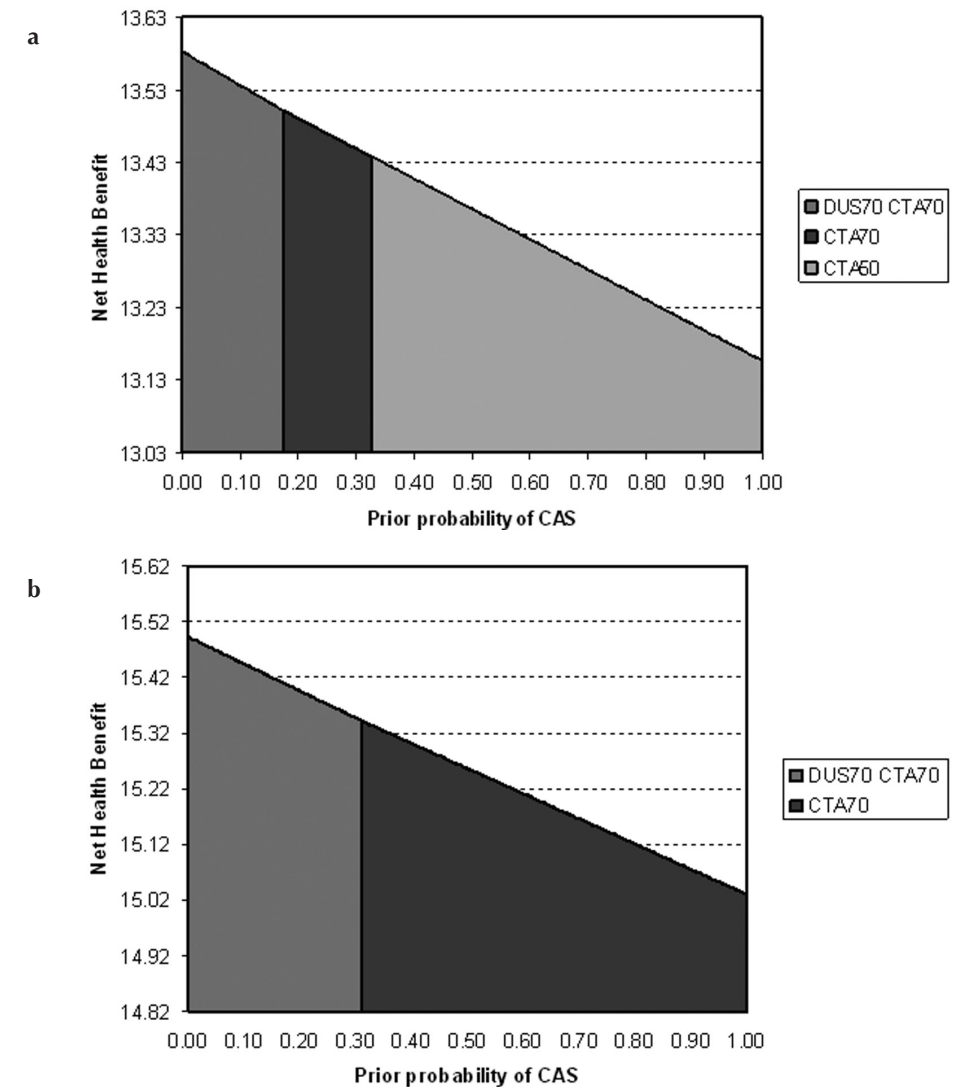


Figure 5: Graphs show results of sensitivity analysis exploring the effect of the prior probability of CAS (x-axis) on the NHB (y-axis) with a WTP of €50 000 per QALY in (a) men and (b) women. Shading = corresponding optimal strategy. 50 = 50%–99% Stenosis, 70 = 70%–99% stenosis, CTA = CT angiography, DUS = duplex US.

Timing of surgery. For men undergoing surgery without delay, the solo CT angiography strategy with a cutoff of 50%–99% stenosis yielded the highest NHB (Fig 6a). With a longer delay, the solo CT angiography strategy with a cutoff of 70%–99% stenosis yielded the highest NHB, followed by the duplex US–CT angiography combination strategy with a cutoff of 70%–99% stenosis, if surgery was performed more than 4 weeks after first symptoms. For women undergoing surgery without delay, the duplex US–CT angiography combination strategy with a cutoff of 50%–99% stenosis had the highest NHB, whereas a cutoff of 70%–99% stenosis would be best if surgery cannot be performed within 2 weeks (Fig 6b).

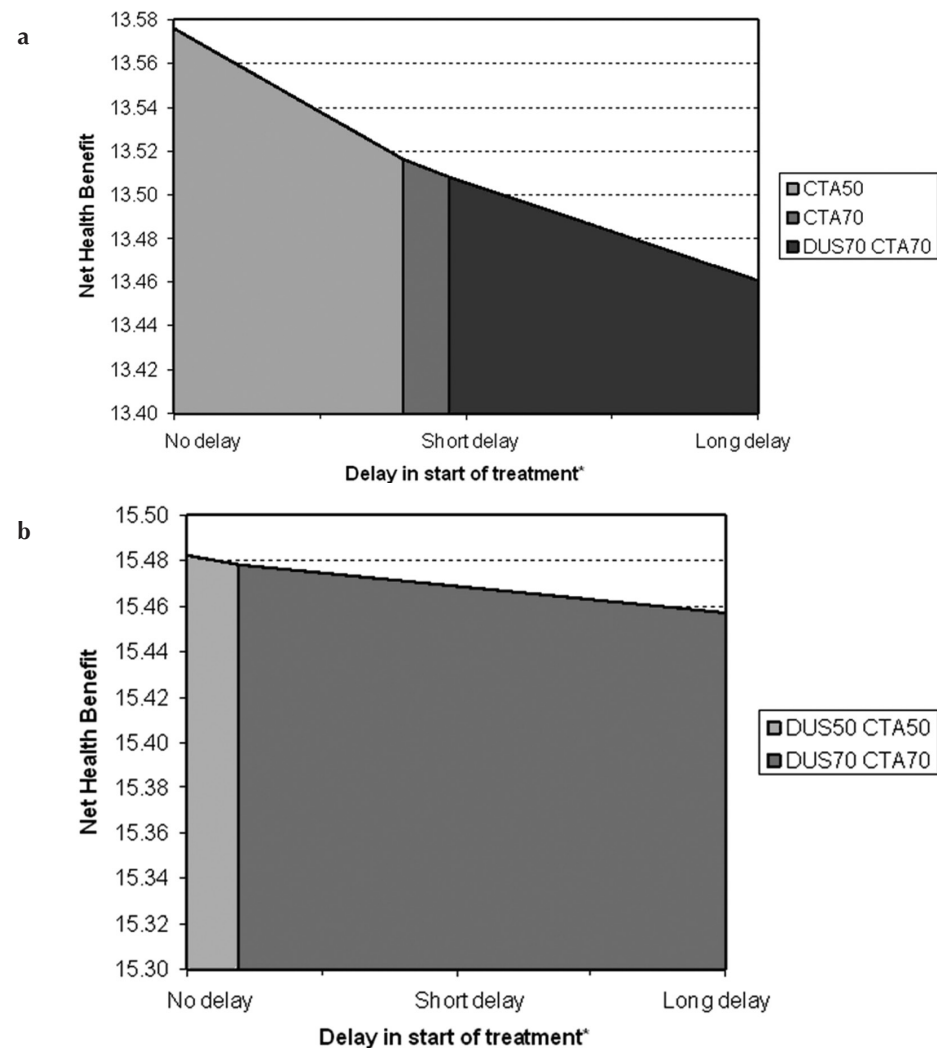


Figure 6: Graphs show results of sensitivity analysis exploring the effect of a delay in treatment after the first symptoms in weeks (x-axis) on the NHB (y-axis) with a WTP of €50 000 per QALY in (a) men and (b) women. Shading = corresponding optimal strategy. □ "Short delay" = delay in treatment ranging from 2 to 4 weeks; "long delay" = delay in treatment of more than 4 weeks.

Discussion

Our study evaluated the cost-effectiveness of various noninvasive tests. The results demonstrated that the duplex US–CT angiography combination strategy with a cut-off of 70%–99% stenosis is the most cost-effective strategy. If the WTP is higher than we assumed—that is, €80 000 per QALY instead of €50 000 per QALY—then the solo CT angiography strategy would be more effective than the combina-

tion strategy at an acceptable ICER in men, whereas in women, the combination strategy would remain optimal. The sensitivity analysis demonstrated that with an increase in patient risk profile or with a higher prior probability of disease, the criterion to perform surgery should be more lenient (50%–99% stenosis) and the solo CT angiography strategy would be preferred to a combination test strategy. Also, if surgery can be performed without delay, a more lenient criterion (50%–99%) for surgery and a single-test strategy with CT angiography would be preferred. Notably, we found that all strategies employing contrast-enhanced MR angiography were dominated by the corresponding CT angiography strategies.

Although we found very small differences in QALYs across the strategies, there were clear differences in costs. This phenomenon is generally found in diagnostic test evaluation.³⁸ Even though differences are small on average, they are nevertheless important because they pertain to a large group of patients and in aggregate can have large consequences. Note that a small average difference in the context of diagnostic test strategies implies that for most patients there is no difference between the evaluated strategies, but for a few patients the consequence can be very large in that a serious complication or event may be avoided with the optimal strategy.

In women, results were less sensitive to changes in the input values than in men. The probabilistic sensitivity analysis demonstrated that whereas for women results were fairly robust, results for men were less certain. The prior probability was lower among women and the risk of surgery was higher, implying that the mean expected gain of performing a diagnostic work-up is less in women; this led to more consistent results favoring less invasive imaging in the sensitivity analysis. This is also reflected in the results of the value-of-information analysis, which demonstrated a high value, especially in men, which suggests that it is worth exploring this issue and performing further studies in this area, especially for men.

As with all decision- and cost-effectiveness models, several assumptions had to be made to keep the model coherent. In finding parameter estimates, we chose to stay as close as possible to the primary data (especially with respect to costs) to ensure the internal consistency of the model, rather than using data from diverse published sources. This may have reduced the generalizability of our results. One assumption concerned the follow-up period and event rates, which were based on the article by Buskens et al.³ Their results dated from 1998, and since then a great deal of new information about event rates in the follow-up period has been published. We adjusted event rates for this new data by including HRRs that were found in the literature for the patient's risk profile and delay between first symptoms and surgery.

Radiation risk was not considered in our model. Although radiation risk is an important consideration in performing CT, the risk for this particular clinical patient population is small in comparison to their risk of cardiovascular events. In particular, the amount of radiation at neck CT angiography is low, only the thyroid is at risk, and the average age of patients with a TIA or minor stroke is high. With a latency period of about 12 years before cancer develops and the high probability that these patients will die of cardiovascular disease before a radiation-induced

cancer can develop, radiation risk is unlikely to influence the decision.³⁹ Finally, the risk of nephrotoxicity was not considered because this is a very small risk, with in most cases only temporary consequences. In patients with renal insufficiency, CT angiography and contrast-enhanced MR angiography are contraindicated; such patients were not considered in this analysis.

For the sensitivity and specificity of duplex US and contrast-enhanced MR angiography, we used data from the meta-analysis by Wardlaw et al.⁸ Other sources of diagnostic performance results of duplex US, CT angiography, and MR angiography were not applicable to our model because they did not report sensitivity and specificity for the criteria that we examined (both 70%–99% and 50%–99% stenoses), because they did not report results with state-of-the-art imaging techniques (ie, contrast-enhanced rather than nonenhanced MR angiography and multidetector instead of single-detector CT angiography), or because the results were not from a large prospectively performed clinical study.^{40,41} In the current analysis, we used sensitivity and specificity data for multidetector CT angiography from a recently completed prospective cohort study rather than from a meta-analysis because to our knowledge, no meta-analysis involving multidetector CT angiography has been published. A meta-analysis involving single-section CT angiography has been performed⁴², but single-section CT angiography is currently no longer a state-of-the-art technique. One small retrospective pilot study of multidetector CT angiography of the carotid arteries⁴³ was published in 2009. This study showed high sensitivity and specificity and supports our estimates.

It is remarkable that in our study, duplex US turned out to be the most costly strategy; this is in stark contrast to the results reported by Buskens et al.³, which clearly showed that duplex US was the most effective and least costly strategy. Buskens et al., however, compared duplex US with nonenhanced rather than contrast-enhanced MR angiography and did not consider CT angiography. Similarly, Wardlaw et al.^{7,8} concluded that duplex US is the most cost-effective strategy. Their data were, however, based on a combination of single- and multidetector CT angiography instead of solely multidetector CT angiography, and only a limited number of studies reporting CT angiography results were available at the time of their analysis. We therefore used a higher sensitivity (91% vs 77%) and a higher specificity (99% vs 95%) for CT angiography than Wardlaw et al; this was justified by a recent study of multidetector CT angiography⁴³ that demonstrated similar values.

Two controversies in the management of CAS were considered in our analysis and proved to be important in choosing a diagnostic work-up: the cutoff value chosen as the indication for surgery (50%–99% vs 70%–99% stenosis) and the delay between first symptoms and surgery. The results highlight how the benefit that can be gained with treatment should influence the diagnostic work-up. Our results suggest that if the patient cannot undergo surgery in a timely fashion, an initial duplex US examination and a 70%–99% stenosis criterion for surgery is indicated. On the other hand, if the patient can undergo surgery in a timely fashion, immediate CT angiography and the use of a lenient criterion (50%–99% stenosis) as the surgery indication is beneficial.

Implementing the results of this study should always be done with consideration of the individual patient and the local situation. The prior probability of CAS and the risk profile of the individual patient or as observed in the local patient population may be very different and affect the choice of work-up.

Similarly, logistics and waiting lists may influence the diagnostic work-up. Furthermore, local expertise with duplex US, CT angiography, and contrast-enhanced MR angiography may influence the decision: If, for example, no local expertise exists with CT angiography of the carotid arteries, whereas contrast-enhanced MR angiography can be performed at low cost, without delay, with good quality, and with high diagnostic performance, then our results justify the use of contrast-enhanced MR angiography instead of CT angiography. Finally, patient behavior, patient preferences, and local treatment options should be considered. Of note, our analysis highlights that if patients present rapidly after their first symptoms and local treatment of patients with TIA or minor stroke is streamlined, a solo CT angiography strategy with lenient criteria for surgery is indicated. The fact that benefit can be gained by streamlining the work-up of patients with TIA or stroke has been pointed out before, but as yet, not all centers are able to organize TIA and stroke care efficiently.^{5,28}

In conclusion, patients with a TIA or minor stroke should undergo duplex US as an initial diagnostic test, followed by CT angiography if the duplex US results are positive, with surgery for 70%–99% stenoses, while in patients with a high risk profile, with a high prior probability of carotid stenosis, or who can undergo surgery without delay, immediate CT angiography and surgery for 50%–99% stenoses are indicated.

References

1. Beneficial effect of carotid endarterectomy in symptomatic patients with high-grade carotid stenosis. North American Symptomatic Carotid Endarterectomy Trial Collaborators. *N Engl J Med* 1991; 325(7):445–453.
2. MRC European Carotid Surgery Trial: interim results for symptomatic patients with severe (70–99%) or with mild (0–29%) carotid stenosis. European Carotid Surgery Trialists' Collaborative Group. *Lancet* 1991; 337(8752):1235–1243.
3. Buskens E, Nederkoorn PJ, Buijs-Van Der Woude T, et al. Imaging of carotid arteries in symptomatic patients: cost-effectiveness of diagnostic strategies. *Radiology* 2004; 233(1):101–112.
4. Barnett HJ, Taylor DW, Eliasziw M, et al. Benefit of carotid endarterectomy in patients with symptomatic moderate or severe stenosis. North American Symptomatic Carotid Endarterectomy Trial Collaborators. *N Engl J Med* 1998; 339(20):1415–1425.
5. Rothwell PM, Eliasziw M, Gutnikov SA, Warlow CP, Barnett HJ; Carotid Endarterectomy Trialists Collaboration. Endarterectomy for symptomatic carotid stenosis in relation to clinical subgroups and timing of surgery. *Lancet* 2004; 363(9413):915–924.
6. Randomised trial of endarterectomy for recently symptomatic carotid stenosis: final results of the MRC European Carotid Surgery Trial (ECST). *Lancet* 1998; 351(9113):1379–1387.
7. Wardlaw JM, Chappell FM, Stevenson M, et al. Accurate, practical and cost-effective assessment of carotid stenosis in the UK. *Health Technol Assess* 2006; 10:iii–iv, ix–x, 1–182.
8. Wardlaw JM, Chappell FM, Best JJ, Wartolowska K, Berry E; NHS Research and Development Health Technology Assessment Carotid Stenosis Imaging Group. Non-invasive imaging compared with intra-arterial angiography in the diagnosis of symptomatic carotid stenosis: a meta-analysis. *Lancet* 2006; 367(9521):1503–1512.
9. U-King-Im JM, Hollingworth W, Trivedi RA, et al. Cost-effectiveness of diagnostic strategies prior to carotid endarterectomy. *Ann Neurol* 2005; 58(4):506–515.
10. Kent KC, Kuntz KM, Patel MR, et al. Peri-operative imaging strategies for carotid endarterectomy: an analysis of morbidity and cost-effectiveness in symptomatic patients. *JAMA* 1995; 274(11):888–893.
11. Bond R, Rerkasem K, Cuffe R, Rothwell PM. A systematic review of the associations between age and sex and the operative risks of carotid endarterectomy. *Cerebrovasc Dis* 2005; 20(2):69–77.
12. Katayama H, Yamaguchi K, Kozuka T, Takashima T, Seez P, Matsuura K. Adverse reactions to ionic and nonionic contrast media: a report from the Japanese Committee on the Safety of Contrast Media. *Radiology* 1990; 175(3):621–628.
13. Willinsky RA, Taylor SM, TerBrugge K, Farb RI, Tomlinson G, Montanera W. Neurologic complications of cerebral angiography: prospective analysis of 2,899 procedures and review of the literature. *Radiology* 2003; 227(2):522–528.
14. Bossuyt PM, Reitsma JB, Bruns DE, et al; Standards for Reporting of Diagnostic Accuracy. Towards complete and accurate reporting of studies of diagnostic accuracy: the STARD Initiative. *Radiology* 2003; 226(1):24–28.
15. Nederkoorn PJ, Mali WP, Eikelboom BC, et al. Preoperative diagnosis of carotid artery stenosis: accuracy of noninvasive testing. *Stroke* 2002; 33(8):2003–2008.
16. Brown MMEJ, Bonati LH. Safety results of the International Carotid Stenting Study (ICSS): early outcome of patients randomised between carotid stenting and endarterectomy for symptomatic carotid stenosis. Stockholm, Sweden: *European Stroke Conference*, 2009.
17. Levy EI, Mocco J, Samuelson RM, Ecker RD, Jahromi BS, Hopkins LN. Optimal treatment of carotid artery disease. *J Am Coll Cardiol* 2008; 51(10):979–985.
18. Janssen MP, de Borst GJ, Mali WP, et al. Carotid stenting versus carotid endarterectomy: evidence basis and cost implications. *Eur J Vasc Endovasc Surg* 2008; 36:258–264.
19. Statline of Central Bureau of Statistics, the Netherlands. statline.cbs.nl. Published 2008. Accessed March 8, 2008.
20. Johnston SC, Rothwell PM, Nguyen-Huynh MN, et al. Validation and refinement of scores to predict very early stroke risk after transient ischaemic attack. *Lancet* 2007; 369(9558):283–292.
21. Rothwell PM, Giles MF, Chandratheva A, et al; Early use of Existing Preventive Strategies for Stroke (EXPRESS) study. Effect of urgent treatment of transient ischaemic attack and minor stroke on early recurrent stroke (EXPRESS study): a prospective population-based sequential comparison. *Lancet* 2007; 370(9596):1432–1442.
22. Sullivan PW, Ghushchyan V. Mapping the EQ-5D index from the SF-12: US general population preferences in a nationally representative sample. *Med Decis Making* 2006; 26(4):401–409.
23. Hallan S, Asberg A, Indredavik B, Widerøe TE. Quality of life after cerebrovascular stroke: a systematic study of patients' preferences for different functional outcomes. *J Intern Med* 1999; 246(3):309–316.
24. Dutch Health Care Insurance Board. Farmacotherapeutic compass. www.fk.cvz.nl. Published 2008. Accessed March 3, 2008.
25. Oostenbrink JB, Koopmanschap MA, Rutten FF. Standardisation of costs: the Dutch Manual for Costing in economic evaluations. *Pharmacoeconomics* 2002; 20(7):443–454.
26. Fryback DG, Dasbach EJ, Klein R, et al. The Beaver Dam Health Outcomes Study: initial catalog of health-state quality factors. *Med Decis Making* 1993; 13(2):89–102.
27. U-King-Im JM, Hollingworth W, Trivedi RA, et al. Contrast-enhanced MR angiography vs intra-arterial digital subtraction angiography for carotid imaging: activity-based cost analysis. *Eur Radiol* 2004; 14(4):730–735.
28. Scotland NHS. Scottish Stroke Care Audit. <http://www.strokeaudit.scot.nhs.uk/Downloads/files/Final%20Proof%20140207.pdf>. Published July 31, 2006. Accessed May 5, 2009.
29. Dutch Council for Public Health and Health Care. Sensible and sustainable care. http://www.rvz.net/data/download/Engelse_vertaling_samenvatting.doc. Published June 2006. Accessed January 6, 2009.
30. Gold MR, Patrick DL, Torrance GW, Fryback DG, et al. Cost-effectiveness in health and medicine. *J Ment Health Policy Econ* 1996; 2:91–92.
31. Siegel JE, Weinstein MC, Russell LB, Gold MR; Panel on Cost-Effectiveness in Health and Medicine. Recommendations for reporting cost-effectiveness analyses. *JAMA* 1996; 276(16):1339–1341.

32. Weinstein MC, Siegel JE, Gold MR, Kamlet MS, Russell LB. Recommendations of the Panel on Cost-effectiveness in Health and Medicine. *JAMA* 1996; 276(15):1253–1258.
33. Brouwer WB, Niessen LW, Postma MJ, Rutten FF. Need for differential discounting of costs and health effects in cost effectiveness analyses. *BMJ* 2005; 331(7514):446–448.
34. National Institute for Clinical Excellence (NICE). Guide to the methods of technology appraisal. Oxford, England: Radcliff Medical Press, 2004.
35. Groot Koerkamp B, Nikken JJ, Oei EH, Stijnen T, Ginai AZ, Hunink MG. Value of information analysis used to determine the necessity of additional research: MR imaging in acute knee trauma as an example. *Radiology* 2008; 246(2):420–425.
36. WHO. World health organization. The global burden of disease. http://www.who.int/healthinfo/global_burden_disease/GBD_report_2004update_full.pdf. Published 2004. Updated 2008. Accessed December 17, 2009.
37. Hollander M, Koudstaal PJ, Bots ML, Grobbee DE, Hofman A, Breteler MM. Incidence, risk, and case fatality of first ever stroke in the elderly population. The Rotterdam Study. *J Neurol Neurosurg Psychiatry* 2003; 74(3):317–321.
38. Weinstein MC, Stason WB. Foundations of cost-effectiveness analysis for health and medical practices. *N Engl J Med* 1977; 296(13):716–721.
39. Einstein AJ, Henzlova MJ, Rajagopalan S. Estimating risk of cancer associated with radiation exposure from 64-slice computed tomography coronary angiography. *JAMA* 2007; 298(3):317–323.
40. Debrey SM, Yu H, Lynch JK, et al. Diagnostic accuracy of magnetic resonance angiography for internal carotid artery disease: a systematic review and meta-analysis. *Stroke* 2008; 39(8):2237–2248.
41. Chappell FM, Wardlaw JM, Young GR, et al. Carotid artery stenosis: accuracy of noninvasive tests—individual patient data meta-analysis. *Radiology* 2009; 251(2):493–502.
42. Koelemay MJ, Nederkoorn PJ, Reitsma JB, Majoie CB. Systematic review of computed tomographic angiography for assessment of carotid artery disease. *Stroke* 2004; 35(10):2306–2312.
43. Puchner S, Popovic M, Wolf F, Reiter M, Lammer J, Bucek RA. Multidetector CTA in the quantification of internal carotid artery stenosis: value of different reformation techniques and axial source images compared with selective carotid arteriography. *J Endovasc Ther* 2009; 16(3):336–342.

Chapter 6
Appendix

Appendix

Model We developed a decision model by using decision-analytical software (DATA Pro 2008 Suite; TreeAge Software) to evaluate the cost-effectiveness of using duplex US (called "DUS" in the model), CT angiography (called "CTA" in the model), contrast-enhanced MR angiography (called "CE-MRA" in the model), or a combination of duplex US and CT angiography or duplex US and contrast-enhanced MR angiography in the diagnosis of a CAS. We compared the single tests and the tests in combination. If the test result was positive, carotid endarterectomy (called "CEA" in the model) followed. If results of the initial test were not interpretable, DSA followed instead. For the combination strategies, only when the first test (duplex US) had a positive result, a second test (CT angiography or contrast-enhanced MR angiography) followed. Short-term outcomes related to the diagnostic imaging tests were modeled with a decision tree, and a Markov model was used to model long-term outcomes. The Markov model, with a cycle length of 1 year, simulated the lifetime consequences depending on changes in length and quality of life caused by having experienced a TIA, a minor stroke, a major stroke, or death (caused either by a cerebrovascular accident ["CVA" in the model] or by a noncerebrovascular event). We created 11 different health states; namely, Alive, PostTIA, Post-TIA2, Post-TIA Stable, Post-Minor, Post-Minor2, Post-Minor Stable, PostMajor, Post-Major2, Post-Major Stable, and Dead. Everyone started in the Alive state, except patients who experienced a stroke caused by carotid endarterectomy or DSA, who proceeded directly to the minor or major stroke state. Depending on whether an event occurred and what type of event, patients moved to other health states in the model. Patients who were symptom free for 3 years moved to the Stable state.

In our model, the variable "Male" coded the sex of the patients. Male = 1 referred to male patients, and Male = 0 referred to female patients. The initial age was 60 years, and each cycle age was increased by 1 year.

In our model, we included strict (70%–99% stenosis) and lenient (50%–99% stenosis) criteria for diagnosing a CAS. CutoffTest50 = 0 referred to the diagnostic test with strict criteria. Cutoff50 = 1 referred to the diagnostic test with lenient criteria. CutoffSurgery50 = 0 referred to strict criteria to perform surgery. Cutoff50 = 1 referred to lenient criteria to perform surgery.

Data Sources

The input data were based on the best available evidence in the literature. The prior probability of disease was based on the results of a clinical study. In this study, 333 patients with a history of TIA or minor stroke and who were suspected of having a CAS were included. All patients underwent duplex US or CT angiography for diagnosing CAS.

Assumptions

Annual Probability of Dying

Noncerebrovascular accident mortality was calculated according to data from the Dutch Bureau of Statistics (19). Using the absolute numbers of deaths from all causes and from cerebrovascular causes in 2006, we calculated the proportion of deaths that were noncerebrovascular for 10-year age categories for men and women separately. We obtained age- and sex-specific mortality rates of the general population from Dutch life table data and multiplied those numbers by the corresponding proportions of noncardiovascular deaths.

Event Rates

Cerebrovascular accident event rates (TIA, minor stroke, major stroke, and cerebrovascular accident-related mortality) in patients with symptoms (minor stroke or TIA) in the study of Buskens et al (3) were used. The event rates were based on whether the patient was treated with carotid endarterectomy (true-positive or false-positive) or not. Patients with false-negative results were assumed to have a higher event rate than patients with true-negative results.

- Variable definitions (where * = multiplication) were as follows:

$$pMajorStroke = pStroke * 0.33$$

$$pMinorStroke = pStroke * 0.67$$

$$pStrokeTN = ((pStroke_{0-49} * p_{0-49}) / (1 - p_{CAS})) + ((1 - Cutoff50) * ((pStroke_{50-69} * p_{50-69}) / (1 - p_{CAS}))) + ((pStrokeOcclusie * p_{100}) / (1 - p_{CAS}))$$

$$pTIATN = ((pTIA_{0-49} * p_{0-49}) / (1 - p_{CAS})) + ((1 - Cutoff50) * ((pTIA_{50-69} * p_{50-69}) / (1 - p_{CAS}))) + ((pTIAOcclusie * p_{100}) / (1 - p_{CAS}))$$

$$RRdieTN = ((RRdie_{0-49} * p_{0-49}) / (1 - p_{CAS})) + (1 - Cutoff50) * ((RRdie_{50-69} * p_{50-69}) / (1 - p_{CAS})) + ((RRdieOcclusie * p_{100}) / (1 - p_{CAS}))$$

- The risk of dying was as follows:

$$pDie = pNon_CVAmortality * RRdie + pMortRadiation$$

Updated Event Rates

To take into account recent published articles in our event rates, we created two variables: Timing and HRR. The variable Timing reflects the change in risk of hav-

ing a TIA or stroke depending on the time between the first symptoms and carotid endarterectomy. The variable HRR reflects the HRR changes in event rate on stroke in patients with a high-risk profile versus those in patients with a low-risk profile. Next, we included the sex differences in stroke risk caused by carotid endarterectomy that were published by Bond et al (11).

The variable Timing was calculated from the article by Rothwell et al (21). In their article, they calculated the risk of having a TIA or stroke after treatment depending on the time frame between first symptoms and therapy (carotid endarterectomy). We compared their probabilities for stroke or TIA depending on the time frame with the rates from the study of Buskens et al (3) and determined the time frame that corresponded to the event rates reported by Buskens et al. The time frame corresponding to the event rates reported by Buskens et al was defined as moderate (23 weeks after first symptoms, HRR = 1.0). In a sensitivity analysis (Figure 6), we compared the changes in NHB by varying the time frame between symptoms and treatment from less than 2 weeks (HRR for stroke = 0.5) to more than 4 weeks (HRR = 2.0).

In the same way, we calculated the HRR for having a stroke depending on the patient's risk profile. Johnston et al (20) compared patients with high-risk profiles (those with diabetes mellitus, hypertension, long duration of stroke, and impairment with or without focal weakness) with patients with low-risk profiles on having a recurrent stroke in symptomatic patients without treatment. We compared the stroke rates of Buskens et al and determined the corresponding risk profile, which was assumed to be moderate (HRR 1, low-risk profile). Sensitivity analysis of the HRR was performed to analyze the changes in NHB for a patient with high-risk versus a low-risk profile.

Bond et al (11) demonstrated that women have a greater risk of experiencing a stroke caused by carotid endarterectomy than men (less benefit of treatment). This was taken into account by multiplying the stroke risk with an odds ratio for women only according to the following formula:

$$p\text{StrokeCEA} = \text{Male} * \text{distprobstrokeCEA} + (1 - \text{male}) * \text{probfactor}(\text{distprobstrokeCEA}; \text{DistOR-femaleComplications}).$$

Perspectives The decision was analyzed from the perspective of the physician, the patient, the hospital, the health care system, and society by using three different recommendations for cost-effectiveness analysis (25).

Recommendation	Perspective (Outcomes Included)	Discount Rate for Costs	Discount Rate for Effectiveness
United Kingdom	Health care (QALYs, health care costs)	0.035	0.035
United States	Society (QALYs, health care costs, patient time and travel costs)	0.030	0.030
The Netherlands	Society (QALYs, health care costs, patient time, travel costs, and friction costs)	0.040	0.015

The analysis from the health care perspective considered QALYs and health care costs and was performed according to United Kingdom recommendations, discounting both future costs and effectiveness at 3.5% (33,34). Subsequently, we performed the cost-effectiveness analysis from the societal perspective according to United States recommendations, which considered QALYs, health care costs, and direct nonhealth care costs (patient time and travel costs) and discounted both future costs and effectiveness at 3% (3032). Finally, an analysis from the societal perspective was performed according to Dutch recommendations, which, in addition to the above, also took productivity losses (friction costs) into account and discounted future costs and effectiveness at 4% and 1.5%, respectively (25).

Friction Costs

Friction costs were defined as costs of productivity losses caused by death or absence from work. The friction period (ie, the time period for replacing an employee after death) has been established at 22 weeks (25). The friction cost per hour (cFriction_hour) was entered in the model for 60-year-old men and women separately. The friction costs for surviving patients were calculated by multiplying the duration of absence from work by sex-specific friction costs per hour for diagnosis and treatment separately (25). The duration of diagnostic procedures was estimated in our cost analysis. According to the standard workable hours per year (n = 1540), we calculated the loss of workable hours.

$$\begin{aligned} \text{TimeDUS} &= 1.33 \text{ hours} & \text{TimeMinorStroke} &= 154/365 * 1540 \\ \text{TimeCTA} &= 1.5 \text{ hours} & \text{TimeMajorStroke} &= 19/365 * 1540 \\ \text{TimeCE-MRA} &= 2 \text{ hours} & \text{TimeTIA} &= 2/365 * 1540 \\ \text{TimeDSA} &= 4.75 \text{ hours} \\ \text{TimeCEA} &= 72 \text{ hours} \end{aligned}$$

$$c\text{Friction_hour} = \text{Male} * \text{Dist_cFriction_Men} + (1 - \text{Male}) * \text{Dist_cFriction_Women}$$

$$c\text{Friction_dead} = c\text{Friction_hour} * (22/52 * 1540)$$

$$c\text{FrictionTreatment} = c\text{Friction_hour} * \text{TimeCEA}$$

$$c\text{FrictionDiagnosis} = c\text{FrictionDiagnosis} + c\text{Friction_hour} * \text{Time_Diagnostic test}$$

$$c\text{Frictionevent} = c\text{Friction_hour} * (\text{minor stroke/major stroke/TIA})$$

Patient Costs

Patient costs consisted of transportation costs to the hospital and the time costs of being absent from work (cPatient_Treatment and cPatient_Diagnosis) to undergo the diagnostic work-up and treatment multiplied by the average income. The aver-

age income ($cTime_patient_hour$) assuming 60% men and, on average, 60-year-old patients was calculated according to data from the Central Bureau of Statistics. Travel costs were based on the standard costs of a hospital visit by car from the Dutch costing manual (25), as follows:

$$cTravel_per_test = Dist_cTravel$$

$$cTime_patient_hour = Dist_cTime_patient_hour$$

$$cPatient_Diagnosis = cPatient_Diagnosis + cPatient_hour * Time_{diagnostic\ test} + cTravel_per_test$$

$$cPatient_Treatment = cPatient_Treatment + cPatient_hour * Time_{CEA} + cTravel_per_test$$

Cost Estimates

Costs were estimated for diagnostic tests, treatment (duplex US, CT angiography, contrast-enhanced MR angiography, DSA, and carotid endarterectomy), and events during follow-up. Costs for duplex US, CT angiography, and DSA were determined with a cost analysis and included direct health care costs (personnel, materials, equipment), indirect health care costs (housing, overhead), direct nonhealth care costs (patient travel and time costs), and indirect nonhealth care costs (production losses).

The costs for contrast-enhanced MR angiography were calculated from the article of U-King-Im et al (27), who compared the cost-effectiveness of DSA with that of contrast-enhanced MR angiography. Because that was an article from the United Kingdom, where the costs were slightly lower, we calculated the ratio between the costs of DSA and those of contrast-enhanced MR angiography. This ratio was used to estimate the costs of contrast-enhanced MR angiography on the basis of our cost estimate for DSA, as follows:

Contrast-enhanced MR angiography in the article of U-King-Im et al: £305.56

DSA in that article: £720.84

Ratio of costs of contrast-enhanced MR angiography to DSA in that article = 0.42
DSA in our article = €906.34

Contrast-enhanced MR angiography = €906.34 * 0.42 = €384.19

The costs for carotid endarterectomy were estimated in a cost analysis of the literature (3,7,44).

Because our decision model was developed to analyze cohorts of patients, the cost estimates in our model represent mean costs.

The costs for events (TIA, minor stroke, and major stroke) were derived from Buskens et al (3).

Quality of Life Estimates

The qualities of life in the different health states of the Markov model were estimated from the literature. The qualities of life in the Alive and Post-TIA states were assumed to be equal because all patients used to be or are symptomatic. The disutility of a TIA was calculated as feeling for 2 days as miserable as if one had had a major stroke ($2/365 * U_{PostMajor}$). The disutilities of major and minor strokes were derived from Sullivan and Ghushchyan (22).

State or Parameter	Quality-of-Life Weight*	Reference	Source or Method†
Alive	0.88 (0.84, 0.92)	Fryback et al (26)	BDHOS
Post-TIA	0.88 (0.84, 0.92)	Fryback et al (26)	BDHOS
Post-minor stroke	0.71 (0.68, 0.74)	Hallan et al (23)	Direct scaling (Frenchay activities index, Montgomery and Aasberg, the modified Rankin Scale)
Post-major stroke	0.31 (0.28, 0.34)	Hallan et al (23)	Direct scaling (Frenchay activities index, Montgomery and Aasberg, the modified Rankin Scale)
Disutility of TIA	$2/365$ Utility of postmajor stroke	Expert opinion	
Disutility of minor stroke	0.0524 (0.0523, 0.0525)	Sullivan and Ghushchyan (22)	EQ-5D
Disutility of major stroke	0.0524 (0.0523, 0.0525)	Sullivan and Ghushchyan (22)	EQ-5D

*Data in parentheses are 95% CIs. BDHOS = Beaver Dam Health Outcomes. EQ-5D = EuroQol 5 dimensions.

Outcome Measures

The NHB was calculated as follows: $NHB = E \cdot C/G$, where E is effectiveness in QALYs, C is the total cost of the strategy concerned, and G is the threshold WTP. NHBs are measures of effectiveness, adjusted for costs and taking into account the WTP per QALY. Given a particular WTP, the strategy with the highest NHB is the most cost effective.

The WTP reflects the amount of money that society is willing to pay for 1 QALY. Threshold WTPs of 50c000 and 80c000 per QALY were used.

Analyses

To assess uncertainty, probabilistic sensitivity analysis was performed by drawing from all variable distributions (in tabular format below) using Monte Carlo simulation of 100c000 samples. Random draws from variable distributions were single draws, which means they were equal for both strategies.

In addition to this, we repeated the analysis to assess the NHB by using different recommendations for cost-effectiveness analyses (Dutch, United Kingdom, or United States recommendations).

We performed several sensitivity analyses on the variables Timing, Prior Probability, and HRR (risk profile).

Variable Definitions

Name	Description	Formula
age	Age	
ageMKV	Age in Markov model	age+_stage
cCEA	Costs of CEA	Dist_Costs_CEA
cCTA	Costs of CTA	Dist_Costs_CTA
cDiagnosis	Costs of diagnosis	
cDSA	Costs of DSA	Dist_Costs_DSA
cDUS	Costs of DUS	Dist_Costs_DUS
cFollowup	Costs of follow-up	Dist_Costs_FollowUp
cFrictionCEA	Friction costs of CEA	$((3/365)*1540)*cFriction_hour$
cFrictionDiagnosis	Friction costs of diagnosis	

Name	Description	Formula
cFrictionMajorStroke	Friction costs of major stroke	$((154/365)*1540)*cFriction_hour$
cFrictionMinorStroke	Friction costs of minor stroke	$cFriction_hour*((19/365)*1540)$
cFrictionTIA	Friction costs of minor stroke	$cFriction_hour*((2/365)*1540)$
cFrictionTreatment	Friction costs of treatment	
cFriction_dead	Friction costs of death	$cFriction_hour*((154/365)*1540)$
cFriction_hour	Friction costs per hour	$Male*Dist_Friction_Costs_Male+(1-Male)*Dist_Friction_Costs_Female$
cMajorStroke	Costs of major stroke	Dist_Costs_MajorStroke
cMajorSY	Costs of major stroke in subsequent year	Dist_Costs_MajorSY
cMinorStroke	Costs of minor stroke	Dist_Costs_MinorStroke
cMinorSY	Costs of minor stroke in subsequent year	Dist_Costs_MinorSY
cMRA	Costs of CE-MRA	Dist_Costs_CE_MRA
cPatient	Patients costs	
cPatient_Diagnosis	Patients costs of diagnosis	
cPatient_Hour	Patients costs per hour	Dist_Costs_Patient_Time_Hour
cPatient_Treatment	Patients cost of treatment	
cTIA	Costs of TIA	
cTIAafterCEA	Costs of TIA after CEA	Dist_Costs_TIAafterCEA
cTIAnoIntervention	Costs of TIA without intervention	Dist_Costs_TIAnoIntervention
cTravel_per_test	Travel costs per test	Dist_Costs_Travel
cTreatment	Treatment costs	
CutoffSurgery50	Surgery for stenosis > 50%	1=operate 50-99% 0= operate 70-99%
CutoffTest50	Test positive > 50%	1= cutoff 50-99% 0= Cutoff 70-99%
Discount_rate_costs	Discount rate costs	
discount_rate_costs_NL	Discount rate costs in Netherlands	
Discount_rate_Eff_NL	Discount rate effectiveness in Netherlands	
Discount_rate_UK	Discount rate in United Kingdom	

Name	Description	Formula
Discount_rate_US	Discount rate in United States	
Dist_Stroke_FollowUpTP_TN	Distribution of strokes during follow-up in the true-positive and true-negative groups	
disutility_Major	Disutility of major stroke	Dist_disutility_Major
disutility_Minor	Disutility of minor stroke	Dist_Disutility_Minor
disutility_TIA	Disutility of TIA	$2/365 * u_{Post_Major}$
HRR	HRR for risk profile	
HRR1	HRR after CEA	
Male		Male=1 Female =0
ORfemaleComplications	Odds ratio for complications in female versus male patients	Dist_OR_Female_Complications
p0_49	Probability of having 0-49% stenosis	1-pDIS
p100	Probability of having occlusion	propOcclusie*pDIS
p50_69	Probability of having 50-69% stenosis	$(1 - \text{propOcclusie} - \text{propSEV}) * pDIS$
p70_99	Probability of having 70-99% stenosis	propSEV*pDIS
pCAS	Probability of having CAS	$p70_99 + \text{CutoffTest50} * p50_69$
pCTAUninterpretable	Probability of CTA being uninterpretable	Dist_Uninterprtble_CTA
pDie	Probability of death	$p_{Non_CVA} mortality * RR_{die} + p_{Mort} Radiation$
pDieMajor	Probability of death from major stroke	$p_{Non_CVA} mortality * RR_{die} Major [tunnel] + p_{Mort} Radiation$
pDieMajorStable	Probability of death in major stable state	$p_{Non_CVA} mortality * RR_{die} Major Stable + p_{Mort} Radiation$
pDieStable	Probability of death in stable state	$p_{Non_CVA} mortality * RR_{die} Stable + p_{Mort} Radiation$
pDIS	Probability of having disease	$Male * Dist_Prop_DIS Male + ((1 - Male) * Dist_Prop_DIS_Female)$
pDUSuninterpretable	Probability of DUS being uninterpretable	Dist_Uninterprtble_DUS

Name	Description	Formula
pMajorStroke	Probability of having major stroke	Dist_Prob_Major_Stroke
pMort_CEA	Probability of death caused by CEA	Dist_Prob_Mort_CEA
pMort_CTA	Probability of death caused by CTA	Dist_Mortality_IVContrast
pMort_DSA	Probability of death caused by DSA	$Dist_Prob_Mort_DSA + Dist_Mortality_IVContrast$
pMort_MRA	Probability of death caused by MRA	Dist(1)
pMRAUninterpretable	Probability of CE-MRA being uninterpretable	Dist_Uninterpretable_MRA
pNon_CVAmortality	Probability of death caused by other than CVA	$(RateToProb(Male * MortalityMen[ageMKV] * Non_CVA_proportion_man[ageMKV] + (1 - Male) * MortalityWomen[ageMKV] * Non_CVA_proportion_Woman[ageMKV]; 1))$
propOcclusie	Proportion of disease caused by occlusion	$Male * Dist_Prop_Occlusie Male + ((1 - Male) * Dist_Prop_Occlusion Female)$
propSEV	Proportion of diseased with 70-99% stenosis	$Male * Dist_Prop_SEV Male + ((1 - Male) * Dist_Prop_SEV Female)$
pSens	Sensitivity of the test	
pSensCE_MRA	Sensitivity of CE-MRA	$(1 - \text{CutoffTest50}) * Dist_Sens_CE_MRA70_99 + \text{CutoffTest50} * Dist_Sens_CE_MRA5099$
pSensCTA	Sensitivity of CTA	$(1 - \text{CutoffTest50}) * Dist_Sens_CTA70_99 + \text{CutoffTest50} * Dist_Sens_CTA5099$
pSensDSA	Sensitivity of DSA	
pSensDUS	Sensitivity of DUS	$(1 - \text{CutoffTest50}) * Dist_Sens_DUS70_99 + \text{CutoffTest50} * Dist_Sens_DUS5099$
pSpec	Specificity of the test	
pSpecCE_MRA	Specificity of CE-MRA	$(1 - \text{CutoffTest50}) * Dist_Spec_CE_MRA70_99 + \text{CutoffTest50} * Dist_Spec_CE_MRA5099$
pSpecCTA	Specificity of CTA	$(1 - \text{CutoffTest50}) * Dist_Spec_CTA70_99 + \text{CutoffTest50} * Dist_Spec_CTA5099$
pSpecDSA	Specificity of DSA	

Name	Description	Formula
pSpecDUS	Specificity of DUS	$(1 - \text{CutoffTest50}) * \text{Dist_Spec_DUS70_99} + \text{CutoffTest50} * \text{Dist_Spec_DUS5099}$
pStrokeAlive	Probability of having stroke in Alive state	$\text{Dist_Stroke_FollowUpTP_FP} * \text{Timing}$
pStrokeCEA	Probability of having stroke after CEA	$\text{Male} * \text{Dist_Prob_Stroke_CEA} + ((1 - \text{Male}) * \text{ProbFactor}(\text{Dist_Prob_Stroke_CEA}; \text{Dist_OR_Female_Complications}))$
pStrokeDSA	Probability of having stroke caused by DSA	$\text{Dist_Prob_Stroke_DSA}$
pStrokeFN	Probability of having stroke in the false-negative group	$((\text{pStroke70_99}[_\text{tunnel}] * \text{p70_99}) / (\text{p70_99} + \text{CutoffTest50} * \text{p50_69})) + (\text{CutoffTest50} * ((\text{pStroke50_69}[_\text{tunnel}] * \text{p50_69}) / (\text{p70_99} + \text{CutoffTest50} * \text{p50_69})))$
pStrokeMajor	Probability of having a stroke after major stroke	$(\text{PstrokeMajorStates}[_\text{tunnel}]) * \text{RR_Dist_Prob}$
pStrokeMinor	Probability of having a stroke after minor stroke	$\text{Dist_Stroke_FollowUpTP_FP} * \text{Timing}$
pStrokeOcclusie	Probability of having a stroke with an occlusion	
pStrokeStable	Probability of having a stroke in the Stable state	$0.02 * \text{RR_Dist_Prob}$
pStrokeTIA	Probability of having a stroke in the TIA state	$\text{Dist_Stroke_FollowUpTP_FP} * \text{Timing}$
pStrokeTN	Probability of having stroke in the true-negative group	$((\text{pStroke0_49}[_\text{tunnel}] * \text{p0_49}) / (1 - (\text{CutoffTest50} * \text{p50_69} + \text{p70_99}))) + ((1 - \text{CutoffTest50}) * ((\text{pStroke50_69}[_\text{tunnel}] * \text{p50_69}) / (1 - (\text{CutoffTest50} * \text{p50_69} + \text{p70_99})))) + ((\text{pStrokeOcclusie} * \text{p100}) / (1 - (\text{CutoffTest50} * \text{p50_69} + \text{p70_99}))))$
pTIAalive	Probability of having a TIA in the Alive state	$\text{Dist_TIA_FollowUpTP_FP} * \text{Timing}$
pTIAFN	Probability of having a TIA in the false-negative group	$\text{RR_Dist_Prob} * (((\text{pTIA70_99}[_\text{tunnel}] * \text{p70_99}) / (\text{p70_99} + \text{CutoffTest50} * \text{p50_69})) + (\text{CutoffTest50} * ((\text{pTIA50_69}[_\text{tunnel}] * \text{p50_69}) / (\text{p70_99} + \text{CutoffTest50} * \text{p50_69}))))$
pTIAminor	Probability of having a TIA after minor stroke	$\text{Dist_TIA2_FollowUpTP_FP} * \text{Timing}$
pTIAocclusie	Probability of having a TIA if carotid artery is occluded	

Name	Description	Formula
pTIAStable	Probability of having a TIA in the Stable state	$0.01 * \text{RR_Dist_Prob}$
pTIATIA	Probability of having a TIA in the TIA state	$\text{Dist_TIA2_FollowUpTP_FP} * \text{Timing}$
pTIATN	Probability of having a TIA in the true-negative group	$\text{RR_Dist_Prob} * (((\text{pTIA0_49}[_\text{tunnel}] * \text{p0_49}) / (1 - (\text{CutoffTest50} * \text{p50_69} + \text{p70_99}))) + (1 - \text{CutoffTest50}) * ((\text{pTIA50_69}[_\text{tunnel}] * \text{p50_69}) / (1 - (\text{CutoffTest50} * \text{p50_69} + \text{p70_99})))) + ((\text{pTIAocclusie} * \text{p100}) / (1 - (\text{CutoffTest50} * \text{p50_69} + \text{p70_99}))))$
pUninterpretable	Probability of test being uninterpretable	
RRdie	Relative risk of death	
RRdieFN	Relative risk of death in the false-negative group	$\text{RR_Dist_Prob} * (((\text{RRdie70_99}[_\text{tunnel}] * \text{p70_99}) / (\text{CutoffTest50} * \text{p50_69} + \text{p70_99})) + (\text{CutoffTest50} * (\text{RRdie50_69}[_\text{tunnel}] * \text{p50_69}) / (\text{CutoffTest50} * \text{p50_69} + \text{p70_99}))))$
RRdieFP	Relative risk of death in the false-positive group	$1.01 * \text{RR_Dist_Prob}$
RRdieMajorStable	Relative risk of death in MajorStable state	$1.02 * \text{RR_Dist_Prob}$
RRdieStable	Relative risk of death in Stable state	
RRdieStableFN	Relative risk of death in Stable state in the false-negative group	$1.02 * \text{RR_Dist_Prob}$
RRdieStableFP	Relative risk of death in Stable state in the false-positive group	$1.01 * \text{RR_Dist_Prob}$
RRdieStableTN	Relative risk of death in Stable state in the true-negative group	$1.0165 * \text{RR_Dist_Prob}$
RRdieStableTP	Relative risk of death in Stable state in the true-positive group	$1.01 * \text{RR_Dist_Prob}$

Name	Description	Formula
RRdieTN	Relative risk of death in the true-negative group	$((RRdie0_49[_tunnel]*p0_49)/(1-(CutoffTest50*p50_69+p70_99)))+(1-CutoffTest50)*((RRdie50_69[_tunnel]*p50_69)/(1-(CutoffTest50*p50_69+p70_99)))+(RRdieOcclude[_tunnel]*p100)/(1-(CutoffTest50*p50_69+p70_99))$
RRdieTP	Relative risk of death in the true-positive group	$1.01*RR_Dist_Prob$
RR_Dist_Prob	Distributions of relative risk	Dist_RR_Probabilities
Time_CEA	Duration of CEA procedure	Dist_Time_CEA
Time_CTA	Duration of CTA procedure	Dist_Time_CTA
Time_DSA	Duration of DSA procedure	Dist_Time_DSA
Time_DUS	Duration of DUS procedure	Dist_Time_DUS
Time_MRA	Duration of CE-MRA procedure	Dist_Time_MRA
Timing	Time between onset of symptoms and surgery	
uAlive	Quality of life in Alive State	Dist_Utility_Alive
uDead	Quality of life in Dead state	
uPost_Major	Quality of life after major stroke	Dist_Utility_MajorStroke
uPost_Minor	Quality of life after minor stroke	Dist_Utility_MinorStroke
uPost_TIA	Quality of life after TIA	Dist_Utility_TIA

Distributions

Variable Name	Description	Type	Parameter 1	Parameter 2	Parameter 3
Dist_Mortality_IVContrast	Distribution of mortality caused by contrast agent allergy	Beta	337c647	2	
Dist_sens_DUS70_99	Distribution of sensitivity of DUS at 70-99% stenosis	Triangular	0.85	0.89	0.92
Dist_sens_CE_MRA70_99	Distribution of sensitivity of CE-MRA at 70-99% stenosis	Triangular	0.88	0.94	0.97
Dist_spec_CE_MRA70_99	Distribution of specificity of CE-MRA at 70-99% stenosis	Triangular	0.89	0.93	0.96
Dist_Costs_DUS	Distribution of costs of DUS	Triangular	0.75*42	42	1.25*42
Dist_Costs_CTA	Distribution of costs of CTA	Triangular	0.75*198	198	1.25*198
Dist_Costs_CE_MRA	Distribution of costs of CE-MRA	Triangular	0.75*384	384	1.25*384
Dist_Costs_DSA	Distribution of costs of DSA	Triangular	0.75*906	906	1.25*906
Dist_Costs_CEA	Distribution of costs of CEA	Triangular	0.75*4535	4535	1.25*4535
Dist_Costs_MinorStroke	Distribution of costs after minor stroke	Triangular	0.75*7654	7654	1.25*7654
Dist_Costs_MajorStroke	Distribution of costs after major stroke	Triangular	0.75*43c650	43650	1.25*43c650
Dist_Costs_TIAafterCEA	Distribution of costs of TIA after CEA	Triangular	0.75*106	106	1.25*106
Dist_Costs_TIAnoIntervention	Distribution of costs of TIA after no intervention	Triangular	0.75*1582	1582	1.25*1582
Dist_Friction_Costs_Male	Distribution of friction costs in men	Triangular	0.75*51	51	1.25*51
Dist_Friction_Costs_Female	Distribution of friction costs in women	Triangular	0.75*39	39	1.25*39
Dist_Costs_Patient_Time_Hour	Distribution of patient costs per hour	Triangular	0.75*(0.29*60)	0.29*60	1.25*(0.29*60)

Variable Name	Description	Type	Parameter 1	Parameter 2	Parameter 3
Dist_Costs_Travel	Distribution of travel costs	Triangular	0.75*5	5	1.25*5
Dist_Time_CTA	Distribution of time of CTA	Triangular	0.75*(90/60)	(90/60)	1.25*(90/60)
Dist_Time_MRA	Distribution of time of CE-MRA	Triangular	0.75*(120/60)	(120/60)	1.25*(120/60)
Dist_Time_DSA	Distribution of time of DSA	Triangular	0.75*(285/60)	(285/60)	1.25*(285/60)
Dist_Time_DUS	Distribution of time of DUS	Triangular	0.75*1.33	1.33	1.25*1.33
Dist_Time_CEA	Distribution of time of CEA	Triangular	0.75*(72)	72	1.25*(72)
Dist_Prob_Major_Stroke	Distribution of probability of having a major stroke	Triangular	0.10	0.33	0.66
Dist_Prob_Mort_CEA	Distribution of probability of dying after CEA	Triangular	0.003	0.0106	0.03
Dist_Prob_Mort_DSA	Distribution of probability of dying after DSA	Triangular	0.0003	0.001	0.003
Dist_Prob_Stroke_CEA	Distribution of probability of stroke after CEA	Triangular	0.015	0.055	0.15
Dist_Prob_Stroke_DSA	Distribution of probability of stroke after DSA	Beta	2899	14	
Dist_Costs_MajorSY	Distribution of costs of a major stroke in subsequent year	Triangular	0.75*25c487	25487	1.25*25c487
Dist_Costs_MinorSY	Distribution of costs of a minor stroke in subsequent year	Triangular	0.75*1310	1310	1.25*1310
Dist_Uninterpretable_MRA	Distribution of a CE-MRA being uninterpretable	Triangular	0.75*0.1145	0.1145	1.25*0.1145
Dist_Utility_Alive	Distribution of the utility of the Alive state	Normal	0.88	0.04	
Dist_Utility_TIA	Distribution of the utility of the TIA state	Normal	0.88	0.04	
Dist_Utility_MajorStroke	Distribution of the utility after major stroke	Normal	0.31	0.03	
Dist_Utility_MinorStroke	Distribution of the utility after minor stroke	Normal	0.71	0.03	
Dist_disutility_Major	Distribution of the disutility after major stroke	Normal	0.0524	0.0001	
Dist_Disutility_Minor	Distribution of the disutility after minor stroke	Normal	0.0524	0.0001	
Dist_RR_Probabilities	Distribution of relative risks	Log-Normal	0	0.114	
Dist_Spec_DUS70_99	Distribution of the specificity of DUS at 70-99% stenosis	Triangular	0.77	0.84	0.89
Dist_Sens_CTA70_99	Distribution of the sensitivity of CTA at 70-99% stenosis	Triangular	0.71	0.91	0.99
Dist_Spec_CTA70_99	Distribution of the specificity of CTA	Triangular	0.98	0.99	1.00
Dist_Uninterpretable_DUS	Distribution of DUS being uninterpretable	Beta	351	7	
Dist_Uninterpretable_CTA	Distribution of CTA being uninterpretable	Beta	351	1	
Dist_Sens_DUS5099	Distribution of the sensitivity of DUS at 50-99% stenosis	Triangular	0.62	0.84	0.95
Dist_Spec_DUS5099	Distribution of the specificity of DUS at 50-99% stenosis	Triangular	0.73	0.83	0.90
Dist_Sens_CTA5099	Distribution of the sensitivity of CTA at 50-99% stenosis	Triangular	0.96	0.999	1.00
Dist_Spec_CTA5099	Distribution of the specificity of CTA at 50-99% stenosis	Triangular	0.96	0.98	0.99
Dist_Sens_CE_MRA5099	Distribution of the sensitivity of CE-MRA at 50-99% stenosis	Triangular	0.90	0.96	0.99
Dist_Spec_CE_MRA5099	Distribution of the specificity of CE-MRA at 50-99% stenosis	Triangular	0.90	0.96	0.99

Variable Name	Description	Type	Parameter 1	Parameter 2	Parameter 3
Dist_Costs_FollowUp	Distribution of the costs in follow-up related to aspirin	Triangular	0.75*20	20	1.25*20
Dist_Stroke_FollowUpTP_FP	Distribution of the probability of stroke after CEA	Triangular	0.01	0.02	0.04
Dist_Prop_OcclusieMale	Distribution of the proportion of diseased men with an occlusion	Beta	32	9	
Dist_Prop_SEVMale	Distribution of the proportion of diseased men with 70-99% stenosis	Beta	32	19	
Dist_TIA_FollowUpTP_FP	Distribution of the probability of TIA after CEA	Triangular	0.005	0.01	0.02
Dist_TIA2_FollowUpTP_FP	Distribution of the probability of TIA in follow-up after CEA	Triangular	0.01	0.02	0.04
Dist_Prop_DISMale	Distribution of the proportion of diseased men with 50-99% stenosis	Beta	194	32	
Dist_OR_Female_Complications	Distribution of the odds ratio for women to experience complications of CEA	Triangular	1.17	1.31	1.47
Dist_Prop_OcclusionFemale	Distribution of the proportion of diseased women with an occlusion	Beta	7	2	
Dist_Prop_SEVFemale	Distribution of the proportion of diseased women with 70-99% stenosis	Beta	7	3	
Dist_Prop_DIS_Female	Distribution of the proportion of diseased women with 50-99% stenosis	Beta	139	7	

Reference

- Gray WA, White HJ, Jr., Barrett DM, Chandran G, Turner R, Reisman M. Carotid stenting and endarterectomy: a clinical and cost comparison of revascularization strategies. *Stroke* 2002; 33:1063-1070.

Supplemental Figure

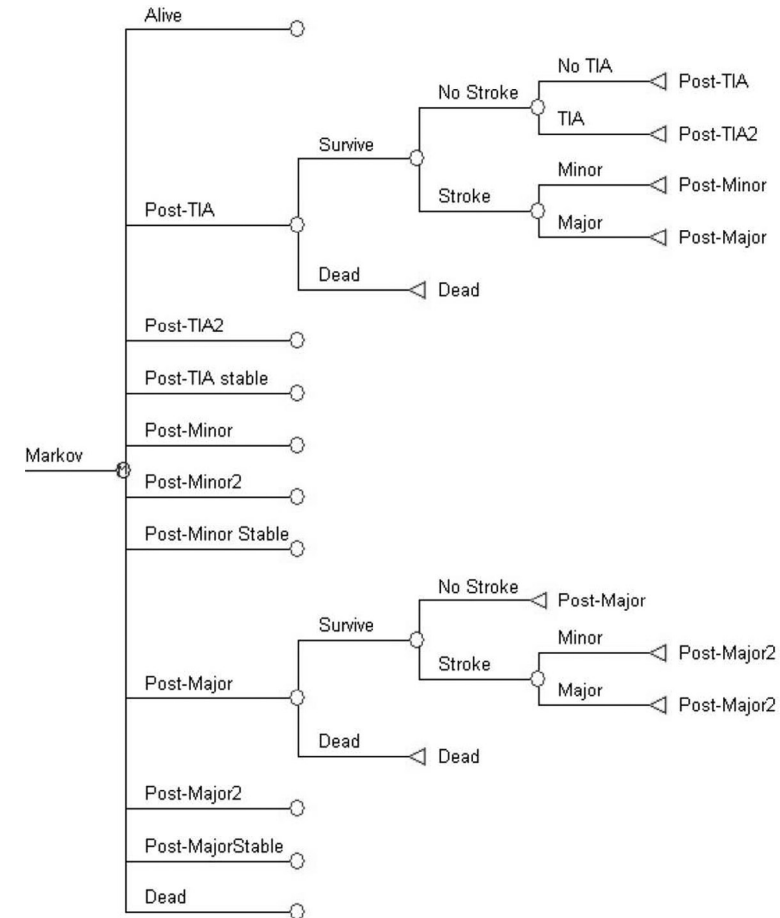


Figure E1: Schematic simplified representation of Markov part of model, which models prognosis. Only the Post-TIA, Post-Minor, and Post-Major health states have been expanded. The other health states have a similar structure.

Chapter 7

Assessment of Atherosclerotic Carotid
Plaque Volume with Multidetector
Computed Tomography Angiography

Assessment of atherosclerotic carotid plaque volume with multidetector computed tomography angiography

Thomas T. de Weert, MD
 Cécile de Monyé, MD
 Erik Meijering, MSc, PhD
 Ronald Booiij, BHS
 Wiro J. Niessen, MSc, PhD
 Diederik W.J. Dippel, MD, PhD
 Aad van der Lugt, MD, PhD

Int J Cardiovasc Imaging 2008; 24:751–759

Abstract

Purpose: The amount of atherosclerotic plaque and its components (calcifications, fibrous tissue, and lipid core) could be better predictors of acute events than the now currently used degree of stenosis. Therefore, we evaluated a dedicated software tool for volume measurements of atherosclerotic carotid plaque and its components in multidetector computed tomography angiography (MDCTA) images.

Materials and methods: Data acquisition was approved by the Institutional Review Board and all patients gave written informed consent. MDCTA images of 56 carotid arteries were analyzed by three observers. Plaque volumes were assessed by manual drawing of the outer vessel contour. The luminal boundary was determined based on a Hounsfield-Unit (HU) threshold. The contribution of different components was measured by the number of voxels within defined ranges of HU-values (calcification >130 HU, fibrous tissue 60-130 HU, lipid core <60 HU). Interobserver variability (IOV) was assessed.

Results: Plaque volume was 1259 ± 621 mm³. The calcified, fibrous and lipid volumes were 238 ± 252 mm³, 647 ± 277 mm³ and 376 ± 283 mm³, respectively. IOV was moderate with interclass correlation coefficients (ICC) ranging from 0.76-0.99 and coefficients of variation (COV) ranging from 3-47%.

Conclusion: In conclusion atherosclerotic carotid plaque volume and plaque component volumes can be assessed with MDCTA with a reasonable observer variability.

Introduction

It is well known that the severity of stenosis is an unreliable estimation of the amount of atherosclerotic plaque. In case of carotid atherosclerotic disease, this is both related to the carotid bulb, in which atherosclerotic plaque accumulates before it compromises the lumen, and to positive remodeling, the phenomenon that an artery may or may not enlarge in response to plaque accumulation.¹ Furthermore, it is current opinion that atherosclerotic plaque rupture plays an important role in acute events, like transient ischemic accidents (TIA) and minor stroke.² Rupture-prone plaques have specific morphological features: the most frequently seen vulnerable plaque type has a large lipid-rich core with a thin fibrous cap² and has proved to be an independent predictor of ischemic cerebrovascular events.³

It is therefore hypothesized that the amount of atherosclerotic plaque and its components (calcifications, fibrous tissue, and lipid core) could be better predictors of acute events than the now clinically used degree of stenosis, and may be useful in the selection of patients who could benefit from therapeutic intervention.

Computed tomography angiography (CTA) has been established as an accurate modality to assess the presence of carotid atherosclerotic plaque and grade the severity of stenosis.⁴ A recent in vitro and in vivo study showed that quantification of the area (two dimensional) of atherosclerotic carotid plaque and its components is possible in axial thin section multidetector computed tomography angiography (MDCTA) images, in good correlation ($R^2 > 0.73$) with histology.^{5,6} Further developments in the quantification software now enable to quantify the volume of atherosclerotic plaque and the volume of different plaque components (three dimensional).

The aim of this study was to evaluate this software tool for atherosclerotic plaque and plaque component volume measurements in MDCTA images of the carotid artery and to assess the observer variability of these measurements.

Methods

Subjects

Twenty patients with a 0-29% stenosis grade (based on NASCET⁷ criteria) and twelve patients for each of the three other stenosis grades (30-49%; 50-69% and 70-99%) at the symptomatic side were retrieved at random from a database ($n=421$) of MDCTA examinations of patients with transient ischemic attack or minor stroke. In all 56 patients MDCTA had been performed as part of a research protocol that was approved by the Institutional Review Board and for which all patients had given written informed consent.

Scanning and image reconstruction

Scanning was performed on a 16-slice MDCT scanner (Siemens, Sensation 16, Erlangen, Germany) with a standardized protocol (120 kVp, 180 mAs, collimation 16x0.75 mm, table feed 12 mm/rotation, pitch 1).⁸ All patients received 80 ml contrast material (320 mg/ml), followed by 40 ml saline, both with an injection rate of 4 ml/sec.⁹ The radiation dose was 2.6 mSv.

Image reconstructions were made with field of view 120 mm, matrix size 512x512 (yielding interpolated pixels of 0.2x0.2 mm, real in-plane resolution is 0.6x0.6 mm), slice thickness 1.0 mm, increment 0.6 mm and with an intermediate reconstruction algorithm (B46: heart-view sharp).⁶

Quantification and characterization

Three observers independently assessed the presence of an atherosclerotic lesion, the length of the atherosclerotic lesion, the location of the bifurcation, lumen attenuation, and plaque volume and plaque component volumes. One of the observers assessed after four months for a second time the volumes in a subset of patients (half the population per stenosis degree, randomly chosen).

The criterion used for the presence of an atherosclerotic lesion was: the presence of a calcification and/or thickening of the vessel wall. The length of the atherosclerotic lesion was defined as the distance between the first (most proximal) image and the last (most distal) image on which the atherosclerotic lesion was present. The location of the bifurcation was defined as the first image with two separate lumina. Lumen attenuation was measured in the most proximal and distal image with atherosclerosis, and the mean lumen attenuation was calculated.

Plaque and plaque component areas were measured with a polymasure plug-in developed by one of the co-authors (E.M.) for the freely available software package ImageJ (Rasband, National Institute of Mental Health, Bethesda, USA). This plug-in made it possible to draw manually regions of interest (ROI) in consecutive axial MDCT images and to automatically calculate the total number of pixels and the number of pixels of different Hounsfield value (HV) ranges within these ROI (Figure 1). The ROI was placed over the outer vessel wall contour and therefore equals plaque area plus lumen area. The different HV ranges are considered to represent the different plaque components; calcification >130 HU, fibrous tissue 60-130 HU and lipid core <60 HU.

The cutoff value between calcifications and fibrous tissue was set at 130 HU; the value currently used for calcium scoring. The cutoff value between fibrous tissue and lipid core was set at 60 HU as assessed in previous studies.^{5,6} The cutoff value between atherosclerotic plaque and lumen was adjusted for each patient and based on the full-width-half-maximum principle (mean lumen attenuation plus mean fibrous tissue attenuation (≈ 88 HU) divided by two). To compensate for partial vol-

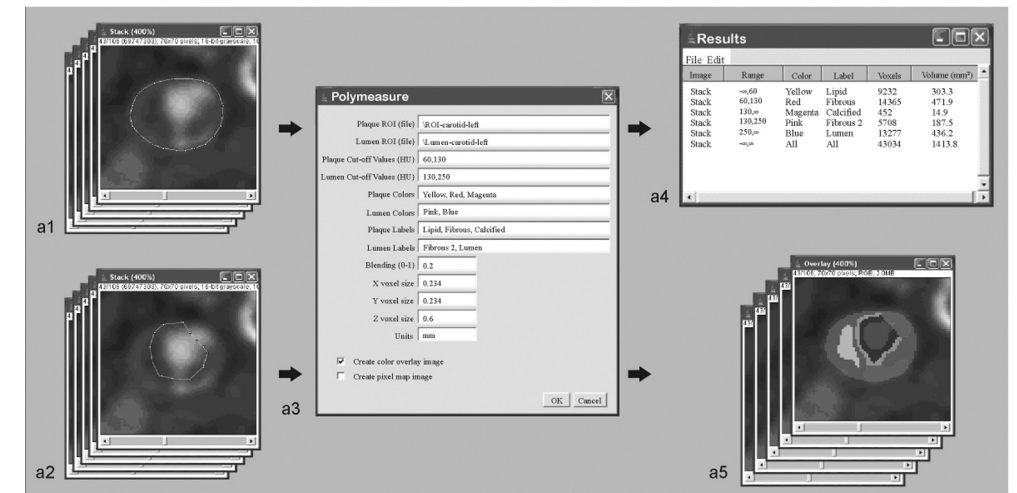


Fig. 1. Semi-automatic assessment of plaque component volumes in a stack of MDCTA images with the ImageJ plug-in 'PolyMeasure'. (a1) This plug-in allows an observer to draw a region of interest (ROI) on consecutive axial MDCTA images. This ROI represents lumen area and atherosclerotic plaque area. (a2) To differentiate lumen area from the atherosclerotic plaque area and from calcified tissue, a second ROI is drawn. This second ROI should include the attenuated lumen area, but should not include any calcifications. (a3) After the input of the cutoff values that differentiate the specific plaque components and the lumen, the plaque components and the lumen can be labeled with a color. After the input of the voxel sizes, (a4) atherosclerotic plaque component volumes and lumen volume are automatically calculated, and (a5) color overlay images are produced on which the plaque components and the lumen have a specific color.

ume effects, related to a high lumen attenuation at the plaque-lumen border, the pixels around the lumen with a HV between 130 HU and the adjusted cutoff value were considered to be fibrous tissue. To assess the border between lumen and atherosclerotic plaque it was necessary to draw a second ROI close to the lumen in each image. Normally, the lumen area was then automatically differentiated from atherosclerotic plaque based on the adjusted cutoff value. But in those plaques in which calcifications bordered the lumen and the two dense structures merged with each other, lumen area and calcifications had to be separated by manual drawing.

The volumes were calculated as the product of the number of pixels, the pixel size and the increment.

Analysis

Firstly, the difference between observers in the assessment of the presence of an atherosclerotic lesion was assessed. Hereafter, consensus on the presence of an atherosclerotic lesion was achieved by a consensus reading between all three ob-

servers. Those image series that were appointed as having atherosclerosis were used for further analysis.

Secondly, differences between observers in the assessment of the length of the atherosclerotic lesion, the location of the bifurcation, lumen attenuation and plaque and plaque component volumes were calculated.

After assessment of the differences, a second consensus reading was held in order to achieve consensus about the length of the atherosclerotic lesion, the location of the bifurcation and lumen attenuation because these features influence the volume measurements. All observers had to adapt their assessments on grounds of this second consensus reading and hereafter plaque and plaque component volumes were calculated again and differences were evaluated. This recalculation provides observer variability measurements due to differences in the assessment of the outer vessel wall contour only.

In order to assess not only the variability in volume measurements, the overlap (similarity index) between the ROIs (outer contour) of the observers was assessed and expressed as a percentage ($2 \times \text{pixels with overlap} / (\text{pixels ROI observer A} + \text{pixels ROI observer B}) \times 100\%$).

Finally, the intra-observer differences in plaque and plaque component volume measurements were assessed.

Statistics

Continuous data were compared with a paired Student's *t*-test for which a *p*-value <0.05 was considered to indicate statistical significance.

Inter-observer differences in the assessment of the length of the atherosclerotic lesion, the location of the bifurcation and lumen attenuation were expressed as the mean \pm the standard deviation (SD), and as a coefficient of variation defined by the SD of the paired difference divided by the mean of the absolute values.

Inter- and intra-observer differences in plaque and plaque component volume measurements were presented with a mean \pm SD, an interclass correlation coefficient (ICC) with 95% confidence interval and a coefficient of variation. The differences were also plotted against the mean value of the measurements (Bland-Altman plot).

Results

In the 36 patients with a stenosis degree of 30% or higher, all observers agreed on the presence of an atherosclerotic lesion. In the 20 patients with 0-29% stenosis, the presence of an atherosclerotic lesion was determined in 9 patients by three

Table 1. Mean values, inter-observer differences, interclass correlation coefficients, coefficients of variation of atherosclerotic plaque features and volume measurements from 46 CTA datasets in which atherosclerosis was considered to be present.

	Mean \pm SD	Diff Obs 1-2	Diff Obs 1-3	Diff Obs 2-3	ICC 95% CI	CoV (range)
Lesion length (mm)	27.3 \pm 10.6	6.1 \pm 4.4*	1.7 \pm 5.2*	4.3 \pm 6.2*	-	-
Image with bifurcation (mm ²)	-	0.5 \pm 3.6	0.3 \pm 1.7	0.2 \pm 3.2	-	-
Lumen attenuation (HU)	217.4 \pm 36.9	0.4 \pm 5.9	0.7 \pm 3.9	0.2 \pm 5.8	-	-
Plaque volume (mm ³)	1259 \pm 621	167 \pm 278*	247 \pm 381*	80 \pm 446	0.79 (0.65-0.87)	23-34%
Calcified volume (mm ³)	238 \pm 252	37 \pm 68*	3 \pm 38	40 \pm 82*	0.96 (0.93-0.98)	13-34%
Fibrous volume (mm ³)	647 \pm 277	77 \pm 144*	92 \pm 191*	15 \pm 210	0.76 (0.63-0.85)	23-31%
Lipid volume (mm ³)	376 \pm 283	48 \pm 141*	153 \pm 204*	105 \pm 236*	0.70 (0.51-0.82)	42-58%
Luminal volume (mm ³)	879 \pm 459	182 \pm 206*	51 \pm 226	132 \pm 240*	0.84 (0.71-0.91)	23-27%
Calcified volume (%)	19 \pm 15	1 \pm 9	4 \pm 9*	2 \pm 6*	0.85 (0.77-0.91)	33-48%
Fibrous volume (%)	54 \pm 12	2 \pm 14	0 \pm 13	2 \pm 7*	0.53 (0.36-0.69)	13-27%
Lipid volume (%)	27 \pm 13	1 \pm 11	3 \pm 11*	5 \pm 8*	0.68 (0.53-0.80)	30-44%

* = *t*-test *p* value < 0.05; Diff = Difference; Obs = Observer; CoV = Coefficient of variation; ICC = Interclass correlation; CI = Confidence interval

observers, in 1 patient by two observers, and in 1 patient by one observer. The consensus reading appointed 10 patients as having atherosclerosis, thus 46 patients were selected for further analysis.

The mean time used by an observer for the analysis of one artery was about 1 hour, almost entirely taken by the drawing of the outer vessel wall.

The assessment of the length of an atherosclerotic lesion was significantly different between observers, while the assessment of the location of the bifurcation and lumen attenuation was not significantly different (*p*>0.27 and *p*>0.49, respectively).

The ICC was good for all volume measurements (range 0.53-0.96). The plaque and plaque component volumes measured by the three observers were significantly different and the coefficients of variation were moderate (range 13-58%) (Table 1).

After the second consensus reading in which consensus was achieved about the length of the atherosclerotic lesion, the location of the bifurcation and lumen attenuation, the ICC improved and was excellent for all volume measurements (ICC>0.80), except for the lipid core volume measurements (ICC=0.76 (0.54-0.87)), for which it was good (Table 2). The coefficients of variation between observers improved for all measurements: plaque volume (17-24%), calcified volume (13-33%), fibrous tissue volume (18-24%), lipid core volume (37-47%) and lumen volume (3-10%) (Table 2). The coefficients of variation between observers for the assessment of calcified volume percentage (15-26%), fibrous volume percentage (10-15%) and lipid core volume percentage (21-30%) were also improved (Table 2).

Table 2. Mean values, inter-observer differences, interclass correlation coefficients, coefficients of variation of volume measurements from 46 CTA datasets in which atherosclerosis was considered to be present and consensus was reached with regard to the lesion length, location of bifurcation and lumen attenuation.

	Mean ± SD	Diff Obs 1-2	Diff Obs 1-3	Diff Obs 2-3	ICC (95 % CI)	CoV (range)
Plaque volume (mm ³)	1223±606	26±194	218±255*	192±300*	0.88 (0.75-0.94)	17-24%
Calcified volume (mm ³)	235±250	28±60*	4±28	31±78*	0.97 (0.95-0.98)	13-33%
Fibrous volume (mm ³)	619±264	21±72*	67±88*	87±106*	0.90 (0.78-0.95)	18-24%
Lipid volume (mm ³)	369±278	20±120	150±168*	130±186*	0.76 (0.54-0.87)	37-47%
Luminal volume (mm ³)	830±421	13±76	6±21	18±86	0.99 (0.98-0.99)	3-10%
Calcified volume (%)	18±15	2±4*	2±3*	4±5*	0.95 (0.89-0.98)	15-26%
Fibrous volume (%)	54±12	2±6	3±5*	1±8	0.84 (0.76-0.91)	10-15%
Lipid volume (%)	27±13	0±7	5±6*	5±8*	0.81 (0.66-0.89)	21-30%

* = t-test *p* value < 0.05; Diff = Difference; Obs = Observer; CoV = Coefficient of variation; ICC = Interclass correlation; CI = Confidence interval

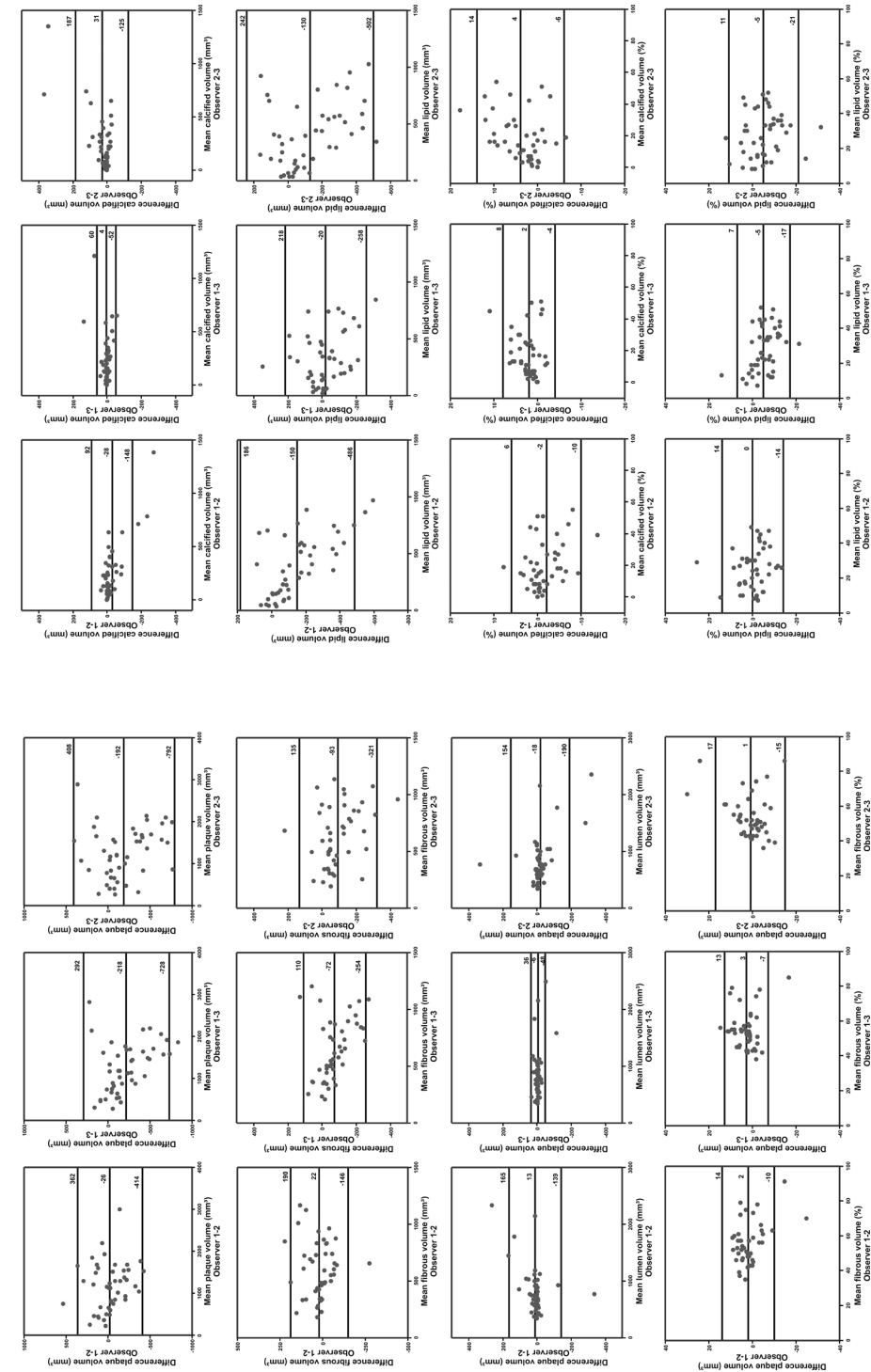


Figure 1. Bland-Altman plots of plaque volume and plaque component volumes assessed by three observers. The horizontal lines express the mean difference and the mean difference ± 2 standard deviations.

From the Bland-Altman plots it can be observed that especially the differences between observers in plaque volume, fibrous tissue volume and lipid core volume measurements increase with a larger volume (Figure I).

The similarity indices (\pm SD) between the ROIs assessed by observer 1 and 2, observer 1 and 3, and observer 2 and 3 were $91.3 \pm 3.0\%$, $90.9 \pm 2.9\%$ and $90.0 \pm 4.5\%$, respectively.

Intra-observer analysis was good with excellent ICC (all > 0.94) and moderate to good coefficients of variation for the assessment of plaque volume (11%), calcified volume (8%), fibrous tissue volume (8%), lipid core volume (25%) and lumen volume (5%) (Table 3). The intra-observer coefficients of variation for the assessment of calcified volume percentage (10%), fibrous volume percentage (6%) and lipid core volume percentage (14%) were also good (Table 3).

The similarity index (\pm SD) between the two series of independently assessed ROIs by observer 1 was $93.7 \pm 1.8\%$.

Table 3. Mean values, intra-observer differences, interclass correlation coefficients, coefficients of variation of volume measurements from 46 CTA datasets in which atherosclerosis was considered to be present and consensus was reached with regard to the lesion length, location of bifurcation and lumen attenuation.

	Mean \pm SD	Difference	ICC (95 % CI)	CoV
Plaque volume (mm ³)	1098 \pm 459	1 \pm 120	0.97 (0.93–0.99)	11%
Calcified volume (mm ³)	218 \pm 186	7 \pm 18	0.99 (0.99–1.00)	8%
Fibrous volume (mm ³)	591 \pm 229	10 \pm 49	0.98 (0.95–0.99)	8%
Lipid volume (mm ³)	289 \pm 205	2 \pm 72	0.94 (0.87–0.97)	25%
Luminal volume (mm ³)	824 \pm 413	14 \pm 40	1.00 (0.99–1.00)	5%
Calcified volume (%)	20 \pm 16	1 \pm 2	0.99 (0.98–1.00)	10%
Fibrous volume (%)	56 \pm 12	1 \pm 3	0.96 (0.91–0.98)	6%
Lipid volume (%)	24 \pm 11	0 \pm 3	0.96 (0.91–0.96)	14%

* = t-test p value < 0.05 ; ICC = Interclass correlation; CI = Confidence interval; CoV = Coefficient of variation

Discussion

Non-invasive in vivo assessment of atherosclerotic plaque volume and the relative contribution of the different plaque components will have important clinical implications: it provides new and probably better parameters, together with the severity of stenosis, for cardiovascular risk assessment, and furthermore the natural history of atherosclerotic disease and the effect of pharmacological intervention can be studied¹⁰. MDCTA has extensively been used to assess the severity of luminal narrowing, and nowadays attention is increasingly paid to the potential role of MDCTA

in qualitative and quantitative evaluation of the atherosclerotic plaque itself. Validation studies in which image-based plaque features are compared with histology, as well as assessment of observer variability, are necessary to establish the final role of MDCTA in qualitative and quantitative atherosclerotic plaque evaluation.

Until now a few coronary in vivo studies have compared the plaque volume assessed with MDCTA and intravascular ultrasound (IVUS). One study found a strong correlation ($r = 0.8$) and an underestimation of the coronary plaque volume assessed with MDCTA compared to IVUS.¹¹ Another study found a moderate correlation ($r = 0.55$) and an overestimation of coronary plaque area assessed with MDCTA compared to IVUS.¹² The discrepancies between these studies might be explained by the results of a third study that found a strong correlation coefficient ($r^2 = 0.69$) with an underestimation of mixed and noncalcified plaque volumes, and a trend to overestimate calcified plaque volumes with MDCTA. In addition, they reported a moderate reproducibility in the assessment of plaque volume, with a coefficient of variation of 37%.¹³

An in vivo study⁵ on carotid atherosclerotic plaques revealed a strong correlation between MDCTA and histology for the assessment of plaque area ($r^2 = 0.73$); in addition, the inter- and intra-observer variability of plaque area measurements with MDCTA was reasonable with coefficients of variation of 19% and 8%, respectively.

To our knowledge, the present study is the first study that shows that in vivo quantification of the volume of atherosclerotic carotid plaque and its components is possible with MDCTA (Figure 2.). Inter-observer variability was moderate with ICC ranging from 0.53-0.96 and coefficients of variation ranging from 13-58%. To evaluate the inter-observer variability caused by the manual drawing of the contours we re-evaluated the data after consensus was reached with regard to the length of atherosclerotic disease, the location of the bifurcation and lumen attenuation, because all these features also influenced the volume measurements. This led to a decreased variability with ICC ranging from 0.76-0.99 and coefficients of variation ranging from 3-47%. Intra-observer variability was less with ICC ranging from 0.94-1.00 and coefficients of variation ranging from 5-25%.

The first problem which causes a variability in volume measurements is the differentiation between a normal vessel wall and a slightly thickened (diseased) vessel wall. In a number of cases, observers disagree with regard to the presence of atherosclerotic disease in carotid arteries with a stenosis of 0-29%. In such cases, the assessed plaque volume in such patients will be very low; the measured plaque volume in the two arteries in which the observers disagree on the presence of atherosclerotic disease was 609 and 245 mm³, while the mean plaque volume of all patients was 1259 ± 621 mm³.

Furthermore, the difficulty in differentiation between a normal vessel wall and a slightly thickened (diseased) vessel wall, influences the assessment of the most proximal and distal image with atherosclerosis and thus the length of the atherosclerotic lesion. Because the plaque volume measurements include the original vessel wall, inclusion of additional images with normal vessel wall increases the amount of measured volumes considerably.

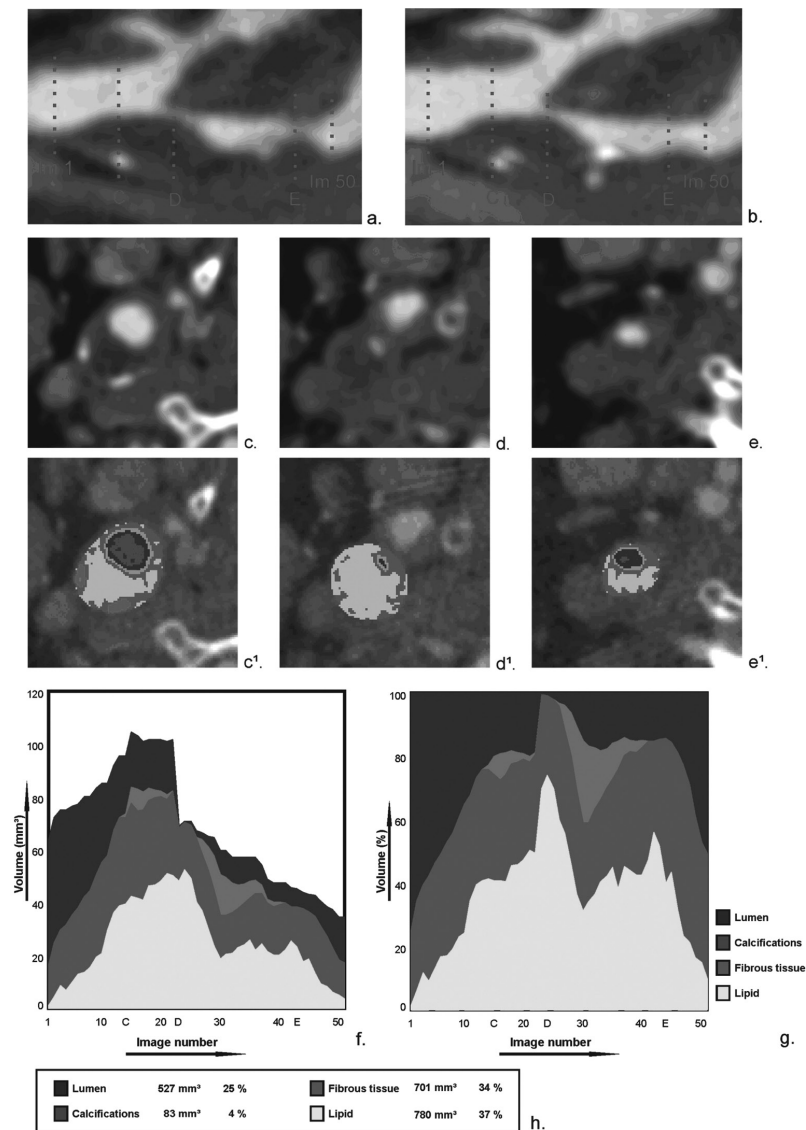


Fig. 2. One mm multiplanar reformat (a) and 2 mm maximum intensity projection (b) in the sagittal plane depicts the carotid bifurcation with an atherosclerotic plaque. The startpoint (Im 1) and endpoint (Im 50) of atherosclerotic plaque volume assessment in this patient, and the position (C, D, E) of the three thin sliced (0.75 mm) axial MDCT images (c, d and e) of the internal carotid artery and their associated color overlay images (c', d' and e') are indicated. A graphical representation of the absolute (f) and relative (g) volume measurements of lumen, calcifications, fibrous tissue, and lipid per MDCT image. The x-axis represents the consecutive MDCT images, the y-axis represents the volume. (h) A table with the total lumen, total calcified, total fibrous tissue and total lipid volume.

The second problem is the manual outlining of the outer border of the vessel wall. Some parts of the vessel wall can easily be differentiated from the surrounding tissue due to the low density of peri-arterial fat or the presence of calcifications at the outer border of the plaque. However, other parts have the same density as the peri- and paravertebral and sternocleidomastoid muscle, which are frequently positioned along the artery. The erroneous manual inclusion of peri-arterial fat in the ROI leads to the classification of this fat as lipid in the plaque. This inclusion will vary between the observers which explains the moderate ICC and the high observer variability in the assessment of lipid volume. The Bland-Altman plots confirm this by showing that the differences in lipid volume between observers 1 and 3, and 2 and 3 depend on the size of the assessed volume, suggesting that observer 3 systematically draws a larger outer contour than the other observers and thus includes more peri-arterial low density tissues. An additional problem in the assessment of the outer border of the vessel wall is, that the size of calcifications is influenced by differences in window-level setting. Because these calcifications are often located at the border of an atherosclerotic plaque, different window-level settings between observers will influence the assessment of the outer vessel wall between observers, and thereby introduce variability in the assessment of plaque volume and calcified volume.

The third problem is the differentiation of contrast-enhanced lumen from atherosclerotic plaque. In some plaque without calcifications at the inner border of the plaque the differentiation is automated and based on a threshold and the only variability is caused by a difference in the measurement of luminal attenuation, which was fortunately low. In case a calcification borders the lumen, a threshold based approach would merge the lumen with the calcification. In such cases manual drawing of the border between lumen and calcification was necessary which introduced a variability in plaque volume and calcium volume measurements.

We expect that improvements in the measurement software will improve the observer variability. Although in our method we assessed volumes, the analysis was performed in axial two-dimensional images. Evaluating the artery both in axial slices and using longitudinal reformats will provide more information on the borders of the vessel wall. This would enable a better continuation of transversal contours in adjacent slices. Also, highlighting specific parts of the vessel outer contour in axial images based on outer vessel contour assessment in longitudinal planes might be helpful. Finally, the differentiation between normal vessel wall and slightly thickened vessel wall can be based on wall thickness measurements, and the length of the atherosclerotic disease can be assessed more reproducibly.

Besides MDCTA, MRI has been used for non-invasive atherosclerotic carotid plaque characterization and quantification. Studies have shown that there is good agreement between in vivo MRI and histology for qualitative¹⁴⁻¹⁶ and quantitative¹⁷ assessment of plaque components, while observer reproducibility has shown to be good to excellent for plaque area^{14-16,18} and plaque component areas.¹⁹ ICC for plaque area were 0.90-0.96 and for lipid core 0.88-0.89. The reproducibility of MRI-based plaque volume measurements has not been extensively studied. One study reported a coefficient of variation for an averaged (over 5 slices) plaque

area of 3.5%²⁰, while another study reported a coefficient of variation of 9.8% for plaque volume.²⁰

Until now carotid intima-media thickness (CIMT) is a validated endpoint in progression/regression studies. CIMT has shown to be an independent risk factor for future myocardial infarction and stroke risk.^{21,22} In addition, CIMT has been related to the presence of future carotid plaque.²³ Lifestyle changes²⁴ and statin therapy²⁵ has a beneficial effect on CIMT. Ultrasound assessment of CIMT is accurate when compared with histology^{26,27}, and has a very good reproducibility (coefficient of variation 2.4-10.6%).²⁸ Interscan coefficient of variation is 5.6%,²⁸ making it a potential valuable tool to evaluate the effectiveness of prevention therapy. Unfortunately, CIMT does not provide us with area and volumetric measurements of the plaque and ignores the presence of different plaque components. This makes CIMT unsuitable for the precise evaluation of pharmacological effects on the advanced atherosclerotic plaque.

The present study investigated the reproducibility of MDCTA-based atherosclerotic plaque volume measurements. It is a limitation that validation with histology has not been performed. Because we investigated a range of carotid artery stenoses, atherosclerotic specimens were not available in most of the patients. In the patients with a stenosis of more than 70% stent placement or surgery was performed. Previous studies^{5,6}, however, have demonstrated a good correlation between area measurements with MDCTA and histology. A second limitation is the inclusion of the vessel wall (tunica media) in the plaque volume measurements. With MDCTA it is not possible to differentiate between the atherosclerotic plaque and the tunica media. This will lead to a systematic overestimation of plaque volume measurements. It is not expected that this overestimation will be a problem for serial evaluation or risk prediction.

Conclusion

In vivo assessment of atherosclerotic plaque and plaque component volumes in carotid arteries with MDCTA is feasible with a moderate reproducibility. A prospective longitudinal study which examines the relationship between cardiovascular risk factors, plaque and plaque component volumes and outcome may determine the value of MDCTA-based stroke risk predictors.

References

1. Glagov S, et al. Compensatory enlargement of human atherosclerotic coronary arteries. *N Engl J Med.* 1987; 316:1371-5.
2. Naghavi M, et al. From vulnerable plaque to vulnerable patient: a call for new definitions and risk assessment strategies: Part I. *Circulation.* 2003; 108:1664-72.
3. Polak JF, et al. Hypoechoic plaque at US of the carotid artery: an independent risk factor for incident stroke in adults aged 65 years or older. Cardiovascular Health Study. *Radiology.* 1998; 208:649-54.
4. Koelemay MJ, et al. Systematic review of computed tomographic angiography for assessment of carotid artery disease. *Stroke.* 2004; 35:2306-12.
5. de Weert TT, et al. In vivo characterization and quantification of atherosclerotic carotid plaque components with multidetector computed tomography and histopathological correlation. *Arterioscler Thromb Vasc Biol.* 2006; 26:2366-72.
6. de Weert TT, et al. In vitro characterization of atherosclerotic carotid plaque with multidetector computed tomography and histopathological correlation. *Eur Radiol.* 2005; 15:1906-14.
7. Beneficial effect of carotid endarterectomy in symptomatic patients with high-grade carotid stenosis. North American Symptomatic Carotid Endarterectomy Trial Collaborators. *N Engl J Med.* 1991; 325:445-53.
8. de Monye C, et al. Optimization of CT angiography of the carotid artery with a 16-MDCT scanner: craniocaudal scan direction reduces contrast material-related perivenous artifacts. *AJR* 2006; 186:1737-45.
9. de Monye C, et al. Sixteen-detector row CT angiography of carotid arteries: comparison of different volumes of contrast material with and without a bolus chaser. *Radiology.* 2005; 237:555-62.
10. Pulido MA, et al. Imaging of atherosclerotic plaque. *Int J Cardiovasc Imaging.* 2004; 20:553-9.
11. Achenbach S, et al. Detection of calcified and noncalcified coronary atherosclerotic plaque by contrast-enhanced, submillimeter multidetector spiral computed tomography: a segment-based comparison with intravascular ultrasound. *Circulation.* 2004; 109:14-7.
12. Moselewski F, et al. Comparison of measurement of cross-sectional coronary atherosclerotic plaque and vessel areas by 16-slice multidetector computed tomography versus intravascular ultrasound. *Am J Cardiol.* 2004; 94:1294-7.
13. Leber AW, et al. Accuracy of 64-slice computed tomography to classify and quantify plaque volumes in the proximal coronary system: a comparative study using intravascular ultrasound. *J Am Coll Cardiol.* 2006; 47:672-7.
14. Cai J, et al. In vivo quantitative measurement of intact fibrous cap and lipid-rich necrotic core size in atherosclerotic carotid plaque: comparison of high-resolution, contrast-enhanced magnetic resonance imaging and histology. *Circulation.* 2005; 112:3437-44.
15. Trivedi RA, et al. Multi-sequence in vivo MRI can quantify fibrous cap and lipid core components in human carotid atherosclerotic plaques. *Eur J Vasc Endovasc Surg.* 2004; 28:207-13.
16. Saam T, et al. Quantitative evaluation of carotid plaque composition by in vivo MRI. *Arterioscler Thromb Vasc Biol.* 2005; 25:234-9.

17. Yuan C, et al. Measurement of atherosclerotic carotid plaque size in vivo using high resolution magnetic resonance imaging. *Circulation*. 1998; 98:2666-71.
18. Takaya N, et al. Intra- and interreader reproducibility of magnetic resonance imaging for quantifying the lipid-rich necrotic core is improved with gadolinium contrast enhancement. *J Magn Reson Imaging*. 2006; 24:203-10.
19. Corti R, et al. Effects of lipid-lowering by simvastatin on human atherosclerotic lesions: a longitudinal study by high-resolution, noninvasive magnetic resonance imaging. *Circulation*. 2001; 104:249-52.
20. Adams GJ, et al. Tracking regression and progression of atherosclerosis in human carotid arteries using high-resolution magnetic resonance imaging. *Magn Reson Imaging*. 2004; 22:1249-58.
21. O'Leary DH, et al. Carotid-artery intima and media thickness as a risk factor for myocardial infarction and stroke in older adults. Cardiovascular Health Study Collaborative Research Group. *N Engl J Med*. 1999; 340:14-22.
22. Touboul PJ, et al. Carotid intima-media thickness, plaques, and Framingham risk score as independent determinants of stroke risk. *Stroke*. 2005; 36:1741-5.
23. Zureik M, et al. Cross-sectional and 4-year longitudinal associations between brachial pulse pressure and common carotid intima-media thickness in a general population. The EVA study. *Stroke*. 1999; 30:550-5.
24. Markus RA, et al. Influence of lifestyle modification on atherosclerotic progression determined by ultrasonographic change in the common carotid intima-media thickness. *Am J Clin Nutr*. 1997; 65:1000-4.
25. Probstfield JL, et al. Results of the primary outcome measure and clinical events from the Asymptomatic Carotid Artery Progression Study. *Am J Cardiol*. 1995; 76:47C-53C.
26. Wong M, et al. Ultrasonic-pathological comparison of the human arterial wall. Verification of intima-media thickness. *Arterioscler Thromb*. 1993; 13:482-6.
27. Pignoli P, et al. Intimal plus medial thickness of the arterial wall: a direct measurement with ultrasound imaging. *Circulation*. 1986; 74:1399-406.
28. Sramek A, et al. Ultrasound assessment of atherosclerotic vessel wall changes: reproducibility of intima-media thickness measurements in carotid and femoral arteries. *Invest Radiol*. 2000; 35:699-706.

Chapter 8

Is a Fetal Origin of the Posterior
Cerebral Artery a Risk Factor for TIA
or Ischemic Stroke? A Study with
16-Multidetector-Row CT Angiography

Is a fetal origin of the posterior cerebral artery a risk factor for TIA or ischemic stroke? A study with 16-multidetector-row CT angiography

Cécile de Monyé, MD
 Diederik W. J. Dippel, MD, PhD
 Theodora A. M. Siepman, MD
 Marcel L. Dijkshoorn, BHS
 Hervé L. J. Tanghe, MD
 Aad van der Lugt, MD, PhD

J Neurol 2008; 255:239–245

Abstract

Background and purpose: Fetal origin of the posterior cerebral artery (PCA) is not uncommon. Whether patients with this anomaly have a higher risk of ischemic stroke in the territory of the PCA is not known. The clinical benefit of screening for a fetal origin in patients with TIA or stroke in the territory of the PCA and an ipsilateral atherosclerotic carotid stenosis is not clear. This study assessed the frequency of a fetal origin of the PCA in patients with a TIA or infarct in the territory of the PCA with 16-multidetector-row CT angiography (CTA).

Methods: 82 patients (52 male; mean age = 64; range 19 to 90 years) with isolated homonymous hemianopia and/or a PCA infarct underwent CTA of the carotid artery and circle of Willis.

Results: A fetal origin of the PCA at the symptomatic side was present in 14 patients (17%) and at the asymptomatic side in 18 patients (22%) (OR: 0.7; 95% CI: 0.3 to 1.7). Severity of stenosis (NASCET criteria) of the ICA at the symptomatic side was <30%, 30–49% and ≥50% in 72, 2 and 8 patients, respectively. Number and frequency of a fetal origin in these groups were 12 (17%), 0 (0%) and 2 (25%), respectively. There was no association between a severe carotid stenosis and a fetal origin of the PCA at the symptomatic side.

Conclusion: This study does not provide arguments for an increased risk of ischemic stroke in the territory of the PCA in patients with a fetal origin of the PCA. A few patients with a TIA or infarct in the territory of the PCA have a fetal origin of the PCA in combination with a high-grade stenosis of the ipsilateral ICA, but not more often than one would expect from chance. Nevertheless, these patients may benefit from carotid endarterectomy.

Introduction

In approximately 5 to 10% of patients with a TIA or minor stroke the ischemia is located in the territory of the posterior cerebral artery (PCA).^{4,13} These patients present with homonymous hemianopia that can be accompanied by a wide spectrum of other features, such as headache, neuropsychological impairment and (often mild) motor and sensory deficits.^{5,8,18,27} A stroke in this territory can be caused by atherosclerotic disease of the vertebral, basilar or posterior cerebral arteries, cardiac embolism, vasospasm (migraine), hemodynamic disorders or hematologic disorders with coagulopathy.^{5,8,18,27}

Most commonly, the PCA derives from the basilar artery. However, in 10–20% of normal subjects the PCA derives from the ICA through a patent posterior communicating artery (PCoA), while the connection with the basilar artery is hypoplastic or even aplastic.^{12,16,20,22,24} Such a fetal origin of the PCA in combination with atherosclerotic disease or dissection of the carotid artery may cause an ischemic stroke in the occipital lobe.^{6,14,17}

Patients with a transient ischemic attack (TIA) or a minor stroke in the territory of the internal carotid artery (ICA) combined with an ipsilateral carotid artery stenosis of more than 70% benefit from carotid endarterectomy.^{1,2} It follows that patients with a TIA or mild stroke in the territory of the PCA who have a fetal origin of the PCA and atherosclerotic disease in the ICA might also be candidates for carotid endarterectomy. With the introduction of multidetector-row CT, CT angiography (CTA) has become an accurate, fast and noninvasive method to analyze the carotid arteries and the anatomy of the circle of Willis.^{9,11,23} Because CTA has significantly less morbidity and mortality than digital subtraction angiography (DSA), it may be used in screening patients with cerebrovascular symptoms in the territory of the PCA.

Whether patients with a fetal origin of the PCA have a higher risk of TIA or ischemic stroke in this arterial distribution is not known.²⁴ The clinical benefit of screening for a fetal origin in patients with TIA or stroke in the territory of the PCA and an ipsilateral atherosclerotic carotid stenosis is not clear.

The purpose of this study was to assess the frequency of a fetal origin of the PCA in a clinical series, and the degree of stenosis of the ipsilateral ICA in patients with a TIA or infarct in the territory of the PCA with 16-multidetector-row CTA.

Methods

Patient selection

In the first (retrospective) part of the study the files of patients with cerebrovascular symptoms who presented at the department of neurology between January 1998 and April 2002 were reviewed and patients who met the inclusion criteria were

invited to participate in the study. In the second (prospective) part of the study that lasted from April 2002 to May 2004, patients who presented at the department of neurology and who met the inclusion criteria were invited to participate in the study. All patients in our study were evaluated in a rapid TIA or stroke service by a neurologist in training and a vascular neurologist, according to a pre-specified protocol. Inclusion criteria for the study were: a) a sudden onset of homonymous hemianopia, without other focal neurological deficits and a normal CT scan of the brain; and b) a sudden onset of homonymous hemianopia with or without other focal neurological deficits and a recent infarction in the territory of the PCA on the CT scan of the brain. When the attack of visual loss was transient, the patient should have covered each eye alternately to exclude monocular blindness, and the attack should not have been accompanied by positive phenomena, nor should the patient have experienced headache during the attack. Patients with a symptomatic lacunar infarction of the thalamus (diameter <15 mm) only, and patients with simultaneously bilateral occipital infarcts were not included. Exclusion criteria were: previous allergic reaction to iodine contrast media, renal insufficiency (serum creatinine >150 mmol/L), Rankin score >3 and age <18 years. The Institutional Review Board approved the study and patients gave written informed consent before inclusion in the study.

Patients underwent a CT scan of the brain and a CTA of the carotid arteries and circle of Willis.

Data acquisition and post processing

CT examinations were performed on a 16-multidetector-row CT scanner (Sensation 16, Siemens Medical Solutions, Forchheim, Germany). Patients were positioned supine on the CT table with the arms along the chest. The CT scan of the brain range reached from the skull base to the vertex parallel to the orbitomeatal line. The CTA scan range reached from the ascending aorta to the intracranial circulation (2 cm above the sella turcica). Scan parameters were: number of detectors 16, collimation 0.75 mm, table feed per rotation 12 mm (pitch 1), rotation time 0.5 s, kV 120, eff. mAs 180, scan direction caudocranial, scan time 10–14 s (depending on individual patient's size and anatomy).

A volume of 80 mL contrast material (Iodixanol 320 mg/mL, Visipaque, Amersham Health, Little Chalfont, UK) was injected using a power injector (EnVision, MedRAD, Pittsburgh, PA, USA) through an 18–20G iv cannula (depending on the size of the vein), in an antecubital vein at 4 mL/s. Synchronization between the passage of contrast material and data acquisition was achieved by real time bolus tracking.⁷

Images were reconstructed with effective slice width 1 mm, reconstruction interval 0.6 mm, FOV 100 mm and convolution kernel B30 f (= medium-smooth). The images were transferred to a stand-alone workstation and evaluated using dedicated analysis software (Leonardo – Siemens Medical Solutions, Forchheim, Germany). For the evaluation of stenosis of the carotid artery multiplanar reconstructions were

used. For the evaluation of the circle of Willis slab maximum intensity projections with a thickness of 6 mm were used in the axial, sagittal and coronal planes and a plane parallel to the clivus for the posterior circulation.

Data collection and analysis

Patient's age at the time of stroke, gender, risk factors (hypertension, hypercholesterolemia, diabetes mellitus, smoking and previous brain- or myocardial infarction) and type of event (TIA or minor stroke) were recorded. Possible and probable causes of cardiac embolism were recorded.³ The CT scan of the brain performed at the time of initial evaluation was evaluated for infarction in the territory of the PCA (occipital lobe or posterior part of the temporal lobe).

In the retrospectively studied patient group the severity of stenosis of the carotid artery was based on the duplex ultrasound (DUS) performed at the time of the initial evaluation. If no DUS was performed at that time, the CTA for the present study that included both the carotid arteries and the circle of Willis was used. In the

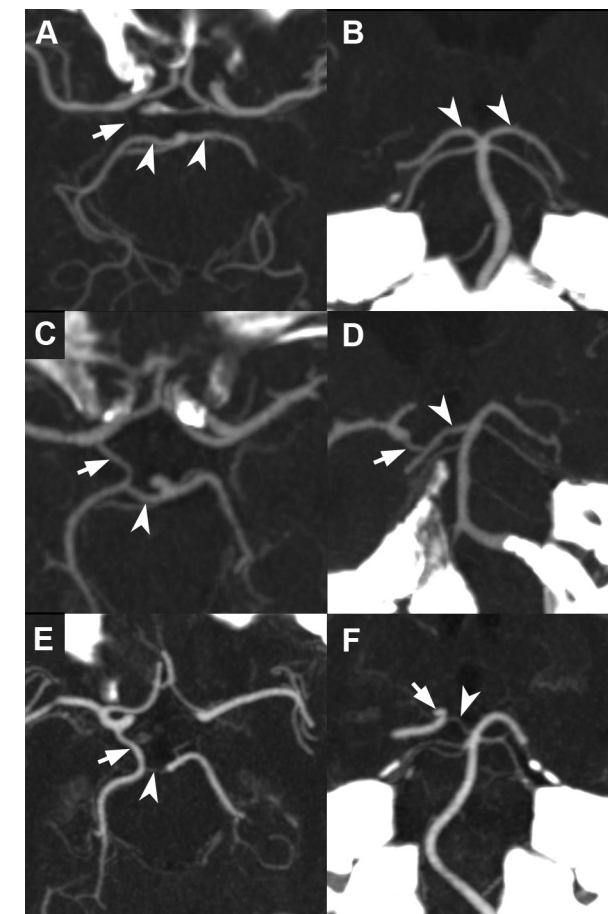


Fig.1 CT angiography of the circle of Willis. Maximum intensity projections (10mm) in an axial plane (a, c, e) and a plane parallel to the clivus (b, d, f).

a and b (78-yr-old man): on both sides the size of the P1 segment of the PCA (arrowheads) is normal and the PCoA is hypoplastic (right side, arrow) or aplastic (left side) (= standard configuration).

c and d (71-yr-old man): on the right side the size of the P1 segment of the PCA (arrowhead) is equal to the size of the PCoA (arrow) (= transitional configuration).

e and f (71-yr-old woman): on the right side the P1 segment of the PCA (arrowhead) is hypoplastic and smaller than the PCoA (arrow) (= fetal origin)

prospectively studied patient group the CTA performed for the present study was evaluated for the severity of stenosis. The severity of stenosis was measured on the CTA scan according to the NASCET criteria¹⁹ and assessed with DUS according to peak systolic velocity (PSV) in the stenosis¹⁵. Multiplanar reformatted images were used for manual measurements of the remaining luminal diameter at a stenosis and the luminal diameter at a normal segment distal to the stenosis. The degree of stenosis was defined as the remaining luminal diameter at the stenosis as percentage of the normal luminal diameter distal to the stenosis. The degree of stenosis was categorized into 0–29%, 30–49 % and ≥ 50 %. The presence of atherosclerosis was scored as mild, moderate or severe. Atherosclerotic disease with a stenosis > 50 % in the posterior circulation from the subclavian artery to the proximal posterior cerebral artery (P1 segment) was assessed.

The size of the PCoA was compared to the P1 segment of the PCA. The diameter of the PCoA was classified as larger than (fetal origin), equal to (transitional configuration) or smaller than (standard configuration) the P1 segment (Fig. 1). Because both a fetal origin and a transitional configuration can lead to embolization of thrombus or atherosclerotic debris from the carotid artery into the PCA, they were combined for analysis and addressed as “fetal origin of the PCA”. In a previous study the accuracy of CTA (93 %) in the assessment of a fetal origin in comparison with DSA and the interobserver variability of CTA ($k = 0.79$) was evaluated.²³

Two radiologists evaluated the CTA of the circle of Willis for a fetal origin of the PCA. They discussed discrepancies in order to reach consensus.

Statistical analysis

Differences in frequency of a fetal origin between subgroups were explored using the Fisher’s exact test. The association between the presence of carotid stenosis and fetal origin of the PCA was studied with contingency table analysis, and expressed as a risk ratio with exact 95 % confidence interval. A p -value < 0.05 was considered statistically significant. We thus estimated the relative risk (odds ratio with 95 % CI) of stroke from a fetal origin in a case control design, by considering the symptomatic PCA as a case, and the asymptomatic PCA as referent, and the presence of a fetal origin as the determinant of stroke risk, after testing whether fetal origin of either PCA occurred independently of each other.

Results

Of the 171 patients who met the inclusion criteria, 82 patients (52 male; mean age = 64; range 19–90 years) participated in the present study. Of these, 41 of 113 patients presented between January 1998 and April 2002 and 41 of 58 patients presented between April 2002 to May 2004. Reasons for not participating in the study were: death ($n = 18$), could not be reached ($n = 9$), renal insufficiency ($n = 3$),

allergy for iodine contrast media ($n = 3$), dementia ($n = 4$), severe disability ($n = 5$), no venous access ($n = 1$), technically inadequate CTA scan ($n = 1$) and no informed consent ($n = 45$). Patient characteristics are shown in Table 1. Possible or probable sources of cardioembolism were atrial fibrillation (5 pts, 6 %), sick sinus syndrome (1 pt), aortic valve stenosis (1 pt), post-CABG (1 pt), and cardiac thrombus (1 pt).

Table 1. Patient Characteristics

	Prospective ($n=41$)		Retrospective ($n=41$)		Total ($n=82$)	
Male	25	(61%)	27	(66%)	52	(63%)
Age: mean (range) years	68	(35-90)	59	(19-82)	64	(19-90)
Event						
TIA	18	(44%)	17	(41%)	35	(43%)
Minor stroke	23	(56%)	24	(59%)	47	(57%)
Relevant infarct on CT						
Yes	20	(49%)	24	(59%)	44	(54%)
No	21	(51%)	17	(41%)	38	(46%)
CT infarction side						
Left	6		15		21	
Right	14		9		23	
Hypertension	28	(68%)	22	(54%)	50	(61%)
Hypercholesterolemia	24	(59%)	31	(76%)	55	(67%)
Diabetes mellitus	8	(20%)	4	(10%)	12	(15%)
Smoking	18	(44%)	15	(37%)	33	(40%)
Peripheral arterial disease	3	(7%)	0	(0%)	3	(4%)
Previous TIA / Stroke	2	(5%)	7	(17%)	9	(11%)
Previous myocardial infarction	7	(17%)	2	(5%)	9	(11%)
Cardioembolism	5	(12%)	4	(10%)	9	(11%)
Possible	1	(2%)	1	(2%)	2	(2%)
Probable	4	(10%)	3	(7%)	7	(9%)
Vertebrobasilar artery disease	11	(27%)	9	(22%)	20	(24%)
Subclavian artery stenosis (>50%)	0	(0%)	2	(5%)	2	(2%)
Vertebral artery stenosis (>50%)	9	(22%)	5	(12%)	14	(17%)
Basilar artery disease	1	(2%)	1	(2%)	2	(2%)
Vertebral artery occlusion	1	(2%)	1	(2%)	2	(2%)

In 12 patients of the retrospectively studied group no DUS was performed at the time of initial evaluation. In these patients the CTA was used to grade the degree of stenosis of the carotid artery. Stenosis of the carotid artery, according to the NASCET criteria¹⁹, at the symptomatic side was 0–29% in 72 cases, 30–49% in 2 cases and 50–99 % in 8 cases (Table 2).

Table 2. Degree of Stenosis and Atherosclerosis of the Carotid Artery of the Symptomatic Side

Stenosis	Atherosclerosis	Prospective	Retrospective	Total
0-29%	No	12	20	32
0-29%	Mild	10	10	20
0-29%	Moderate	8	8	16
0-29%	Severe	3	1	4
30-49%	Severe	2	0	2
50-69%	Severe	2	1	3
70-99%	Severe	4	1	5
Total		41	41	82

A fetal origin of the PCA was found in 14 patients (17%) at the symptomatic side and in 18 patients (22%) at the asymptomatic side (OR: 0.7; 95% CI: 0.3 to 1.7) (Table 3). Bilateral fetal origin occurred in 5 patients (6%). The frequency of a fetal origin of the PCA on the symptomatic side in different subgroups is shown in Table 4. A fetal origin of the PCA was not associated with gender, age at time of presentation (age < or \geq 65, years), type of event (TIA or stroke) or presence of an infarct on the CT scan of the brain.

Table 3. Configuration of the Circle of Willis Ipsilateral and Contralateral to the Symptomatic Side: Diameter of Posterior Communicating Artery (PCoA) in Comparison with Diameter of the P1 Segment of the Posterior Cerebral Artery (P1)

	PCoA < P1	PCoA > P1	PCoA = P1
Ipsilateral	68	12	2
Contralateral	64	15	3

Patients with a fetal origin of the symptomatic PCA did not more often have an ipsilateral carotid artery stenosis ($p = 0.62$; Fisher's exact test, 2-sided). Conversely, patients with a severe carotid stenosis ipsilateral to the symptomatic hemisphere were not more likely to have an ipsilateral fetal origin of the PCA than patients without a severe carotid stenosis (RR 1.5, 95% CI: 0.4–5.7). Exclusion of patients with possible or probable cardioembolism did not change our results, nor did exclusion of patients with a transitional configuration.

Discussion

In this study we screened patients who had a TIA or ischemic stroke in the territory of the PCA with CTA, for a fetal origin of the PCA: the frequency of a fetal origin of the PCA at the symptomatic side is not higher than the frequency at the asymptomatic side or than the reported frequencies in the literature.^{10,18,25} Moreover, in our

study no association was found between the presence of a fetal origin of the PCA and an ipsilateral severe ($\geq 50\%$) carotid artery stenosis.

The present study has several limitations. First, to allow thrombo-emboli from the carotid artery to pass through the PCoA to the PCA, there has to be antegrade flow in the PCoA, i.e. from the carotid artery to the P2 segment of the PCA. CTA is not able to provide hemodynamic information concerning blood flow direction in individual vessels. In case of a transitional configuration of the PCA on CTA it is not certain that there is indeed antegrade flow in the PCoA. In a previous study, however, we showed that DSA revealed complete filling of the PCA after injection of the ICA in 12 of the 13 cases with a transitional configuration.²³

Table 4. Frequency of a Fetal Origin on the Ipsilateral Side in Different Subgroups

	Total	Fetal origin	
Gender			
Male	52	8	(15%)
Female	30	6	(20%)
Age at time of presentation			
< 65 years	37	8	(22%)
> 65 years	45	6	(13%)
Event			
TIA	35	6	(17%)
Stroke	47	8	(17%)
Relevant infarct on CT			
Yes	44	5	(11%)
No	38	9	(24%)
Ipsilateral carotid stenosis			
0-29%, no atherosclerosis	32	6	(19%)
0-29%, atherosclerosis	40	6	(15%)
30-49%	2	0	(0%)
> 50%	8	2	(25%)
Total	82	14	(17%)

Second, DUS and CTA were used to grade the degree of stenosis of the carotid artery. Recently, Wardlaw et al. showed in a meta-analysis that noninvasive imaging of a symptomatic carotid artery stenosis could replace intra-arterial carotid angiography for 70–99% stenosis, but still more data are required to determine their accuracy, especially at 50–69% stenoses.²⁶ In our study we grouped both categories together, because both have an increased risk of stroke. Because the incidence of a fetal origin of the PCA is low and patients with occipital stroke are not treated with carotid endarterectomy in our hospital, it would not have been ethical to perform intra-arterial carotid angiography in these patients.

Third, our study investigated a small number of patients. The fact that we could not prove an association between the presence of a fetal origin of the PCA and an ipsilateral severe carotid artery stenosis could be caused by the small number of patients with severe carotid artery stenosis in our study. However, when all ipsilateral atherosclerotic carotid artery lesions were considered as symptomatic carotid lesions there was still no association with the presence of a fetal origin of the PCA ($p = 0.77$). Still, our results do not make a relative risk of PCA-stroke associated with a fetal origin of the ipsilateral PCA of 1.5 to 1.7 entirely unlikely, as these values fall within the range of the 95% CI. In order to obtain even more precise estimates, additional studies will be necessary.

Fourth, the retrospective nature of the first part of our study is a limitation. This may have jeopardized the accuracy and completeness of our data. However, the protocolized approach in our rapid TIA and stroke service by a neurologist in training and a vascular neurologist, determines that relevant data have been systematically sought and recorded.

Fifth, we did not exclude patients with a possible source of cardioembolism. We wanted our inclusion criteria to match the standard clinical situation, where one wonders whether ischemia in the PCA territory could be attributed to carotid disease. We therefore included all patients with a clinical diagnosis of ischemia in the territory of the posterior cerebral artery that could be attributed to thromboembolism.

In other patient series with infarction in the PCA territory similar data on the combination of a fetal origin and ICA arterial disease have been reported.^{21,27} Yamamoto et al. reported 1 of 79 cases with a PCA territory infarct.²⁷ Steinke et al. attributed two of 74 cases to carotid artery disease with a fetal origin of the PCA.²¹ However, in both those studies angiographic examinations were not performed in all cases. Graf et al. performed CTA in 103 cases with ischemic stroke or TIA in the posterior circulation and in 8 cases a fetal origin of the PCA was found¹⁰; however, whether this was considered as the cause of the PCA infarcts in their series was not reported.

This study does not provide arguments for an increased risk of ischemic stroke in the territory of the PCA in patients with a fetal origin of the PCA. Nevertheless, in an individual patient with a TIA or infarct in the territory of the PCA this could still be the most likely cause and therefore the patient might benefit from carotid endarterectomy. A cost-effectiveness study should be performed to investigate whether screening patients with a recent TIA or infarct in the territory of the PCA for a fetal origin and atherosclerotic disease of the ipsilateral carotid artery is justified.

Acknowledgments:

Grant support: College voor Zorgverzekeringen/Vereniging Academische Ziekenhuizen, Doelmatigheidsproject 01116.

References

1. North American Symptomatic Carotid Endarterectomy Trial Collaborators. Beneficial effect of carotid endarterectomy in symptomatic patients with high-grade carotid stenosis. *N Engl J Med* 1991; 325:445–453.
2. European Carotid Surgery Trialists' Collaborative Group. MRC European Carotid Surgery Trial: interim results for symptomatic patients with severe (70–99 %) or with mild (0–29 %) carotid stenosis. *Lancet* 1991; 337:1235–1243.
3. Ay H, Furie KL, Singhal A, Smith WS, Sorensen AG, Koroshetz WJ. An evidence-based causative classification system for acute ischemic stroke. *Ann Neurol* 2005; 58:688–697.
4. Bogousslavsky J, Van Melle G, Regli F. The Lausanne Stroke Registry: analysis of 1,000 consecutive patients with first stroke. *Stroke* 1988; 19:1083–1092.
5. Brandt T, Thie A, Caplan LR, Hacke W. Infarcts in the brain areas supplied by the posterior cerebral artery, Clinical aspects, pathogenesis and prognosis. *Nervenarzt* 1995; 66:267–274.
6. Cohen SN. Occipital infarction with hemianopsia from carotid occlusive disease. *Stroke* 1989; 20:1433–1434.
7. de Monye C, Cademartiri F, de Weert TT, Siepmann DA, Dippel DW, van Der Lugt A. Sixteen-detector row CT angiography of carotid arteries: comparison of different volumes of contrast material with and without a bolus chaser. *Radiology* 2005; 237:555–562.
8. Fisher CM. The posterior cerebral artery syndrome. *Can J Neurol Sci* 1986; 13:232–239.
9. Fleischmann D. Present and future trends in multiple detector-row CT applications: CT angiography. *Eur Radiol* 2002; 12(Suppl 2):S11–S15.
10. Graf J, Skutta B, Kuhn FP, Ferbert A. Computed tomographic angiography findings in 103 patients following vascular events in the posterior circulation: potential and clinical relevance. *J Neurol* 2000; 247:760–766.
11. Hollingworth W, Nathens AB, Kanne JP, Crandall ML, Crummy TA, Hallam DK, Wang MC, Jarvik JG. The diagnostic accuracy of computed tomography angiography for traumatic or atherosclerotic lesions of the carotid and vertebral arteries: a systematic review. *Eur J Radiol* 2003; 48:88–102.
12. Jongen JC, Franke CL, Soeterboek AA, Versteeg CW, Ramos LM, van Gijn J. Blood supply of the posterior cerebral artery by the carotid system on angiograms. *J Neurol* 2002; 249:455–460.
13. Kleihues P, Hizawa K. The infarct of the posterior cerebral artery: pathogenesis and topographical relationship to the visual cortex. *Arch Psychiatr Nervenkr* 1966; 208:263–284.
14. Kuker W, Mull M, Block F, Thron A. Carotid artery dissections presenting as isolated posterior cerebral artery infarctions. *J Neurol* 1997; 244:324–327.
15. Nederkoorn PJ, Mali WP, Eikelboom BC, Elgersma OE, Buskens E, Hunink MG, Kappelle LJ, Buijs PC, Wust AF, van der Lugt A, van der Graaf Y. Preoperative diagnosis of carotid artery stenosis: accuracy of noninvasive testing. *Stroke* 2002; 33:2003–2008.
16. Pedroza A, Dujovny M, Artero JC, Umansky F, Berman SK, Diaz FG, Ausman JL, Mirchandani HG. Microanatomy of the posterior communicating artery. *Neurosurgery* 1987; 20:228–235.

17. Pessin MS, Kwan ES, Scott RM, Hedges TR 3rd. Occipital infarction with hemianopsia from carotid occlusive disease. *Stroke* 1989; 20:409–411.
18. Pessin MS, Lathi ES, Cohen MB, Kwan ES, Hedges TR 3rd, Caplan LR. Clinical features and mechanism of occipital infarction. *Ann Neurol* 1987; 21:290–299.
19. Rothwell PM, Eliasziw M, Gutnikov SA, Fox AJ, Taylor DW, Mayberg MR, Warlow CP, Barnett HJ. Analysis of pooled data from the randomised controlled trials of endarterectomy for symptomatic carotid stenosis. *Lancet* 2003; 361:107–116.
20. Saeki N, Rhoton AL Jr. Microsurgical anatomy of the upper basilar artery and the posterior circle of Willis. *J Neurosurg* 1977; 46:563–578.
21. Steinke W, Mangold J, Schwartz A, Hennerici M. Mechanisms of infarction in the superficial posterior cerebral artery territory. *J Neurol* 1997; 244:571–578.
22. Tulleken CA, Luiten ML. The basilar artery bifurcation: microscopical anatomy. *Acta Neurochir (Wien)* 1987; 85:50–55.
23. van der Lugt A, Buter TC, Govaere F, Siepmann DA, Tanghe HL, Dippel DW. Accuracy of CT angiography in the assessment of a fetal origin of the posterior cerebral artery. *Eur Radiol* 2004; 14:1627–1633.
24. van Raamt AF, Mali WP, van Laar PJ, van der Graaf Y. The fetal variant of the Circle of Willis and its influence on the cerebral collateral circulation. *Cerebrovasc Dis* 2006; 22:217–224.
25. Velthuis BK, van Leeuwen MS, Witkamp TD, Ramos LM, Berkelbach van der Sprenkel JW, Rinkel GJ. Surgical anatomy of the cerebral arteries in patients with subarachnoid hemorrhage: comparison of computerized tomography angiography and digital subtraction angiography. *J Neurosurg* 2001; 95:206–212.
26. Wardlaw JM, Chappell FM, Best JJ, Wartolowska K, Berry E. Noninvasive imaging compared with intraarterial angiography in the diagnosis of symptomatic carotid stenosis: a meta-analysis. *Lancet* 2006; 367:1503–1512.
27. Yamamoto Y, Georgiadis AL, Chang HM, Caplan LR. Posterior cerebral artery territory infarcts in the New England Medical Center Posterior Circulation Registry. *Arch Neurol* 1999; 56:824–832.

Chapter 9

MDCT Detection of Fibromuscular
Dysplasia of the Internal Carotid Artery

MDCT detection of fibromuscular dysplasia of the internal carotid artery

Cécile de Monyé, MD
 Diederik W. J. Dippel, MD, PhD
 Marcel L. Dijkshoorn, BHS
 Hervé L. J. Tanghe, MD
 Aad van der Lugt, MD, PhD

AJR 2007; 188:W367–W369

Abstract

Objective: The purpose of this article is to describe two cases in which fibromuscular dysplasia of the internal carotid artery was diagnosed with CT angiography.

Conclusions: CT angiography can depict the characteristic findings of fibromuscular dysplasia. If patients with cerebrovascular symptoms undergo screening with CT angiography of the supraortic vessels, more cases of fibromuscular dysplasia will be recognized as a cause of neurologic symptoms.

Introduction

Fibromuscular dysplasia (FMD) of the cervical arteries is a possible cause of stroke. It can be detected with conventional angiography and less sensitively with duplex sonography and MR angiography. In 2002, we started a study in which we used CT angiography (CTA) to screen patients with symptoms of transient ischemic attack or minor stroke for atherosclerosis and stenosis of the carotid artery. Since then, two cases of FMD of the internal carotid artery (ICA) have been encountered in a group of 400 consecutively screened patients. To our knowledge, except for a report by Castillo and Wilson¹, descriptions of CTA of FMD of the carotid artery have not been published. Castillo and Wilson in 1994 reported the cases of two patients with carotid FMD diagnosed with digital subtraction angiography although CTA findings suggested carotid occlusion. We present two cases in which FMD of the ICA was diagnosed with CTA.

Observed Cases

Patient 1

A 39-year-old woman presented with acute hemiparesis of the left side of the body and mild dysarthria. The patient was a heavy smoker and used oral contraceptives. Findings on CT of the brain were normal. Duplex sonography of the carotid arteries showed no signs of atherosclerosis. CTA of the carotid arteries, from the ascending aorta to the intracranial circulation, was performed with a 16-MDCT scanner (Sensation 16, Siemens Medical Solutions). Scanning parameters were as follows: individual detector width, 0.75 mm; table feed per rotation, 12 mm (pitch of 1);

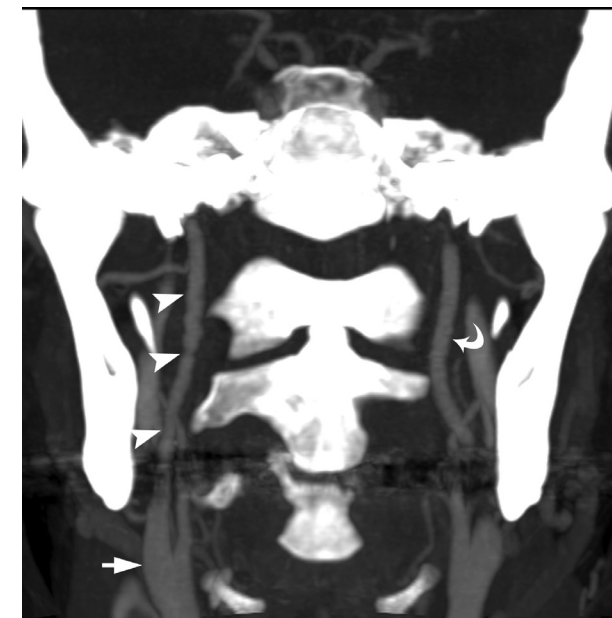


Fig. 1 39-year-old woman with acute hemiparesis of left side of body and mild dysarthria. Coronally reformatted CT angiogram of right and left internal carotid arteries shows string-of-beads appearance of right internal carotid artery (arrowheads). Left internal carotid artery (curved arrow) is normal. Signs of atherosclerosis, especially at level of carotid bifurcation (straight arrow), are absent.

gantry rotation time, 0.5 second; 120 kV; effective tube current, 180 mAs; scanning time, 10–14 seconds. Eighty milliliters of contrast material (iodixanol 320 mg I/mL, Visipaque, Amersham Health) and a 40-mL saline bolus chaser were injected through an 18- to 20-gauge IV cannula in an antecubital vein, both at an injection rate of 4 mL/s with a double-head power injector (Stellant, Medrad). Synchronization between passage of contrast material and data acquisition was achieved with real-time bolus tracking. Images were reconstructed with the following parameters: effective slice width, 1 mm; reconstruction interval, 0.6 mm; field of view, 120 mm; convolution kernel, B30f (medium smooth). CTA showed no signs of atherosclerosis in any vessel, and the anatomic features of the circle of Willis were normal. The right ICA had a typical string-of-beads appearance at the level of the first, second, and third cervical vertebrae (Fig. 1). The left ICA and vertebral arteries had no abnormalities. Therapy with alteplase was started within 3 hours after onset of symptoms and resulted in partial resolution of symptoms. The patient was treated with antiplatelet drugs and did not experience new symptoms during follow-up.

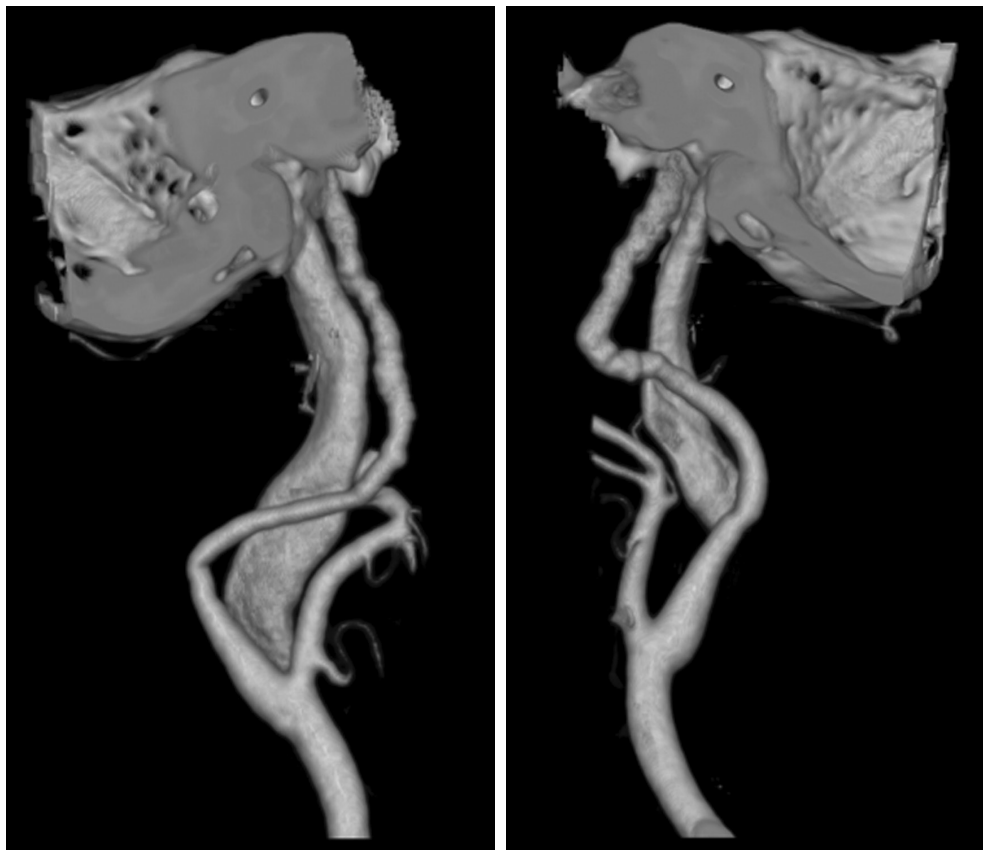


Fig. 2 78-year-old woman with left amaurosis fugax. A and B, Volume-rendered CT angiograms of left (A) and right (B) carotid arteries. String-of-beads appearance of internal carotid artery is visible at distal extracranial internal carotid artery on both sides.

Patient 2

A 78-year-old woman presented with left amaurosis fugax and mild hypertension. CT of the brain showed no abnormalities. Duplex sonography of the carotid arteries showed no signs of atherosclerosis. CTA performed with the protocol used for patient 1 showed only small calcifications in the brachiocephalic trunk and the left subclavian artery. There were no signs of atherosclerosis in other vessels. The distal cervical portion of both ICAs had a typical string-of-beads appearance (Fig. 2). The vertebral arteries had no abnormalities. The patient was treated with antihypertensive and antiplatelet drugs and had no symptoms during follow-up.

Discussion

FMD is an uncommon segmental, nonatheromatous, noninflammatory arterial disease of unknown causation that affects small to medium-sized vessels in many areas of the body. The renal arteries are the most commonly affected, followed by the cervicocephalic vessels.² Cervicocephalic FMD involves the extracranial part of the ICA in nearly 75% of patients.³ The vertebral artery is involved in 15–25% of patients, and multiple vessels are involved in 60–75% of patients.³ FMD of the cervicocephalic vessels is most often encountered in the fifth decade of life and occurs predominantly in women.

Cervicocephalic FMD is often asymptomatic and an incidental finding on imaging or at autopsy. It also, however, can manifest itself with a variety of specific neurologic symptoms, including transient ischemic attack, amaurosis fugax, and stroke or nonspecific symptoms such as headache and tinnitus.²

On arteriograms, the most common appearance of FMD is multifocal concentric luminal narrowing alternating with areas of mural dilatation that are wider than the original lumen.⁴ This finding is also described as the string-of-beads appearance and is present in 80–90% of patients with FMD.⁵ Less common imaging findings include focal or tubular stenosis, a septum, and a diverticulum.⁵ The condition is also associated with arterial dissection, intracranial aneurysms, and arteriovenous fistulas. Duplex sonography and color Doppler imaging can depict FMD of the ICA only when the lesion is located proximally.⁶ Color Doppler imaging reveals the segmental string-of-beads pattern with alternating regions of luminal narrowing and vascular dilatation distal to a completely normal segment of vessel. High-grade distal FMD stenosis also can be detected on the basis of indirect hemodynamic criteria. On time-of-flight MR angiography, artifacts caused by patient motion and swallowing or related to in-plane flow and susceptibility gradients may mimic the appearance of FMD and tend to decrease both sensitivity and specificity for detection of cervicocephalic FMD. The increased resolution and decreased scanning time of contrast-enhanced MR angiography may solve this problem.

Cervicocephalic FMD is an uncommon cause of cerebral ischemia. The diagnostic evaluation of patients with cerebrovascular symptoms commonly includes CT of

the brain and duplex sonography of the cervical arteries to detect significant atherosclerotic disease in the carotid artery. Until recently, duplex sonography was used as a screening instrument to select patients for digital subtraction angiography. The implication is that with this policy, assessment of FMD relies on the sensitivity of duplex sonography in detection of this disease. FMD is most commonly localized in the middle and distal portions of the ICA at the level of the first and second cervical vertebrae. This unfavorable localization results in much lower sensitivity of duplex sonography than of angiography in the detection of FMD of the ICA.⁶ Therefore, many cases of cervical FMD as a cause of cerebral ischemia can be missed.

With the introduction of helical CT scanners, especially MDCT scanners, CTA of the carotid artery has entered clinical practice. The technique has high sensitivity and specificity in the detection of carotid artery stenosis and may replace digital subtraction angiography and MR angiography. Because it is noninvasive, faster, and more accurate than duplex sonography, CTA may replace sonography in screening for vascular abnormalities in patients with cerebrovascular symptoms. Since 2002, all patients in our department with ischemic neurologic symptoms have been screened with CTA. Among the 400 patients screened as of this writing, we encountered two (0.5%) cases of FMD, a higher frequency than reported in a review of autopsies (0.02%)⁷ and equal to the frequencies in reviews of cerebral angiography (0.25–0.68%).⁷ The higher incidence of FMD in our series compared with that in the autopsy series can be explained by the higher frequency of FMD in a population with ischemic neurologic symptoms. Both patients had the characteristic string-of-beads appearance of the ICA, one unilateral and one bilateral. Neither of the patients had atherosclerotic lesions at the carotid bifurcation, although coexistent atherosclerotic involvement of the carotid bifurcation is found in approximately 25% of cases.⁸

In conclusion, CTA can depict the characteristic findings of FMD. It is expected that if patients with cerebrovascular symptoms are screened with CTA of the supraaortic vessels, more cases of FMD will be recognized as a possible cause of the neurologic symptoms.

References

1. Castillo M, Wilson JD. CT angiography of the common carotid artery bifurcation: comparison between two techniques and conventional angiography. *Neuroradiology* 1994; 36:602–604
2. Slovut DP, Olin JW. Fibromuscular dysplasia. *N Engl J Med* 2004; 350:1862–1871
3. Osborn AG. Nonatheromatous causes of arterial narrowing and occlusion. In: *Diagnostic neuroradiology*. St. Louis, MO: Mosby, 1994; 369–382
4. Furie DM, Tien RD. Fibromuscular dysplasia of arteries of the head and neck: imaging findings. *AJR* 1994; 162:1205–1209
5. Osborn AG, Anderson RE. Angiographic spectrum of cervical and intracranial fibromuscular dysplasia. *Stroke* 1977; 8:617–626
6. Arning C, Grzyska U. Color Doppler imaging of cervicocephalic fibromuscular dysplasia. *Cardiovasc Ultrasound* 2004; 2:7
7. Schievink WI, Bjornsson J. Fibromuscular dysplasia of the internal carotid artery: a clinicopathological study. *Clin Neuropathol* 1996; 15:2–6
8. Wesen CA, Elliott BM. Fibromuscular dysplasia of the carotid arteries. *Am J Surg* 1986; 151:448–451

Chapter 10

Summary and Conclusions

Summary and conclusions

This thesis evaluates the role of multidetector computed tomography (MDCT) angiography in the diagnostic work-up of patients with symptoms of transient ischemic attack (TIA) or ischemic stroke. The work in this thesis is focused on three topics. One: the optimization of the computed tomography angiography (CTA) scan protocol. Two: the accuracy of CTA in the detection of carotid artery stenosis and plaque composition. Three: the role of CTA in the workup of rare causes of ischemic stroke.

Optimization of the scan protocol

Optimization of the contrast material injection protocol with a saline bolus chaser was evaluated in **chapter 2**. Because contrast material is expensive and potentially nephrotoxic, the amount of contrast material administered should be as low as possible. MDCT scanners allow performance of CTA of the carotid arteries with increased coverage from the aortic arch to the circle of Willis, improved spatial resolution, and shorter acquisition times. The short acquisition time may lead to lower doses of contrast material. Furthermore, the addition of a saline bolus chaser after the contrast material injection can reduce the volume of contrast material without a subsequent decrease in arterial attenuation. This study revealed that the addition of a 40 ml bolus chaser to 80 ml contrast material results in significantly higher attenuation of the supra-aortic arteries compared to 80 ml contrast material alone. Decreasing the amount of contrast material to 60 ml with the use of a 40 ml bolus chaser results in significantly lower attenuation compared to 80 ml contrast material alone. The maximum attenuation was reached in the proximal internal carotid artery in all three groups, which is the site of most interest. The study also revealed that the vessel enhancement was inversely correlated with body weight. We concluded that in patients weighing less than 75 kg, 60 ml contrast material with 40 ml bolus chaser was sufficient for optimal vessel attenuation.

With bolus tracking, CTA scanning can be optimally synchronized with the passage of contrast material in the arteries.¹ Scan direction is normally based on the direction of the blood flow. The presence of undiluted contrast material in the subclavian vein, brachiocephalic vein, and superior vena cava produces artifacts that project over the ascending aorta and the origin of the supra-aortic arteries. Such artifacts can obscure adjacent structures and thus hide or suggest stenosis or occlusion of the proximal supra-aortic arteries.^{2,3} Our study described in **chapter 3** showed that a craniocaudal scan direction in comparison with a caudocranial scan direction resulted in much lower attenuation of the superior vena cava and a reduction of the number of perivenous artifacts. Although arterial attenuation slightly decreased, a better evaluation of the ascending aorta and supra-aortic arteries was possible.

The considerably shorter acquisition times of CTA with the MDCT scanners require a high arterial attenuation in a shorter period of time. Especially in imaging of the coronary arteries, which is hampered by their small size and tortuous course and, when a stenosis or obstruction is present, by reduced blood flow, high arterial attenuation is desirable. A way to achieve this is to use a contrast material with higher iodine concentration. In **chapter 4**, the attenuation achieved in the coronary arteries and great vessels of the thorax after administration of 2 contrast materials with high iodine concentration (iopromide 370 mg/ml and iomeprol 400 mg/ml) was compared. With all other injection variables (volume, injection rate) and examination parameters kept constant, significantly higher attenuation was found in all vessels with the contrast material with the highest concentration of iodine (400 mg/ml). These findings suggest that modest increases in the concentration of iodine can lead to significant increases in the attenuation observed and thereby improve the visualization of the vessels of interest.

In these studies CTA was performed on a 16-detector row CT scanner. Based on these studies, to achieve the best evaluation of the supra-aortic arteries, we recommend a scan protocol with a 40-mL saline bolus chaser, a craniocaudal scan direction and a contrast material volume adjusted for weight; use 60 mL of contrast material in patients weighing 75 kg or less and use 80 mL of contrast material in patients weighing more than 75 kg. The use of contrast material with a high iodine concentration in CTA of the supra-aortic arteries has not been studied but might further reduce the amount of contrast material needed.

Since the time of these studies improvements of technique have gone incredibly fast. Today CT scanners with up to 320 detectors are available and used in daily clinical practice. Scan times are further reduced and spatial and temporal resolution are further improved. Scan protocols will have to be adjusted for the ultra short acquisition times. It is not expected that the amount of contrast material can be further decreased.

The diagnostic imaging work-up of carotid artery disease

Carotid endarterectomy reduces the risk of stroke in patients with high-grade symptomatic carotid artery stenosis of 70–99% (NASCET criteria) and may also benefit patients with milder stenosis of 50–69%. Accurate carotid imaging to assess the severity of stenosis is important to avoid operating on patients with less severe stenoses in whom the risk of surgery may not outweigh the benefit. The gold standard for the assessment of carotid stenosis was digital subtraction angiography (DSA). DSA is invasive and has a complication rate of 0.5% in patients with symptomatic ischemic cerebrovascular disease.⁴ Logistical reasons may delay the DSA, which will lead to an increase in time between the first cerebrovascular event and treatment. Less invasive imaging tests, such as duplex ultrasound (DUS), (contrast-enhanced) magnetic resonance angiography (MRA) and CTA have been proven to be accurate enough to replace DSA. DUS is probably the most widely accessible test and therefore it seems reasonable to use it as a first line investigation. However, because of its relative low sensitivity and operator dependence, most surgeons hesitate to rely on DUS alone. A different less invasive test before carotid endarterectomy is used to confirm the DUS test result. Contrast-enhanced MRA is an accurate technique, but is expensive, lower in availability and has a higher percentage of contraindications than CT angiography. Also, the longer duration of the examination can be a problem in acute patients. Recent significant improvement in MDCT technology made CTA probably as accurate as contrast-enhanced MRA.

In **chapter 5** the accuracy of CTA and DUS in detecting a significant stenosis of the symptomatic internal carotid artery in the diagnostic work-up of patients with amaurosis fugax, TIA or minor stroke in the setting of routine clinical practice was studied. The study was designed to test CTA as a first-line investigation. A large group of consecutive patients with amaurosis fugax, TIA or minor ischemic stroke was included. CTA was performed in a patient population without selection based on prior imaging and only the symptomatic artery was included in the analysis.

The results of this study showed a sensitivity of CTA of 91% (95%CI, 71-99%) and a specificity of 99% (95%CI, 98-100%) for 70%-99% stenoses. For 50%-99% stenoses the sensitivity was 100% (95%CI, 88-100%) and the specificity was 98% (95%CI, 96-99%). The sensitivity of DUS on the contrary was much lower: 59% (95%CI, 36-79%) for 70%-99% stenoses and 79% (95%CI, 59-92%) for 50%-99% stenoses, while the specificity of DUS is comparable to the specificity of CTA. We concluded that CTA can provide an accurate and fast diagnosis in patients suspected of having a carotid stenosis in the setting of routine clinical practice.

In **chapter 6** the cost-effectiveness of MDCT angiography alone was compared to other imaging strategies in patients with a TIA or a minor stroke who are suspected of having a carotid artery stenosis. Particular attention was paid to the time window between the first ischemic symptoms and carotid endarterectomy and the cut-off value chosen as an indication for surgery (70%–99% vs. 50%–99% stenosis). The results of this study show that MDCT angiography alone or combined with DUS is the most cost-effective diagnostic test strategy for suspected carotid artery stenosis in the work-up of patients with a recent TIA or minor ischemic stroke. In patients with a TIA or minor stroke, the diagnostic work-up should be DUS as the initial diagnostic test; CTA should then be performed if the DUS results are positive, assuming carotid endarterectomy is performed 2–4 weeks after presentation in patients harboring stenoses of 70%–99%. In patients with a high-risk profile, with a high prior probability of carotid artery stenosis, or who can undergo surgery within 2 weeks after the initial symptoms, immediate CTA and surgery for stenoses of 50%–99% are indicated.

Although the severity of stenosis caused by atherosclerosis in the carotid bifurcation is the most important risk factor for (recurrent) stroke and is used to decide which patients could benefit from carotid endarterectomy, pathological and clinical studies have shown that other atherosclerotic plaque features play a role in an acute ischemic event. Atherosclerotic plaque volume, composition and morphology could be parameters, which may help in a better risk prediction and selection of patients who could benefit from surgical intervention. Plaques containing a necrotic lipid core covered by a thin fibrous cap (known as unstable or vulnerable plaque) are prone to rupture, releasing thromboembolic particles to the brain. Therefore, noninvasive, in vivo assessment of plaque components in the carotid artery would be useful in therapy determination. In **chapter 7** we evaluated a dedicated software tool for volume measurements of atherosclerotic carotid plaque and its components in MDCT angiography images and assessed the observer variability of these measurements. This study shows that in vivo assessment of atherosclerotic plaque and plaque component volumes in carotid arteries with MDCT angiography is feasible with a moderate reproducibility.

Today most centres consider non-invasive techniques, alone or in combination, to be accurate enough to replace DSA in the routine assessment of carotid disease. A recent meta-analysis of the available evidence by the Health and Technology Assessment review on carotid imaging in the UK supports this.⁵ The use of non-invasive diagnostic strategies enables more patients to receive endarterectomy more quickly than the use of DSA and produces greater net benefit compared with

DSA.⁵ DSA is mostly replaced by contrast-enhanced MRA or CTA. Both techniques can also provide information about plaque morphology and plaque constituents, which might add further prognostic information to luminal stenosis alone. Large prospective studies are mandatory to evaluate the predictive value of MRI- or CT-assessed atherosclerotic plaque characteristics in stroke patients or patients with an increased risk of atherosclerotic disease.

Rare causes of ischemic stroke

Cerebral infarctions are usually classified into the traditional diagnostic categories of large-artery atherothrombosis, cardiogenic embolism and small-artery disease. Ischemic stroke of unusual etiology includes patients with rare causes of stroke, such as non-atherosclerotic vasculopathies, hypercoagulable states, or hematologic conditions. Today neurologists have an increased need to distinguish it from other ischemic stroke subtypes as these rare causes of stroke have a different treatment approach and outcome. Imaging may play a crucial role in detection of rare causes of ischemic stroke.

In **chapter 8** an anomaly of the intracranial arteries is discussed: a fetal origin of the posterior cerebral artery. In 10–20 % of normal subjects the posterior cerebral artery (PCA) derives from the internal carotid artery (ICA) through a patent posterior communicating artery, while the connection with the basilar artery is hypoplastic or even aplastic. Such a fetal origin of the PCA in combination with atherosclerotic disease or dissection of the carotid artery may cause an ischemic stroke in the occipital lobe. This study assessed the frequency of a fetal origin of the PCA in a clinical series, and the degree of stenosis of the ipsilateral ICA in patients with a TIA or infarct in the territory of the PCA with 16-multidetector-row CTA. There was no association between a severe carotid stenosis and a fetal origin of the PCA at the symptomatic side. Therefore this study does not provide arguments for an increased risk of ischemic stroke in the territory of the PCA in patients with a fetal origin of the PCA. Nevertheless, in an individual patient with a TIA or infarct in the territory of the PCA this could still be the most likely cause and therefore the patient might benefit from carotid endarterectomy. This study showed that evaluation of the circle of Willis in ischemic stroke is relevant for the evaluation of the underlying disease and its pathophysiological pathway. A cost-effectiveness study should be performed to investigate whether screening patients with a recent TIA or infarct in the territory of the PCA for a fetal origin and atherosclerotic disease of the ipsilateral carotid artery is justified.

In **chapter 9** cervicocephalic fibromuscular dysplasia (FMD) is discussed as a rare cause of stroke. Cervicocephalic FMD involves the extracranial ICA in nearly 75% of patients. It is often asymptomatic, but it can also present with a variety of specific neurologic symptoms including TIA, amaurosis fugax and stroke or non-specific symptoms such as headache and tinnitus. It can be detected with conventional angiography and less sensitively with DUS and MRA. To our knowledge, we were the first to describe FMD of the carotid artery detected by CTA. We presented two

patients with ischemic neurologic symptoms in whom CTA showed the characteristic “string-of-beads appearance” of the ICA. It is expected that by screening patients with cerebrovascular symptoms with CTA of the supra-aortic vessels more cases of FMD will be recognized as possible cause of the neurologic symptoms.

References

1. Haage P, Schmitz-Rode T, Hubner D, Piroth W, Gunther RW. Reduction of contrast material dose and artifacts by a saline flush using a double power injector in helical CT of the thorax. *AJR* 2000; 174:1049-53.
2. Rubin GD, Lane MJ, Bloch DA, Leung AN, Stark P. Optimization of thoracic spiral CT: effects of iodinated contrast medium concentration. *Radiology* 1996; 201:785-91.
3. Loubeyre P, Debard I, Nemoz C, Minh VA. High opacification of hilar pulmonary vessels with a small amount of nonionic contrast medium for general thoracic CT: a prospective study. *AJR* 2002; 178:1377-81.
4. Johnston DC, Chapman KM, Goldstein LB. Low rate of complications of cerebral angiography in routine clinical practice. *Neurology* 2001; 57:2012-4.
5. Wardlaw JM, Chappell FM, Stevenson M, et al. Accurate, practical and cost-effective assessment of carotid stenosis in the UK. *Health Technol Assess* 2006; 10:iii-iv,ix-x,1-182.

Chapter 11

Samenvatting en Conclusies

Samenvatting en conclusies

Dit proefschrift evalueert het gebruik van multidetector computed tomography (MDCT) angiografie in de diagnostische work-up van patiënten met symptomen van een voorbijgaande ischemische aanval (TIA) of herseninfarct. De onderzoeken in dit proefschrift zijn onderverdeeld in drie onderwerpen. Eén: de optimalisering van het computed tomography angiography (CTA) scan protocol. Twee: de accurate van CTA in de opsporing van arteria carotis stenose en plaque samenstelling. Drie: de rol van CTA in de work-up van zeldzame oorzaken van een herseninfarct.

Optimalisering van het scan protocol

In **hoofdstuk 2** wordt de optimalisering van het contrastmiddel injectie protocol door het inspuiten van een zoutoplossing direct na het beëindigen van het inspuiten van het contrastmiddel geëvalueerd. De zoutoplossing zorgt ervoor dat het gehele volume van het contrastmiddel in de grote vaten terecht komt en wordt gebruikt voor afbeelding van de bloedvaten. Omdat contrastmiddel duur is en potentieel nefrotoxisch, is het noodzakelijk de toegediende hoeveelheid contrastmiddel zo laag mogelijk gehouden worden. MDCT scanners maken CTA van de arteria carotis mogelijk met een groter scanbereik van de aortaboog tot en met de Cirkel van Willis, een verbeterde spatiële resolutie, en een kortere acquisitie tijd. De kortere acquisitie tijd kan lijden tot kleinere hoeveelheden toe te dienen contrastmiddel. Bovendien zou de toediening van een zoutoplossing na het contrastmiddel het volume van het toe te dienen contrastmiddel reduceren zonder te resulteren in een afname van de vaataankleuring. Dit onderzoek toont aan dat het toevoegen van een bolus chaser van 40 ml zoutoplossing aan de toediening van 80 ml contrastmiddel resulteert in een significant hogere aankleuring van de supra-aortale arteriën in vergelijking met de toediening van alleen 80 ml contrastmiddel. Het verminderen van de hoeveelheid contrastmiddel van 80 ml naar 60 ml bij het gebruik van een 40 ml bolus chaser resulteert echter in een significant lagere vaataankleuring in vergelijking met de toediening van alleen 80 ml contrastmiddel. In alle drie de groepen wordt de maximale aankleuring bereikt in de proximale arteria carotis interna, de locatie welke het meest van belang is. Uit het onderzoek blijkt ook dat de vaataankleuring omgekeerd evenredig gecorreleerd is met het lichaamsgewicht. We concluderen dat bij patiënten die minder wegen dan 75 kg, 60 ml contrastmiddel met 40 ml bolus chaser voldoende is voor een optimale vaataankleuring.

Met bolus tracking kan de CTA scan optimaal worden gesynchroniseerd met de passage van contrast materiaal door de arteriën.¹ De scan richting wordt normaal gesproken aangepast aan de richting van de bloedstroom. De aanwezigheid van onverdund contrastmiddel in de vena subclavia, vena brachiocephalica en de vena cava superior veroorzaakt artefacten die projecteren over de aorta ascendens en de oorsprong van de supra-aortale arteriën. Deze artefacten kunnen er voor zorgen dat aangrenzende structuren niet meer goed zichtbaar zijn en zo een stenose of occlusie van de proximale supra-aortale arteriën verbergen of juist suggereren.^{2,3} Uit ons onderzoek beschreven in **hoofdstuk 3** blijkt dat een craniocaudale scanrichting in vergelijking met een caudocraniale scanrichting resulteert in een lagere vaataankleuring van de vena cava superior en een vermindering van het aantal peri-veneuze artefacten. Hoewel de arteriële vaataankleuring licht daalt is een betere evaluatie van de aorta ascendens en supra-aortale arteriën mogelijk.

De aanzienlijk kortere acquisitie tijden van CTA met de huidige MDCT scanners vereisen een hoge arteriële vaataankleuring in een kortere tijd. Vooral in de beeldvorming van de coronair arteriën, die wordt bemoeilijkt door hun kleine omvang en bochtige verloop, en wanneer een stenose of occlusie aanwezig is, door de verminderde doorstroming, is een hoge arteriële vaataankleuring gewenst. Een manier om dit te bereiken is een contrastmiddel te gebruiken met een hogere concentratie jodium. In **hoofdstuk 4** wordt de vaataankleuring in de coronair arteriën en de

grote vaten van de thorax vergeleken na toediening van 2 contrastmiddelen met een hoge jodium concentratie (iopromide 370 MGI / ml en iomeprol 400 MGI / ml). Alle andere injectie variabelen (volume, injectiesnelheid) en onderzoeksparementers werden constant gehouden. De vaataankleuring is significant hoger in alle arteriën bij gebruik van het contrastmiddel met de hoogste concentratie jodium (400 MGI / ml). Deze bevindingen suggereren dat een bescheiden verhoging van de concentratie jodium kan leiden tot een aanzienlijke stijging van de waargenomen vaataankleuring en daarmee een verbetering van de visualisatie van de bloedvaten.

In alle drie de studies (**hoofdstuk 2-4**) werd CTA uitgevoerd op een 16 detector CT-scanner. Op basis van deze studies adviseren wij een scan protocol toe te passen met een craniocaudale scan richting waarbij 40-ml fysiologisch zoutoplossing wordt ingespoten direct na de injectie met contrastmiddel, en waarbij het contrastmiddel volume wordt aangepast aan het lichaamsgewicht; gebruik 60 ml contrastmiddel bij patiënten met een gewicht van 75 kg of minder en 80 ml contrastmiddel bij patiënten die meer wegen dan 75 kg. Het gebruik van contrastmiddel met een zeer hoge jodium concentratie in CTA van de supra-aortale vaten is niet onderzocht, maar zou de hoeveelheid contrastmiddel die nodig is verder kunnen verlagen.

Sinds de uitvoering van deze studies zijn de verbeteringen in techniek ongelooflijk snel gegaan. Vandaag de dag zijn CT-scanners met maximaal 320 detectoren verkrijgbaar en in de dagelijkse klinische praktijk in gebruik. Scantijden zijn verder verlaagd en de spatiële en temporele resolutie zijn verder verbeterd. Scan protocollen moeten worden aangepast voor de ultra korte acquisitie tijden. Ondanks deze verbeteringen verwachten we niet dat de hoeveelheid contrastmiddel verder kan worden verlaagd.

De diagnostische beeldvorming van carotis stenose en plaque samenstelling.

Carotis endarteriëctomie vermindert het risico op een herseninfarct bij patiënten met een hooggradige symptomatische carotis stenose van 70-99% (NASCET criteria) en kan ook gunstig zijn voor patiënten met een mildere stenose van 50-69%. Een accurate beoordeling van de ernst van de stenose is belangrijk om operaties te voorkomen bij patiënten met minder ernstige vernauwingen bij wie het risico van een operatie niet opweegt tegen het voordeel. De gouden standaard voor de beoordeling van carotis stenose was digitale subtractie angiografie (DSA). DSA is invasief en heeft een complicatie percentage van 0,5% bij patiënten met symptomatische ischemische cerebrovasculaire ziekte.⁴ Daarnaast kunnen logistieke redenen de uitvoering van de DSA vertragen, waardoor de tijd tussen de start van de symptomen en de behandeling toeneemt. Minder invasieve beeldvormende onderzoeken, zoals duplex-echografie (DUS), (contrastversterkende) magnetische resonantie angiografie (MRA) en CTA hebben bewezen dat ze accuraat genoeg zijn om DSA te vervangen. DUS is waarschijnlijk de meest toegankelijke test en daarom lijkt het redelijk om het te gebruiken als het eerste onderzoek. Vanwege de relatief lage sensitiviteit en de gebruikersafhankelijkheid, aarzelen de meeste chirurgen om alleen te vertrouwen op DUS. Een andere minder invasieve test voorafgaand aan

carotis endarteriëctomie wordt daarom gebruikt om het DUS resultaat te bevestigen. Contrastversterkende MRA is een nauwkeurige techniek, maar is duur, minder beschikbaar en heeft een hoger percentage van contra-indicaties dan CTA. Ook kan de langere duur van het onderzoek een probleem geven in acute patiënten. Recente verbetering van de MDCT technologie maakt CTA waarschijnlijk net zo nauwkeurig als contrastversterkende MRA.

In **hoofdstuk 5** wordt de nauwkeurigheid bestudeerd van CTA en DUS bij het opsporen van een significante stenose van de symptomatische arteria carotis interna in de diagnostische work-up van patiënten met een TIA of klein herseninfarct in de setting van de dagelijkse klinische praktijk. De studie is opgezet om CTA te testen als een eerstelijns onderzoek. Een grote groep van opeenvolgende patiënten met een TIA of klein herseninfarct werd geïncludeerd. CTA werd uitgevoerd in een patiëntenpopulatie zonder selectie op basis van voorafgaande beeldvorming en alleen de symptomatische slagader werd opgenomen in de analyse. De resultaten van deze studie tonen een sensitiviteit van CTA van 91% (95% BI, 71-99%) en een specificiteit van 99% (95% CI, 98-100%) voor 70%-99% stenosen. Voor 50%-99% stenose is de sensitiviteit 100% (95% CI, 88-100%) en de specificiteit 98% (95% BI, 96-99%). De sensitiviteit van DUS daarentegen is veel lager: 59% (95% BI, 36-79%) voor 70%-99% stenosen en 79% (95% BI, 59-92%) voor 50%-99% stenosen, terwijl de specificiteit van DUS vergelijkbaar is met de specificiteit van CTA. We concluderen dat CTA een nauwkeurige en snelle diagnose geeft, bij patiënten verdacht van het hebben van een carotis stenose in de setting van de dagelijkse klinische praktijk.

In **hoofdstuk 6** wordt de kosteneffectiviteit van MDCT angiografie vergeleken met andere beeldvormende strategieën bij patiënten met een TIA of klein herseninfarct die verdacht worden van een carotis stenose. Bijzondere aandacht is besteed aan het tijdvenster tussen de eerste ischemische symptomen en carotis endarteriëctomie en aan de drempel waarde die gekozen wordt voor een operatie-indicatie (70%-99% vs 50%-99% stenose). De resultaten van deze studie tonen aan dat MDCT angiografie alleen of in combinatie met DUS de meest kosteneffectieve diagnostische test strategie is voor het aantonen of uitsluiten van een carotis stenose in de work-up van patiënten met een recente TIA of klein herseninfarct. Bij patiënten met een TIA of klein herseninfarct moet DUS de eerste diagnostische test in de diagnostische work-up zijn; CTA dient dan te worden uitgevoerd als de DUS resultaten positief zijn, ervan uitgaande dat carotis endarteriëctomie wordt uitgevoerd 2-4 weken na de presentatie bij patiënten met stenosen van 70%-99%. Direct CTA en carotis endarteriëctomie voor stenosen van 50%-99% is geïndiceerd bij patiënten met een hoog risicoprofiel, met een hoge voorafgaande kans op carotis stenose, of die geopereerd kunnen worden binnen 2 weken na de eerste symptomen.

Hoewel de ernst van de vernauwing als gevolg van atherosclerose in de carotis bifurcatie de belangrijkste risicofactor is voor een nieuw herseninfarct en wordt gebruikt om te bepalen welke patiënten baat kunnen hebben bij carotis endarteriëctomie, hebben pathologische en klinische studies aangetoond dat andere atherosclerotische plaque kenmerken een rol spelen bij acute ischemie. Atherosclerotische plaque volume, plaque samenstelling en plaque morfologie zouden parameters kunnen zijn, die kunnen helpen bij een betere risicovoorspelling en selectie van

patiënten die baat kunnen hebben bij een chirurgische ingreep. Plaques met een necrotische vet kern, die wordt bedekt met een dunne fibreuze kap (bekend als instabiele of kwetsbare plaque) zijn gevoelig voor scheuren, waardoor trombo-embolische deeltjes los laten en naar de hersenen gaan. Daarom zou niet-invasieve, in vivo bepaling van plaque componenten in de halsslagader bruikbaar kunnen zijn in de bepaling van de therapie. In **hoofdstuk 7** hebben we een speciale software tool geëvalueerd voor volume metingen van atherosclerotische plaque en plaque componenten in de arteria carotis op MDCT angiografie beelden. Tevens hebben we de observer variabiliteit van deze metingen beoordeeld. Deze studie toont aan dat in vivo evaluatie van de atherosclerotische plaque en plaque component volumes in de arteria carotis met MDCT angiografie haalbaar. De reproduceerbaarheid is echter nog matig.

Tegenwoordig beschouwen de meeste centra niet-invasieve technieken, alleen of in combinatie, nauwkeurig genoeg om DSA te vervangen in de routinematige beoordeling van atherosclerose van de arteria carotis. Een recente meta-analyse van de beschikbare gegevens door de Health and Technology Assessment over arteria carotis beeldvorming in het Verenigd Koninkrijk ondersteunt dit.⁵ Door het gebruik van niet-invasieve diagnostische strategieën kunnen meer patiënten sneller endarteriëctomie ondergaan dan bij het gebruik van DSA en is het netto voordeel groter in vergelijking met DSA.⁵ DSA wordt meestal vervangen door contrastversterkende MRA of CTA. Beide technieken kunnen ook informatie geven over plaque morfologie en plaque bestanddelen, die verder prognostische informatie kan toevoegen aan de stenosegraad alleen. Grote prospectieve studies zijn nodig om de voorspellende waarde van MRI-of CT-beoordeling van atherosclerotische plaque kenmerken in patiënten met een herseninfarct of patiënten met een verhoogd risico op atherosclerose te evalueren.

Zeldzame oorzaken van herseninfarct

Herseninfarcten worden meestal ingedeeld in de traditionele diagnostische categorieën van atherotrombose van de grote arteriën, embolieën afkomstig uit het hart en ziekte van de kleine vaatjes in de hersenen. Zeldzame oorzaken van een herseninfarct zijn o.a. niet-atherosclerotische vaatafwijkingen, hypercoagulatie en hematologische aandoeningen. Tegenwoordig hebben neurologen een toegenomen interesse om deze oorzaken te onderscheiden van de bekende herseninfarct subtypes omdat deze zeldzame oorzaken een andere benadering van de behandeling behoeven en een andere prognose hebben. Beeldvorming kan een cruciale rol spelen in de detectie van zeldzame oorzaken van een herseninfarct.

In **hoofdstuk 8** wordt een anomalie van de intracraniële bloedvaten besproken: een foetale oorsprong van de arteria cerebri posterior. In 10-20% van de bevolking wordt de arteria cerebri posterior (ACP) gevoed door de arteria carotis interna (ACI) door middel van een open gebleven arteria communicans posterior, terwijl de verbinding met de arteria basilaris hypoplastisch of zelfs aplastisch is. Een foetale oorsprong van de ACP in combinatie met atherosclerose of een dissectie van de

arteria carotis kan leiden tot een herseninfarct in de occipitale hersenkwab. Deze studie onderzocht met 16-multidetector CTA de frequentie van een foetale oorsprong van de ACP en de mate van stenose van de ipsilaterale ACI in een klinische patiëntengroep bestaande uit patiënten met een TIA of infarct in het stroomgebied van de ACP. Er was geen verband tussen een ernstige carotis stenose en een foetale oorsprong van de ACP aan de symptomatische zijde. Daarom biedt dit onderzoek geen argumenten voor een verhoogd risico op een herseninfarct in het stroomgebied van de ACP bij patiënten met een foetale oorsprong van de ACP. Niettemin kan bij een individuele patiënt met een TIA of herseninfarct in het stroomgebied van de ACP, een carotis stenose nog steeds de meest waarschijnlijke oorzaak zijn en heeft de patiënt in dat geval baat bij een carotis endarteriëctomie. Deze studie toont aan dat de evaluatie van de cirkel van Willis bij een herseninfarct relevant is voor de beoordeling van de onderliggende ziekte en pathofysiologie. Een kosten-effectiviteits analyse moet worden uitgevoerd om te onderzoeken of het screenen op een foetale oorsprong van patiënten met een recente TIA of herseninfarct in het stroomgebied van de ACP en atherosclerose van de ipsilaterale arteria carotis gerechtvaardigd is.

In **hoofdstuk 9** wordt cervicocraniële fibromusculaire dysplasie (FMD) besproken als een zeldzame oorzaak van een herseninfarct. Cervicocraniële FMD heeft betrekking op de extracraniële ACI in bijna 75% van de patiënten. Het is vaak asymptomatisch, maar het kan zich ook presenteren met een verscheidenheid aan specifieke neurologische symptomen, waaronder TIA en herseninfarct of niet-specifieke symptomen zoals hoofdpijn en oorsuizen. Het kan worden gedetecteerd met conventionele angiografie en minder gevoelig met DUS en MRA. Voor zover wij weten, waren we de eersten die FMD van de arteria carotis gedetecteerd met CTA beschrijven. We presenteren twee patiënten met ischemische neurologische symptomen bij wie CTA het karakteristieke kralensnoerpatroon van de ACI toonde. De verwachting is dat door het screenen van patiënten met cerebrovasculaire symptomen met CTA van de supra-aortale vaten meer gevallen van FMD zullen worden erkend als mogelijke oorzaak van de neurologische symptomen.

References

1. Haage P, Schmitz-Rode T, Hubner D, Piroth W, Gunther RW. Reduction of contrast material dose and artifacts by a saline flush using a double power injector in helical CT of the thorax. *AJR* 2000; 174:1049-53.
2. Rubin GD, Lane MJ, Bloch DA, Leung AN, Stark P. Optimization of thoracic spiral CT: effects of iodinated contrast medium concentration. *Radiology* 1996; 201:785-91.
3. Loubeyre P, Debard I, Nemoz C, Minh VA. High opacification of hilar pulmonary vessels with a small amount of nonionic contrast medium for general thoracic CT: a prospective study. *AJR* 2002; 178:1377-81.
4. Johnston DC, Chapman KM, Goldstein LB. Low rate of complications of cerebral angiography in routine clinical practice. *Neurology* 2001; 57:2012-4.
5. Wardlaw JM, Chappell FM, Stevenson M, et al. Accurate, practical and cost-effective assessment of carotid stenosis in the UK. *Health Technol Assess* 2006; 10:iii-iv,ix-x,1-182.

Chapter 12
Dankwoord

Dankwoord

Velen hebben een bijdrage geleverd aan de totstandkoming van dit proefschrift. Een aantal van hen wil ik graag in het bijzonder bedanken.

Allereerst wil ik Prof.dr. Aad van der Lugt bedanken, in eerste instantie mijn co-promotor, uiteindelijk zelfs mijn promotor. Zijn enthousiasme lokte mij de research in en zijn visie was de drijfveer van dit onderzoek. Veel dank voor de prettige begeleiding, de interesse in mijn werk en leven en het begrip dat de afronding “iets langer” heeft geduurd.

Daarnaast wil ik Prof.dr. Diederik Dippel bedanken, mijn tweede promotor. Voor mij iets meer op de achtergrond aanwezig, maar zeker niet minder betrokken bij alles. Altijd bereikbaar voor neurologische en statistische vragen. Bedankt voor de fijne samenwerking.

De overige commissieleden wil ik graag bedanken voor het beoordelen van mijn proefschrift: Prof.dr. W.P.T. Mali, Prof.dr. H. J.M. Verhagen en Prof.dr. Myriam Hunink in het bijzonder voor haar betrokkenheid, adviezen en steun gedurende de hele studie.

Prof.dr. Gabriel Krestin, mijn opleider, wil ik bedanken voor alle mogelijkheden die hij mij heeft geboden en het geduld en vertrouwen in de goede afloop van onderzoek en opleiding.

Daarnaast dank aan alle betrokkenen van de afdeling radiologie, neurologie en beeldverwerking in het Erasmus MC, zonder wie dit proefschrift niet mogelijk was geweest, zoals alle medeauteurs, mijn collega onderzoekers, het trial bureau, alle duplex en CT laboranten, (oud-)collega arts-assistenten en radiologen, het secretariaat en vele anderen.

List of Publications

List of Publications

Tholen AT, de Mony  C, Genders TS, Buskens E, Dippel DW, van der Lugt A, Hunink MG. Suspected carotid artery stenosis: cost-effectiveness of CT angiography in work-up of patients with recent TIA or minor ischemic stroke. *Radiology* 2010; 256(2):585-97

Rozie S, de Weert TT, de Mony  C, Homburg PJ, Tanghe HL, Dippel DW, van der Lugt A. Atherosclerotic plaque volume and composition in symptomatic carotid arteries assessed with multidetector CT angiography; relationship with severity of stenosis and cardiovascular risk factors. *Eur Radiol* 2009; 19(9):2294-301

De Weert TT, de Mony  C, Meijering E, Booij R, Niessen WJ, Dippel DW, van der Lugt A. Assessment of atherosclerotic carotid plaque volume with multidetector computed tomography angiography. *Int J Cardiovasc Imaging* 2008; 24(7):751-9

De Mony  C, Dippel DW, Siepman TA, Dijkshoorn ML, Tanghe HL, van der Lugt A. Is a fetal origin of the posterior cerebral artery a risk factor for TIA or ischemic stroke? A study with 16-multidetector-row CT angiography. *J Neurol* 2008; 255(2):239-45.

De Mony  C, Dippel DW, Dijkshoorn ML, Tanghe HL, van der Lugt A. MDCT detection of fibromuscular dysplasia of the internal carotid artery. *AJR* 2007; 188(4):W367-9

Van Velsen EF, Niessen WJ, de Weert TT, de Mony  C, van der Lugt A, Meijering E, Stokking R. Evaluation of an improved technique for lumen path definition and lumen segmentation of atherosclerotic vessels in CT angiography. *Eur Radiol* 2007; 17(7):1738-45

De Mony  C, de Weert TT, Zaalberg W, Cademartiri F, Siepman DA, Dippel DW, van der Lugt A. Optimization of CT angiography of the carotid artery with a 16-MDCT scanner: craniocaudal scan direction reduces contrast material-related perivenous artifacts. *AJR* 2006; 186(6):1737-45

Cademartiri F, de Mony  C, Pugliese F, Mollet NR, Runza G, van der Lugt A, Midiri M, de Feyter PJ, Lagalla R, Krestin GP. High iodine concentration contrast material for noninvasive multislice computed tomography coronary angiography: iopromide 370 versus iomeprol 400. *Invest Radiol* 2006; 41(3):349-53

Gratama van Andel HA, Meijering E, van der Lugt A, Vrooman HA, de Mony  C, Stokking R. Evaluation of an improved technique for automated center lumen line definition in cardiovascular image data. *Eur Radiol* 2006; 16(2):391-8

De Mony  C, Cademartiri F, de Weert TT, Siepman DA, Dippel DW, van Der Lugt A. Sixteen-detector row CT angiography of carotid arteries: comparison of different volumes of contrast material with and without a bolus chaser. *Radiology* 2005; 237(2):555-62.

De Mony  C, Karcher DS, Boelaert JR, Gordeuk VR Bone marrow macrophage iron grade and survival of HIV-seropositive patients *AIDS* 1999; 13(3):375-80

PhD Portfolio

PhD Portfolio

Name PhD student: Cécile de Monyé
 Erasmus MC Department: Radiology
 Research School: COEUR

PhD period: October 2002-August 2009
 Promotor(s): Prof.Dr. A. van der Lugt
 Prof.Dr. D.W.J. Dippel

1. PhD training

	Year	Workload ECTS
General courses		
- Classical Methods for Data-analysis, NIHES, Rotterdam	2004	6.0
Specific courses (e.g. Research school, Medical Training)		
- Atherosclerosis Research, COEUR training modules, Rotterdam	2004	1.5
- Cardiovascular Imaging and Diagnostics, COEUR training modules, Rotterdam	2004	1.5
- Neurovascular Diseases, COEUR training modules, Rotterdam	2004	1.5
- Peripheral Vascular Diseases: AAA, COEUR training modules, Rotterdam	2005	1.5
Seminars and workshops		
- COEUR Research seminars	2003, 2004	2.0
Presentations		
- <i>CT Angiography of the Carotid Artery</i> COEUR Research Seminar	2003	0.6
- Vaatdagen	2003	0.6
- Radiologen dagen	2003	0.6
- <i>CT, CTA en CT Perfusie in patiënten met cerebrovasculaire afwijkingen</i> Groot Referaat, Erasmus MC, Rotterdam & regio	2004	1.0
- <i>16-slice multidetector CT angiography of the carotid artery, the new modality of choice</i> RSNA	2003	1.8
- <i>Comparison of CTA with DUS in the vascular work-up of patients with cerebrovascular symptoms</i> RSNA	2004	1.8

- <i>Craniocaudal scan direction reduces contrast material-related perivenous artifacts</i> ECR	2005	1.8
- <i>Fetal origin of the posterior cerebral artery in patients with a TIA or infarct in the territory of the posterior cerebral artery assessed with 16-multidetector-row CT angiography</i> European Stroke Conference	2006	1.8
(Inter)national conferences		
- Radiologen dagen	2002-2008	0.6
- Vaatdagen	2003	0.6
- RSNA	2004	1.5
- ECR	2005	1.5

Other

2. Teaching

	Year	Workload (Hours/ECTS)
Lecturing		
Supervising practicals and excursions, Tutoring		
Supervising Master's theses		
Other		

Curriculum Vitae

De auteur van dit proefschrift werd geboren op 24 januari 1972 in Eindhoven. Na het behalen van haar eindexamen Gymnasium- β aan het Lorentz Lyceum te Eindhoven in 1990, ging zij Geneeskunde studeren aan de Universiteit Utrecht. Tijdens deze studie heeft zij zich onder andere ingezet als bestuurslid van de Medische Studenten Faculteitsvereniging Utrecht "Sams". Alvorens aan haar co-schappen te beginnen heeft zij in 1996 ruim een half jaar wetenschappelijk onderzoek verricht in de Verenigde Staten onder supervisie van Prof.dr. V.R. Gordeuk aan de George Washington University, Washington DC, USA. Dit heeft geresulteerd in een publicatie in het wetenschappelijk tijdschrift "AIDS". Zij behaalde haar arts-examen in 1999. Na enkele maanden als burgerarts bij de Koninklijke Landmacht te hebben gewerkt, begon zij als arts-assistent chirurgie in het Groene Hart Ziekenhuis te Gouda. In April 2000 startte zij haar opleiding radiologie in het Erasmus MC in Rotterdam (opleider Prof.dr. G.P. Krestin). Tijdens haar opleiding begon zij in 2002 aan het onderzoek beschreven in dit proefschrift onder leiding van Prof.dr. A. van der Lugt. Van 2003 tot 2007 onderbrak zij haar opleiding om zich volledig op dit onderzoek te kunnen richten. In augustus 2009 rondde zij haar opleiding tot radio- loog af en startte aansluitend haar fellowship mammaradiologie in het Erasmus MC Daniel den Hoed Kliniek. Sinds augustus 2011 is zij mammaradioloog en staf lid van de afdeling radiologie van het Erasmus MC Rotterdam.

